TECHNISCHE UNIVERSITÄT WIEN
Vienna University of Technology

DIPLOMARBEIT

Comparative Mathematical Modelling of Groundwater Pollution

Ausgeführt am Institut für

Analysis & Scientific Computing

der Technischen Universität Wien
unter der Anleitung von

Ao.Univ.Prof. Dipl.-Ing. Dr.techn. Felix Breitenecker

und Dipl-Ing. Martin Bicher
als verantwortlich mitwirkenden Assistenten
durch

Stefanie Nadine Winkler

Gernotgasse 5/10
A-1150 Wien

Wien, am 7. Mai 2014

Dedication and Acknowledgement

This thesis is dedicated to
the best grandfather in the world

Emmerich Zügner

I would like to express my gratitude to my supervisor Prof. Dr. Felix Breitenecker for guidance and the possibility to become a member of the research group. I appreciate the feedback and discussion inputs offered bbty Martin Bicher, Irene Hafner and all the colleagues who supported me in the last phase of my master thesis. I want to thank all friends who filled my time at university with laughs and joy and appreciated their help solving mathematical mysteries like Sherlock Holmes.
My deepest appreciation goes to my family, to my brother for sharing a wonderful childhood and my parents who give me the possibility of an excellent education. Additionally they motivated me to study a music instrument. My musical education is now an important part of me, makes hard times easier and brings joy into my life. I owe a debt of gratitude to my dear boyfriend who stays with me the whole time no matter how much time I have to share.
Thank you all for the great support.

Kurzfassung

In den unterschiedlichsten naturwissenschaftlichen und wirtschaftlichen Disziplinen spielt die Diffusion eine wichtige Rolle. In der Biologie wird beispielsweise die Reaktionsgleichung dazu benutzt, tierische Musterbildung nachzubauen. Auch in der Wirtschaft wird Diffusion verwendet um den Ankauf und Verkauf von Aktienfonds zu berechnen. Diese Arbeit widmet sich der sogenannten Smoluchowski Gleichung und wurde von einem Benchmark der europäischen Simulationsgemeinschaft inspiriert. Dieser Benchmark befasst sich mit der Thematik der Grundwasserverschmutzung und deren Simulation. Man stelle sich einfach eine Schmutzquelle inmitten eines beliebigen Gewässers vor. Diese Quelle emittiert immerwährend oder auch nur zeitweise Schmutzpartikel welche sich im Folgenden auf dem ganzen Gebiet verteilen. Um dieses Verhalten simulieren zu können benötigt man die zugrunde liegende mathematische Gleichung. In diesem Fall handelt es sich um die Analyse von diffusem Verhalten unter Einfluss von Geschwindigkeitsfeldern. Diverse Ansätze, beginnend bei analytischen Lösungen bis hin zu chaotischen Bewegungssimulationen, werden verwendet um dieses Verhalten abzubilden.

Der erste Teil der Arbeit beschäftigt sich ausschließlich mit der Problemanalyse auf einem eindimensionalen Gebiet. Im zweiten Teil wird das Gebiet zu einem zweidimensionalen Raum erweitert. In jeder Dimension werden grundsätzlich drei verschiedene Ansätze verfolgt. Als erstes wird auf dem angegebenen Gebiet und unter unterschiedlichen Voraussetzungen nach einer analytischen Lösung gesucht. Da analytische Lösungen in der Regel nicht einfach aufzufinden sind, konzentriert sich die zweite Herangehensweise auf numerische Lösungen. Diesbezüglich können zwei wichtige Verfahren genannt werden, die finite Differenzen und die finite Elemente Methode. Stochastische Prozesse als auch das Prinzip des Random Walks werden im dritten Teil verwendet um Diffusion zu simulieren. Diese alternativen Methoden beschäftigen sich mit der chaotischen Bewegung kleinster Teile.

Im Fokus dieser Arbeit steht der Vergleich dieser verschiedenen Ansätze in Hinblick auf Effizienz, Handhabung und Implementierung. Es werden sowohl Vorzüge als auch Nachteile, Gemeinsamkeiten sowie Unterschiede herausgearbeitet werden. Das Zusammenspiel der einzelnen Parameter und deren Auswirkungen auf die Simulationszeiten und -ergebnisse wird untersucht. Verfahren, die sich für diese Art von Aufgabenstellung weniger eignen, werden in dieser Arbeit ebenfalls angesprochen. Da in der hier betrachteten Problemstellung eine analytische Lösung angegeben werden kann, können die verschiedenen Methoden mit dieser als ultimativer Bestapproximation verglichen werden.
Zum Abschluss werden alle verwendeten Methoden und ihre Eigenschaften nochmals Revue passieren und ein Ausblick auf weitere mögliche Ansätze und Methoden gegeben.

Abstract

The theme of this master thesis was motivated by a benchmark of the Federation of European Simulation Societies, EUROSIM. The Benchmark deals with the problem of groundwater pollution. A two-dimensional domain filled with water may be considered. In the middle of this area a pollution source is located. This source emits solid constantly or at certain points in time. The distribution of this pollution on the regarded domain is analyzed. For simulation some mathematical background is summarized. The basic equation for pollution distribution is the diffusion equation. Different kinds of this equation are used. In chemistry as well as in biology the reaction-diffusion equation plays a very important role. Of course there are also physical applications of the diffusion, e.g. the heat equation. However, diffusion is also used to foresee the behavior of buyers of stocks in the financial market. In this work the focus is on the convection-diffusion equation. Using this equation the distributive behavior of the pollution influenced by a velocity field is described. Several approaches, ranging from analytical solutions to some chaotic particle movement, are used for realization.

In the first part of this thesis the problem definition is restricted to a one-dimensional domain. The second part deals with the already mentioned two-dimensional analysis. In both parts there are three different kinds of simulations used. Analysis always starts with an analytical solution of the equation using certain conditions. In reality it is not always possible to find such analytical solutions. Therefore the second approach covers two commonly used numerical methods, the finite differences and finite element method. Alternative implementations are given using the principle of microscopic particle movements, also known as Brownian motion, as well as the random walk. These processes can be described using stochastic theory including probability theory.

An important part of this work is the comparison of these different approaches regarding efficiency, accuracy and implementation. All the disadvantages and advantages will be shown. Also the similarities and differences between them are lined out. The interaction of the different parameters and their influences regarding simulation time and results are examined. This work also includes methods which are not appropriate to simulate diffusion in a useable way. For most of the used conditions an analytical solution can be given. Therefore an exact prototype for the perfect approximation is given and can be used for comparison.
In the end all the different used approaches and their properties are summarized. Also an outlook to other possible implementations is given.

Contents

CHAPTER 1

Introduction

The famous second order diffusion differential equation occurs in various different fields. For example in physics an application of diffusion would be the heat transport. The physical quantity is temperature and heat flow, respectively. Heat is transported from regions with higher temperature to regions with lower temperature. Consider a room with a heating source, e.g. a radiator. Every radiator is made of metal and filled with water. If the sensor signals that the room temperature is too low water is heated and leaded to the radiator. Due to the fact that the radiator is leaded the heat of the hot water is emitted the surrounding air. The distribution of the heat from the radiator into the room can be described with the heat equation.

$$\frac{\partial u}{\partial t} - \alpha \nabla^2 u = 0 \tag{1.1}$$

Another application can be found in biology. Pattern formation on fish's skin or cat fur look as if they are random [Bon97]. In fact the strips and points obey mathematical rules. Basis for these mathematical rules are reaction-diffusion simulations reproducing color patterns found in nature. [Tur52]

$$\frac{\partial q}{\partial t} = D \nabla^2 q + R(q) \tag{1.2}$$

The reaction-diffusion mechanism is based on interactions of a short-range self-enhancing reaction and a long-range antagonistic reaction, in other words an activator A and its inhibitor B. The behavior of activator and inhibitor is defined by certain reaction-diffusion equations with different diffusion coefficients D_A and D_B. Considering condition $D_A \ll D_B$, B disappears from regions around reaction centers of A and a pattern formation arises. [Mur89]

Similar to the application in biology, chemistry also uses reaction-diffusion equations (1.2). Additional to a diffusive part as in (1.1) the equation describes reactions between different elements. Reactions of two different substances can lead to new chemical bounds, thus new occurring elements. Therefore simulation based on reaction-diffusion are mainly used to describe the

distribution of different substances over a certain time. Reactions only take place at some local sites. [SMF10]

Diffusion is not only useful to analyze problems in natural science. In the last centuries the importance of the financial market has increased. The Black Schole Model is an implementation based on diffusion used in the financial market. This model is based on a convection-reaction-diffusion equation.

$$\frac{\partial V}{\partial t} + \frac{1}{2}\sigma^2 S^2 \frac{\partial^2 V}{\partial S^2} + rS\frac{\partial V}{\partial S} - rV = 0 \tag{1.3}$$

Quantity is the price of a derivative V as a function of stock price S and time t. [Coe02] The coefficient σ and r define the standard deviation of the stock's returns and the force of interest. The Black Schole Model focuses on the price variation of financial instruments, e.g. the European call option.

The four examples above show a part of the applications using mathematical equations containing diffusion. The research areas are widespread and involve important fields of study influencing various scientific discoveries. The basic idea of this work is the usage of diffusion for analyzing pollution in groundwater. In a minimized environment simplifying assumptions will result in different models and implementations reflecting diffusive behavior. More precisely the convection-diffusion equation will be used to simulate the expansion of soil injected by a source of pollution. Two different case studies are considered. On the one hand an instantaneous source is used. On the other hand the case of a constantly releasing source is regarded.

1.1 Modeling and Simulation

History of Modeling and Simulation.
The following paragraph is based on [AEM98]. Since the early stages of modeling and simulation in the 1920s a fascinating evolution happened. In that former times the needed technology was available only at a handful of university groups. Nowadays every engineer can choose which simulation tool fits best for his purpose. Between 1920 and 1950 analog techniques dominated this field. The significant change took place when digital computers where available.
The first simulators were analog and based on ordinary differential equations and block diagrams. The basic idea was developing a physical device that obeys differential equations. The first tool simulating dynamical systems, the mechanical differential analyzer, was developed around 1931 by V. Bush. In 1947 a paper of Ragazzini demonstrated that simulations can be done electronically instead of mechanically. That paper had a great impact on technology. Mechanics were replaced by electronics. Triggered by Selfridge digital computers appeared around 1955. Selfridge showed that differential analyzers could be replaced by digital computers. By 1967 more than 23 different programs for digital computers were available. The first appearance of a graphical environments representing models in block structure was in the mid 1970s. Due to the limited input-output facilities they were rarely used. After the development of modern work stations and raster graphics these environments got more popular. In 1980s matrix environments which additionally provided modeling tools appeared, e.g. MATLAB. The graphical

block diagram modeling was established in different languages around 1991. Another approach focused on the power of symbolic computations. This leads to an evolution of object-oriented languages, starting around 1973. Due to this development environments like Dymola which offered complete components for simulation (1990s) were established. Nowadays the modern approaches build on non-causal modeling with mathematical equations and use object-oriented constructs to facilitate reuse of modeling knowledge.

Classification of models.
In general models can be classified in different ways. First of all one can differ between static and dynamic models. An analysis of recorded data belongs to the group of static models. There are data of an observed system before and after certain changes but no data regarding the actual change. A model providing also the behavior of a system during changes as well as before and after, is called a dynamic model.
Additional to the separation between static and dynamic models other classifications concerning the observed parameter can be made. [IK03]

- time continuous
- time discrete
- spatial continuous
- time and spatial continuous

Models which are continuous in time are described by a differential equation as a function of time. Therefore this equation enables to calculate the state of a system at any point in time. Not every process can be reproduced using a time continuous model. As opposed to that there are time discrete models. In some cases it happens that data can only be measured at certain points in time. Another reason for discrete models are data which can not be continuous, e.g. thinking of population elicitation data only contains integers. These data are called discrete and so does the type of model. For modeling these problem data can sometimes be transformed into a differential equation using time series analysis. If a model concernes not only changes in time but also behavior in a continuous space it is called spatial continuous model. These kind of models are based on partial differential equations. An example for this class of models would be simulating vibration of strings with the wave equation.
The last class are stochastic models. In nature not all processes are predictable e.g. the decay of radioactive materials. There are assumptions and expectations how much material will be decayed after a certain amount of time but no one knows when it will happen exactly. The underlying mathematics belong to the theory of probability. Such models are based on differential equations whereas quantity is a stochastic process and therefore the equation describes a stochastic process itself.

In Modeling and Simulation depending on the focus different model approaches can be used for a certain problem. Even if the problem can be solved analytically most of the time it is helpful to find other formulations of the problem. Also the regarded diffusion problem can be

simulated with different models. The underlying partial differential equation suggests the use of spatial continuous models. In the following chapters different spatial continuous models using different methods will be introduced. Additionally a stochastic approach is implemented using the principle of Random Walk.

1.2 Motivation

There are many different interesting applications for diffusion but the motivation for this master thesis was a benchmark [Cra75] prepared by a German speaking research group for modeling and simulation. This benchmark deals with the pollution of groundwater in a simplified way. In the following considered surroundings and circumstances are described. Instead of using a difficult realistic geometry of a groundwater flux a rectangle is used. This rectangle is embedded in a Cartesian coordination system. In the origin of this coordinate system a source of pollution is placed as shown in figure 1.1.

Figure 1.1: A schematic illustration of the described area.

There are two different scenarios discussed in this thesis. On the one hand a constantly releasing source is observed. This is also the case which is described in the mentioned benchmark. On the other hand a different approach analyzes an instantaneous source of pollution. This process describing the spread out of pollution in the rectangle can be implemented with the diffusion equation.

$$\frac{\partial c}{\partial t} = D \cdot \nabla^2 c \tag{1.4}$$

In equation (1.4) the variable c stands for the concentration of pollution. The concentration is a function of time t and space x. In general the dimension of space is arbitrary $n \geq 1$. The parameter D stands for the diffusion coefficient. This coefficient influences the reduction of the peak and the spreading of pollution. The intuitive result of the pollution expansion is given in figure 1.2.

Additional to diffusion of pollution there exists a flow in positive x-direction, also called convection. Due to this flow the equation (1.4) has to be adapted. It results in the convection-diffusion equation, usually called *Smoluchowski equation*. [Cra75]

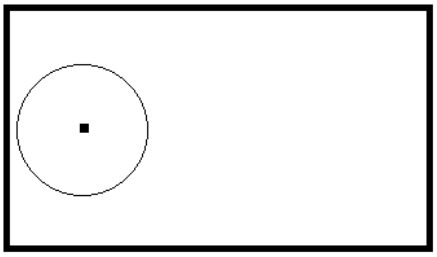

Figure 1.2: Diffusion of the pollution injected constantly by the source.

$$\frac{\partial c}{\partial t} = D \cdot \nabla^2 c - v \cdot \nabla c \tag{1.5}$$

The flux effects the pollution expansion. Instead of a distribution around the source a movement towards the right boundary occurs. In case of a natural flow there would by an inlet and outlet for the fluid. Therefore domain changes from a finite to a semi-finite domain are observed. That means that every kind of reflection is neglected. The illustration of the regarded area changes are shown in figure 1.3.

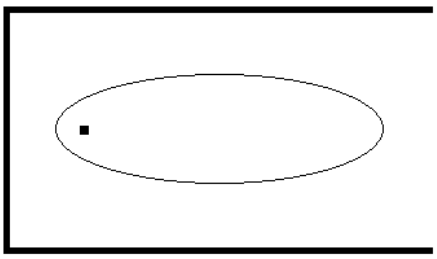

Figure 1.3: Convected diffusion in a semi-finite domain is shown.

In the benchmark a special diffusion equation is given. Compared to (1.5) the given equation has a different form.

$$\frac{\partial c}{\partial t} - \frac{u}{R}\frac{\partial c}{\partial t} = \frac{\alpha_L u}{R}\frac{\partial^2 c}{\partial x^2} + \frac{\alpha_T u}{R}\frac{\partial^2 c}{\partial y^2} - \lambda c \tag{1.6}$$

One can see immediately that the convection part is missing because no first derivate is found. Instead of that a retardation factor λ is given. The retardation factor could stand for a pump or anything else responsible for discharging pollution. Regarding the focus of this work discharging is no point of interest so the parameter λ can be set to zero. Concerning dispersive constants α_L and α_T, which stand for the dispersion in x-direction - longitudinal - and y-direction - transverse, respectively, another assumption can be made. These two constants

are assumed to be equal, therefore we define $\alpha = \alpha_L = \alpha_T$. Hence, the equation (1.6) can be written as:

$$\left(1 - \frac{u}{R}\right) \cdot \frac{\partial c}{\partial t} = \frac{\alpha u}{R} \cdot \left(\frac{\partial^2 c}{\partial x^2} + \frac{\partial^2 c}{\partial y^2}\right) \tag{1.7}$$

The diffusion coefficient D regarding (1.5) can be defined after a small transformation. In (1.7) the convective transport is missing. In this context the considerable variable for flux velocity is v.

$$\frac{\partial c}{\partial t} = D\Delta c - v\nabla c \tag{1.8}$$

$$D = \frac{\alpha u}{R - u} \tag{1.9}$$

Due to the fact that the flow is considered only along x-direction, ∇c can be replaced by $\frac{\partial c}{\partial x}$ independently of actual space dimension. In the following the mathematical and physical derivation respectively of the regarded convection-diffusion equation are described.

1.3 Convection-Diffusion Equation

The process of transport can be separated into two different parts. On the one hand there is an oriented transport process named convection. On the other hand there is a chaotic process, the diffusion. The diffusive transport is a consequence of many randomized individual motions. In fact the motion of every single molecule itself is randomized and minimal but taking into account all molecules, a uniform movement from regions with higher to regions with lower concentration occurs. This behavior is mathematically formalized in *Fick's First Law*:

$$J_d : \mathbb{R}^n \to \mathbb{R}^n \quad \text{with} \quad J_d(\mathbf{x}) = -D(\mathbf{x}) \cdot \nabla c(\mathbf{x}) \tag{1.10}$$

In 1855 the physiologist Adolf Fick first talked about his laws for transporting mass through a diffusive medium. Fick's First Law describes the relation between diffusive flux and concentration under a steady state assumption. It declares that the flux is proportional to the concentration gradient going from regions with high concentration to regions with low concentration. [LT05] In (1.10) J_d stands for the diffusion flux. It is a function of space x influenced by the diffusion coefficient D and the concentration c. In general the diffusion coefficient varies in space. In the following cases only constant diffusion coefficients are established. The negative sign in (1.10) entails diffusion in opposite direction to the gradient of concentration - from a region with high to a region with low concentration. According to the *Einstein-Smoluchowski-relation* the diffusion coefficient depends on the mobility μ of particles and the temperature T. The variable k_B terms the Boltzmann constant. This relation can also be formulated in a microscopic way where λ stands for the length a particle jumps during diffusion within time frame τ. Therefore $\frac{\lambda}{\tau}$ can be taken as mean velocity of the particle and λ as the mean travel path.

$$D = \mu \cdot k_B \cdot T = \frac{\lambda^2}{2\tau} \tag{1.11}$$

The oriented part of the transport, the convection, accrues due to a flux. The flux can be quantified by a velocity field **v** describing the flow in all directions. This velocity field can be a function of space but in the following study a constant velocity v is considered. Due to flux velocity the concentration c of a certain substance at point **x** will be transported to the place $\mathbf{x} + tv$ after time step t. Therefore the convective flux of mass $J_c : R^n \to R^n$ can be written as:

$$J_c(\mathbf{x}) = v \cdot c(\mathbf{x}). \tag{1.12}$$

In a closed system the *conservation law* claims that a particular measurable property does not change even if physical or chemical processes happen. In this case this law describes the relation between the time rate of change regarding the concentration of a certain quantity c and the change in space regarding the flux J.

$$\frac{\partial c}{\partial t} + \nabla \cdot J(\mathbf{x}) = 0 \tag{1.13}$$

The combination of diffusion and convection results in the sum of both flux equations (1.10) and (1.12). Replacing the flux J in equation (1.13) with $J = J_c + J_d$ leads to the diffusion equation.

$$\frac{\partial c}{\partial t} + \nabla \cdot J = 0 \Rightarrow \frac{\partial c}{\partial t} + \nabla \left(-D \cdot \nabla c + v \cdot c\right) = 0 \tag{1.14}$$

$$\Rightarrow \frac{\partial c}{\partial t} = \nabla \left(D \cdot \nabla c\right) - \nabla \left(v \cdot c\right) \tag{1.15}$$

For a constant diffusion coefficient and a constant velocity field the diffusion equation can be written as:

$$\frac{\partial c}{\partial t} = D \cdot \nabla^2 c - v \cdot \nabla \left(c\right). \tag{1.16}$$

Concerning the described problem in section 1.2 the convection-diffusion equation will be needed in two dimensions with a flux only in x-direction. In this work not only the two dimensional case but also the simplified problem in one dimension is a point of interest.

$$\frac{\partial c}{\partial t} = D\left(\frac{\partial^2 c}{\partial x^2} + \frac{\partial^2 c}{\partial y^2}\right) - v\frac{\partial c}{\partial x} \tag{1.17}$$

$$\frac{\partial c}{\partial t} = D\frac{\partial^2 c}{\partial x^2} - v\frac{\partial c}{\partial x} \tag{1.18}$$

1.4 Mathematics of Diffusion

In this section some common equation and theorems important for diffusion are summarized. Regarding characterizing convection-diffusion equations the French physicist Jean Claude Eugène Péclet introduced the *Péclet number*. It describes the interaction of convection and diffusion and is defined as the ratio of convection to diffusion of a certain quantity. For diffusion of particles the formula can be written as:

$$Pe = \frac{\text{convective transport rate}}{\text{diffusive transport rate}} \Rightarrow Pe_l = \frac{vl}{D} \tag{1.19}$$

The variables stand for the convection field v, the characteristic length l and the mass diffusion coefficient D. A high Péclet number results in a prevalent convective transport whereas a small number leads to dominant diffusive behavior. Another important equation regarding the flow description is an analogue to Fick's Law, *Darcy's Law*.

$$Q = -K \cdot A \cdot \frac{dh}{dl} \tag{1.20}$$

Equation (1.20) represents a special solution of the homogenous *Navier-Stokes equation*. It describes the flow of a fluid trough a porous medium and is derived form the constitutive equation. In other words, it is the proportional relation between the pressure decrease over a given distance and the flow rate through a perforated medium. K describes the hydraulic conductivity, Q is the rate of flow and A the cross section area. Therefore $\frac{dh}{dl}$ describes the hydraulic gradient with respect to length l.
Regarding stochastic differential equations the *Langevin equation* describes Brownian motion.

In particular the random movement of particles in a fluid is indicated. Thereby collisions with the molecules of the fluid are taken into account.

$$m\frac{d^2x}{dt^2} = -\lambda\frac{dx}{dt} + \eta(t) \tag{1.21}$$

The variables m, λ and η in (1.21) represent the mass of a particle, damping coefficient and the effect of collision of molecules in a fluid, respectively. The force $\eta(t)$ has a Gaussian probability distribution.

1.5 Partial Differential Equations

This section is based on lecture notes [JÖ8]. All the applications at the beginning use different implementations of diffusion. Regardless of whether the convection-diffusion, reaction-diffusion or pure diffusion equation is considered, the basic theory are partial differential equations. The difference between an ordinary and a partial differential equation is that the function's

derivatives with respect to only a part of the variables are used, also called partial derivatives. The diffusion equation (1.18) is a linear partial differential equation of second order which means that the maximal order of occurring partial derivatives is two and all the terms are linear. Therefore the solution of the diffusion equation has to be differentiable twice, in other words $u \in C^2(\Omega, \mathbb{R})$. In most cases the partial differential equations are not continuous and no such solutions $u \in C^2(\Omega, \mathbb{R})$ can be found. In these cases a generalized solution also called weak solution can be given. This method will be introduced later on.
Three different types of partial differential equations can be distinguished named elliptic, parabolic and hyperbolic. For defining the three classes a quasilinear second order partial differential equation is considered.

$$L(u) := \sum_{i,j=1}^{n} a_{ij} \frac{\partial^2 u}{\partial x_i \partial x_j} = f \tag{1.22}$$

Matrix $A = (a_{i,j})_{i,j \leq n}$ in (1.22) is symmetric and can depend on spatial coordinates x, the regarded quantity u and its gradient ∇u. In the following cases the Matrix A is constant. Its eigenvalues λ_i characterize the equation.

Definition 1.5.1.
- (1.22) is called *elliptic* if $\lambda_i > 0$ for all $i \in (1, 2, .., n)$.
- (1.22) is called *hyperbolic* if there is a j with $\lambda_j > 0$ and $\lambda_i < 0$ for all $i \neq j$ or vice versa.
- (1.22) is called *parabolic* if there is a j with $\lambda_j = 0$ and λ_i for all $i \neq j$ have the same algebraic sign.

Regarding the general formulation of the diffusion equation

$$u_t - \Delta u = f$$

the matrix A for the variables $(t, x_1, x_2, .., x_n)$ can be written as

$$A = \begin{pmatrix} 0 & 0 & 0 & \dots & 0 \\ 0 & -1 & 0 & \dots & 0 \\ 0 & 0 & -1 & & \vdots \\ \vdots & \vdots & & \ddots & 0 \\ 0 & \dots & 0 & 0 & -1 \end{pmatrix}.$$

Comparing the eigenvalues with the definition from above the equation of interest is classified as a parabolic differential equation.
Partial differential equations are usually defined on an open but bounded region Ω. The edge of

this region is denoted as $\partial\Omega$. In this context the *Gauss divergence theorem* is introduced.

Theorem 1.5.2.
Given is an open and bounded region Ω with $\partial\Omega \in C^1$ and v is the outward pointing unit normal field of the boundary $\partial\Omega$. Let u be $\in C^1\left(\overline{\Omega}, \mathbb{R}^n\right)$

$$\int_\Omega \text{div}F \; dx = \int_{\partial\Omega} F \cdot v \; ds \tag{1.23}$$

whereas the right hand side is a surface integral.

Hence, the partial integration can be derived using $\text{div}(Fu) = \nabla u \cdot F + u \, \text{div}F$:

$$\int_\Omega u \cdot \text{div}F \; dx = -\int_\Omega \nabla u \cdot F \; dx + \int_{\partial\Omega} u \, (F \cdot v) \, ds.$$

This theorem will be used for the weak solution of the convection-diffusion equation. In order to get a unique solution of a partial differential equation some conditions are necessary. On the one hand an initial condition is given, in this case the concentration at $c(x, 0) = c_0(x)$. One the other hand the interaction with the environment is defined by boundary conditions. One can differ between three different types of boundary conditions:

- *Dirichlet boundary condition*: $c = g_1$ on $\partial\Omega$
- *Neumann boundary condition*: $-\kappa\nabla \cdot v = h_1$ on $\partial\Omega$
- *Robin boundary condition*: $-\kappa\nabla \cdot v = \alpha c + h_2$ on $\partial\Omega$

The Dirichlet boundary condition gives values at the boundaries themselves but the Neumann and Robin conditions determine the flux of heat going through $\partial\Omega$. In the analyzed case studies the Dirichlet and Neumann boundary conditions will be used depending on the formulation of the problem.

Considering a non continuous right hand side f in (1.22) no classical two times differentiable solution can be found. The term solution is expanded by so-called weak solutions. In order to get such solutions a weak formulation of the regarded partial differential equation is necessary. To motivate this method the following partial differential equation with Dirichlet boundary conditions is considered.

$$-\Delta u + u = f \tag{1.24}$$

The equation is multiplied by a so-called test function $\varphi \in H := \{\varphi \in C^1(\Omega) : \varphi = 0 \text{ on } \partial\Omega\}$. Using the Gauss theorem for integration over Ω (1.24) results in the weak formulation.

$$\int_\Omega (\nabla u \nabla \varphi + uv) dx = \int_\Omega f\varphi \, dx$$

Now the solution u of this equation has to fulfill $u \in H$. Looking closely at this formulation it can be shown that the right hand side is a scalar product and the lhs is a continuous and linear functional. Therefore the Riesz representation theorem can be used to guarantee a unique solution of the weak formulation. But this theorem takes effect only if H is a Hilbert space. In order to characterize such spaces a new scalar product and norm on $C^\infty(\overline{\Omega})$ are introduced.

$$(u,v)_{H^k} = \sum_{|\alpha|\leq k} \int_\Omega D^\alpha u D^\alpha v dx \qquad |u|_{H^k(\Omega)} = \sqrt{(u,u)_H^k} \quad \text{with} \quad k \in N \tag{1.25}$$

The closure of $C^\infty(\overline{\Omega})$ and of $C_0^\infty(\overline{\Omega})$, respectively regarding the norm in (1.25) is called Sobolev space. For the first closure a different characterization can be given.

$$H^k = \overline{C^\infty(\overline{\Omega})} = \{u \in L^2(\Omega) : D^\alpha u \in L^2(\Omega) \text{ for all } |\alpha| \leq k\}$$
$$H_0^k = \overline{C_0^\infty(\overline{\Omega})}$$

In order to get the weak formulation and its solution the Sobolev space plays an important role. In the section concerning finite element method the Sobolev space will be used.

CHAPTER 2

Convective Diffusion in one Dimension

In the following the convection-diffusion equation in one dimension is considered. The one dimensional problem deals with two different initial conditions. On the one hand the source releases pollution only at the beginning $t = 0$. On the other hand the initial condition describes a constantly releasing source of pollution which is actually only used in 2.1.2.

$$\frac{\partial c}{\partial t} = D\frac{\partial^2 c}{\partial x^2} - v\frac{\partial c}{\partial x} \tag{2.1}$$

This chapter covers everything from the derivation of an analytical solution to the point of different mathematical respectively numerical methods to solve equation (2.1). In the first section an analytical solution of the convection-diffusion equation on both an infinite and a semi-finite domain is discussed. In the second section numerical solutions of the equation are shown. Two methods are used, the finite difference method and the finite element method. Different random walk approaches are the focus of the third section. These approaches are connected to stochastic perspectives of equation (2.1).

2.1 Analytical Solution

In this section the analytical solutions for the Smoluchowski equation under different conditions are described. First of all the solution of diffusion on an infinite domain is observed.

2.1.1 Infinite Domain

The infinite solution is based on [SK00]. In this case an infinite domain is considered. That means that $x \in (-\infty, \infty)$ and the Dirichlet boundary condition is used. The initial condition

describes an instantaneous release of pollution. The according equation system can be written as follows.

$$\frac{\partial c}{\partial t} = D\frac{\partial^2 c}{\partial x^2} - v\frac{\partial c}{\partial x} \qquad \text{with} \qquad \begin{aligned} c(x,t) &= \delta(x) \\ \lim_{x\to\pm\infty} c(x,t) &= 0. \end{aligned} \tag{2.2}$$

In order to solve (2.2) two variables are introduced.

$$\tau = Dt, \qquad b = \frac{v}{D}.$$

With these new variables the convection-diffusion equation can be written as

$$D \cdot \frac{\partial c(x,\tau)}{\partial \tau} = D \cdot \frac{\partial^2 c(x,\tau)}{\partial x^2} - Db \cdot \frac{\partial c(x,\tau)}{\partial x} \tag{2.3}$$

$$\Leftrightarrow \frac{\partial c(x,\tau)}{\partial \tau} = \frac{\partial^2 c(x,\tau)}{\partial x^2} - b\frac{\partial c(x,\tau)}{\partial x}. \tag{2.4}$$

Time-dependent coordinates are set as

$$y = x - b\tau, \qquad y_0 = b\tau_0.$$

Inserting the spatial variables into (2.4) gives

$$\frac{\partial c(y,\tau)}{\partial \tau} - b\frac{\partial c(y,\tau)}{\partial y} = \frac{\partial^2 c(y,\tau)}{\partial y^2} - b\frac{\partial c(y,\tau)}{\partial y} \tag{2.5}$$

$$\Leftrightarrow \frac{\partial c(y,\tau)}{\partial \tau} = \frac{\partial^2 c(y,\tau)}{\partial y^2}. \tag{2.6}$$

This simplified equation can be solved with the Laplace-Transformation method. The equation (2.6) will be multiplied by $e^{-p\tau}$ and integrated over τ. The partial differential equation transforms into an ordinary differential equation.

$$\overline{c}(y,\tau) = \frac{1}{p}\frac{\partial^2 \overline{c}(y,\tau)}{\partial y^2}, \tag{2.7}$$

whereas the Laplace transform of $c(y,\tau)$ is given as

$$\overline{c}(y,\tau) = \int_0^\infty \mathrm{e}^{-pt}\, c(y,\tau) d\tau.$$

Equation (2.7) can be solved with the approach e^{-Ay}. Regarding the boundary conditions one receives

$$\overline{c}(y,\tau) = \mathrm{e}^{-\sqrt{p}y} \tag{2.8}$$

After an inverse Laplace-Transformation of (2.8) and the substitution to the origin parameters a solution for the initial problem (2.2) can be given.

$$c(x,t) = \frac{1}{\sqrt{4\pi Dt}}\,\mathrm{e}^{-\frac{(x-vt)^2}{4Dt}} \tag{2.9}$$

In the chapter 1.3 the equation was separated into an oriented transport and a randomized one. In the following figure this idea is taken up again. The left picture shows the effect based on the convective transport. Over certain time steps the Gaussian curve is moving to the right due to the velocity field of the flux. In the right picture the diffusion part is outlined. The time steps are the same as in the convection graphic and show the shrinking amplitude of the Gaussian curve.

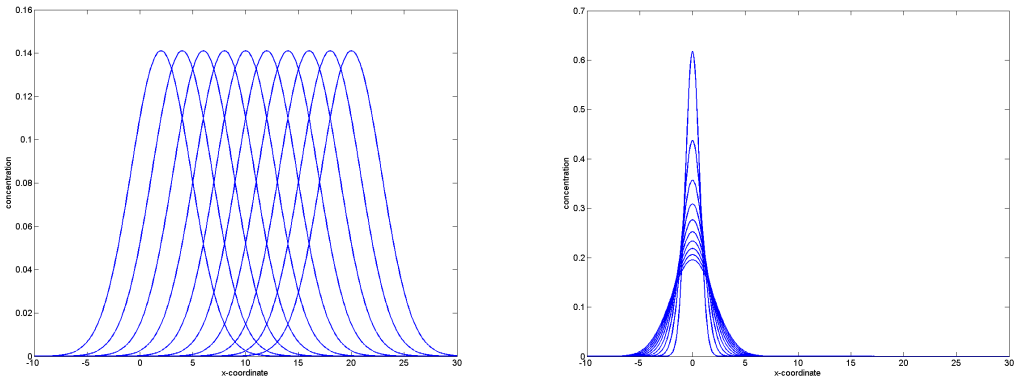

Figure 2.1: left: convection part of (2.9), right: diffusion part of (2.9)

The basis equations for creating the graphics in figure 2.1 are adaptions of the solution (2.9). To receive the convection without any diffusive movement the parameter t in the pre-exponential factor $\frac{1}{\sqrt{4\pi Dt}}$ has to be considered constant. The time t in the exponential function itself takes on different values to visualize the development of this solution. Regarding the diffusive movement the modification of the equation is easy to understand. The term $v \cdot t$ containing the velocity field of the flow is eliminated. Figure 2.1 shows the modified solutions for different time steps $t = 100, 200,..,1000$. The flux velocity v and the diffusion coefficient D are set arbitrary to the value $0.02[m/s]$.

Figure 2.2 shows (2.9) for the same time steps as in 2.1. The flux velocity v and diffusion coefficient c are also equally chosen. Due to the diffusion the peak decreases over time. The influence of the convection part is clearly visible. There is an initial peak set at $t = 0$ in $x = 0$. For $t > 0$ no further pollution is injected in the system. Therefore the positive velocity of the fluid transports the diffusing pollution to the right.

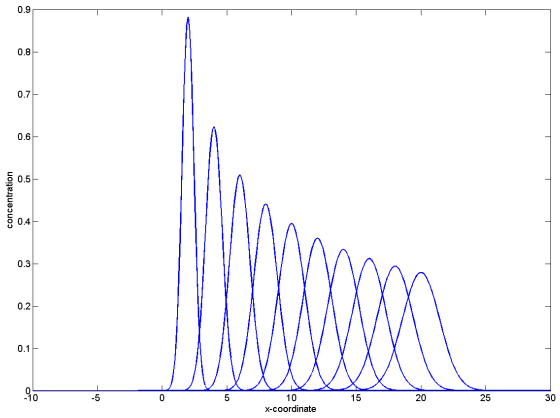

Figure 2.2: The convected diffusion of the pollution injected by the source is shown.

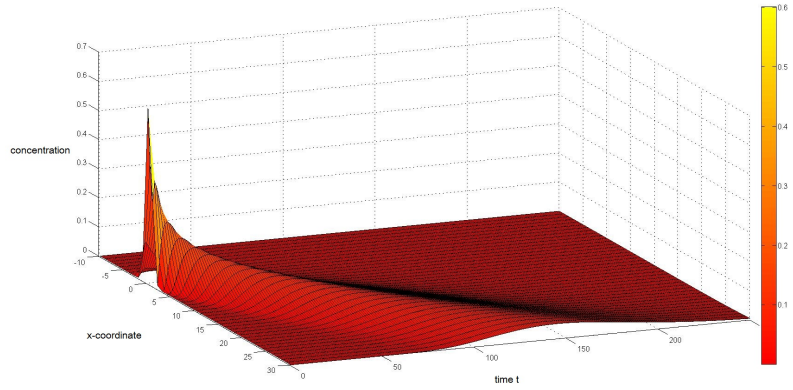

[a]

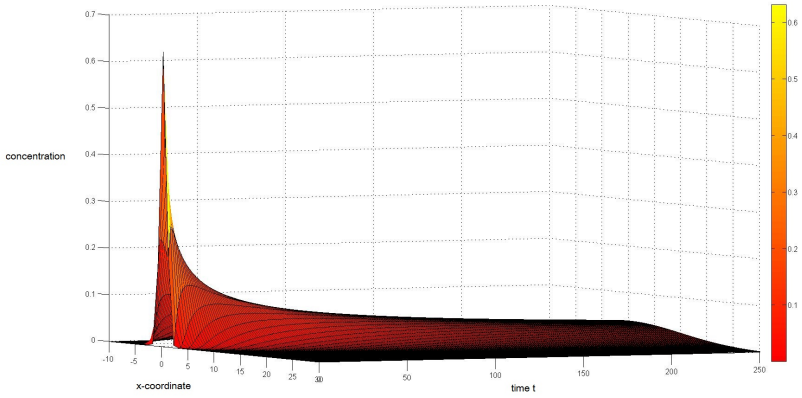

[b]

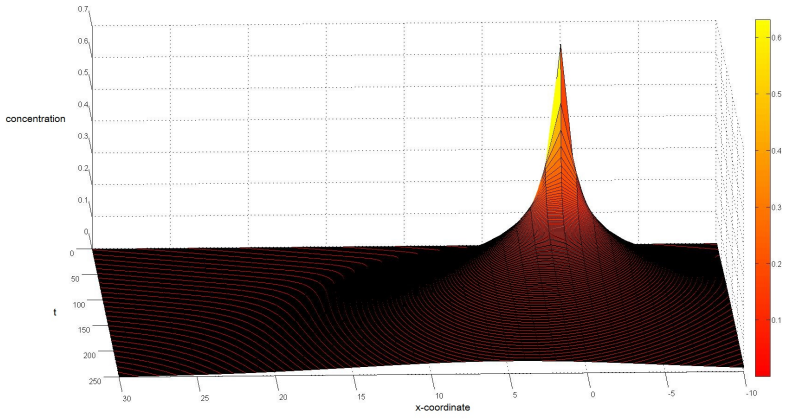

[c]

Figure 2.3: One dimensional analytical solutions using differnet velocities.

Figure 2.3 shows three plots of the analytical solution over time. In figure [a] the parameter setting is velocity $v = 0.2$ and diffusion coefficient $D = 0.2$. Compared to the setting of the two dimensional figures before these two variables are increased by 10 times. The simulation sketches the progress of the pollution concentration over $t_{end} = 250s$. One can see that all pollution leaves the region of interest in the time span $t \in (100, 200)$. As a consequence the velocity is defined as $v = 0.02$ for plot [b]. This graphic shows the process from the time axis point of view. No pollution leaves the area but its dissemination on the regarded region is becoming more homogenous. In other words the maximum of the bell curve decreases under a value of $c < 0.06$. Figure [c] shows the progress from x-direction in inverse chronology. In the back the peak of the initial condition is visible. In the front, in other words the concentration curve at $t = 250s$ is nearly equal to the x-axis. The different plots show the different aspects of the convection-diffusion equation. Plot [a] focuses on the influence of convection whereas [b] and [c] show the diffusive movement from different viewing angles.

2.1.2 Semi-finite Domain

Based on [OB61] the analytical solution of convection-diffusion on a semi-finite domain is derivated. The concentration in the medium is zero at $t = 0$ except at the source at $x = 0$. There the initial concentration c_0 is set. The mathematical formulation of the problem is given.

$$\frac{\partial c}{\partial t} = D\frac{\partial^2 c}{\partial x^2} + v\frac{\partial c}{\partial x} \qquad \text{with} \qquad \begin{aligned} &c(0,t) = c_0, t \geq 0 \\ &c(x,0) = 0, x \geq 0 \\ &\lim_{x\to\infty} c(x,t) = 0, t \geq 0 \end{aligned} \tag{2.10}$$

If the substitution $c(x,t) = \Gamma(x,t)\exp\left(\frac{ux}{2D} - \frac{u^2 t}{4D}\right) = \Gamma(x,t)f(x,t)$ is introduced the derivatives change to the following.

$$\frac{\partial c(x,t)}{\partial t} = \frac{\partial \Gamma(x,t)}{\partial t} f(x,t) - \Gamma(x,t)\frac{u^2}{4D} f(x,t)$$
$$\frac{\partial c(x,t)}{\partial x} = \frac{\partial \Gamma(x,t)}{\partial x} f(x,t) + \Gamma(x,t)\frac{u}{2D} f(x,t)$$
$$\frac{\partial^2 c(x,t)}{\partial x^2} = \frac{\partial^2 \Gamma(x,t)}{\partial x^2} f(x,t) + \frac{u}{D}\frac{\partial \Gamma(x,t)}{\partial x} f(x,t) + \Gamma(x,t)\frac{u^2}{4D^2} f(x,t)$$

These changed derivatives inserted in the equation (2.10) give a new differential equation with modified boundary conditions.

$$\frac{\partial \Gamma(x,t)}{\partial t} = D\frac{\partial^2 \Gamma(x,t)}{\partial x^2} \qquad \text{with} \qquad \begin{aligned} &\Gamma(0,t) = c_0 \exp\frac{u^2 t}{4D}, t \geq 0 \\ &\Gamma(x,0) = 0, x \geq 0 \\ &\lim_{x\to\infty} \Gamma(x,t) = 0, t \geq 0 \end{aligned}$$

The Dunhamel's theorem says that the solution of the initial value problem can be used to find the solution for the inhomogeneous problem whereas $\phi(\lambda)$ symbols the solution of the modified initial value problem. The solution of the problem with time-independent boundary conditions can be formulated as an integral of the solution of a time-independent problem. Using the Duhamel's theorem the following boundary conditions are considered. [CJ70]

$$\frac{\partial \Gamma(x,t)}{\partial t} = D\frac{\partial^2 \Gamma(x,t)}{\partial x^2} \qquad \text{with} \qquad \begin{aligned} &\Gamma(0,t) = 1, t \geq 0 \\ &\Gamma(x,0) = 0, x \geq 0 \\ &\Gamma(\infty,t) = 0, t \geq 0 \end{aligned} \tag{2.11}$$

$$\Gamma(x,t) = \int_0^t \phi(\lambda)\frac{\partial}{\partial t} F(x, t-\lambda) d\lambda \tag{2.12}$$

In (2.12) F stands for the solution of the adapted problem corresponding to Duhamel's theorem. Similar to the analytical solution for an infinite domain the Laplace-Transformation is used.

$$\overline{\Gamma}(x,p) = \int_0^\infty \Gamma(x,t)\, \mathrm{e}^{-pt}\, dt$$

Every term of equation (2.12) multiplied by e^{-pt} and then integrated transforms the equation into an ordinary differential equation.

$$\overline{\Gamma}(x,t) = \frac{p}{D}\frac{\partial^2 \overline{\Gamma}(x,t)}{\partial x^2} \tag{2.13}$$

A general solution of this equation (2.13) can be given.

$$\overline{\Gamma}(x,t) = Ae^{-\sqrt{\frac{p}{D}}x} + Be^{\sqrt{\frac{p}{D}}x} \qquad \text{with} \qquad \begin{aligned} &\overline{\Gamma}(0,t) = \frac{1}{p}, t \geq 0 \\ &\overline{\Gamma}(x,0) = 0, x \geq 0 \\ &\overline{\Gamma}(\infty,t) = 0, t \geq 0 \end{aligned}$$

Due to the boundary condition $\overline{\Gamma}(x,t) = 0$ if $x \to \infty$ the constant B has to be zero. Regarding the initial condition $\overline{\Gamma}(0,t) = \frac{1}{p}$ the constant A is given as $A = \frac{1}{p}$. Therefore a solution for (2.13) is obtained.

$$\overline{\Gamma}(x,t) = \frac{1}{D}\,\mathrm{e}^{-\sqrt{\frac{p}{D}}x}$$

To receive the solution $\Gamma(x,t)$ the inverse Laplace-Transformation is applied. Due to the table of Laplace-Transformations [Cra75] the solution can be written as

$$\Gamma(x,t) = 1 - \operatorname{erf}\left(\frac{x}{2\sqrt{Dt}}\right) = \frac{2}{\pi}\int_{\frac{x}{2\sqrt{Dt}}}^{\infty} \mathrm{e}^{-\eta^2}\,d\eta$$

Hence, the solution of the adapted probelm (2.12) is

$$\Gamma(x,t) = \int_0^t \phi(\tau)\frac{\partial}{\partial t}\left[\frac{2}{\pi}\int_{\frac{x}{2\sqrt{D(t-\tau)}}}^{\infty} \mathrm{e}^{-\eta^2}\,d\eta\right]d\tau. \tag{2.14}$$

The function $\mathrm{e}^{-\eta^2}$ is continuous therefore it is possible to differentiate within the integral. Hence, (2.14) results in

$$\Gamma(x,t) = \frac{x}{\pi\sqrt{D}}\int_0^t \phi(\tau)\,\mathrm{e}^{\frac{-x^2}{4D(t-\tau)}}\,\frac{d\tau}{(t-\tau)^{\frac{3}{2}}}. \tag{2.15}$$

Defining a new parameter

$$\lambda = \frac{x}{2\sqrt{D(t-\tau)}}$$

and considering that $\phi(t) = C_0\,\mathrm{e}^{\frac{u^2 t}{4D}}$ is the certain solution mentioned in Duhamel's theorem the equation (2.15) can be written as

$$\Gamma(x,t) = C_0 \frac{2}{\sqrt{\pi}} e^{\frac{u^2 t}{4D}} \int_{\frac{x}{2\sqrt{Dt}}}^{\infty} \mathrm{e}^{\frac{-x^2 u^2}{16 D^2 \lambda^2}}\, d\lambda \tag{2.16}$$

$$= C_0 \frac{2}{\sqrt{\pi}} \mathrm{e}^{\frac{u^2 t}{4D}} \left[\int_0^{\infty} \mathrm{e}^{\frac{-\epsilon^2}{\lambda^2} - \lambda^2}\, d\lambda - \int_0^{\alpha} \mathrm{e}^{\frac{-\epsilon^2}{\lambda^2} - \lambda^2}\, d\lambda \right] \tag{2.17}$$

$$\text{with} \qquad \alpha = \frac{x}{2\sqrt{Dt}} \quad \text{and} \quad \epsilon = \frac{xu}{4D} \tag{2.18}$$

Dividing the solution in (2.18) into two separate integrals I_1 and I_2 the following results can be assumed [PF56], [OB61].

$$\begin{aligned} I_1 &= \int_0^{\infty} \mathrm{e}^{\frac{-\epsilon^2}{\lambda^2}}\, d\lambda = \frac{\sqrt{\pi}}{2} \mathrm{e}^{-2\epsilon} \\ I_2 &= \int_0^{\alpha} \mathrm{e}^{\frac{-\epsilon^2}{\lambda^2} - \lambda^2}\, d\lambda = \frac{\sqrt{\pi}}{4} \left[\mathrm{e}^{-2\epsilon} \left(1 + \operatorname{erf}\left(\alpha - \frac{\epsilon}{\alpha} \right) \right) - \mathrm{e}^{2\epsilon} \left(\operatorname{erfc}\left(\alpha + \frac{\epsilon}{\alpha} \right) \right) \right] \\ I_1 - I_2 &= \frac{\sqrt{\pi}}{4} \left[\mathrm{e}^{-2\epsilon} \operatorname{erfc}\left(\alpha - \frac{\epsilon}{\alpha} \right) + \mathrm{e}^{2\epsilon} \operatorname{erfc}\left(\alpha + \frac{\epsilon}{\alpha} \right) \right] \end{aligned} \tag{2.19}$$

$$\Rightarrow \Gamma(x,t) = \frac{C_0}{2} \mathrm{e}^{\frac{u^2 t}{4D}} \left[\mathrm{e}^{-2\epsilon} \operatorname{erfc}\left(\alpha - \frac{\epsilon}{\alpha} \right) + \mathrm{e}^{2\epsilon} \operatorname{erfc}\left(\alpha + \frac{\epsilon}{\alpha} \right) \right].$$

With (2.19), the inverse substitution of the parameter defined in (2.18) and remembering $c(x,t) = \Gamma(x,t) \exp\left(\frac{ux}{2D} - \frac{u^2 t}{4D} \right)$ the finial solution is

$$C(x,t) = \frac{C_0}{2} \left[\operatorname{erfc}\left(\frac{x - ut}{2\sqrt{Dt}} \right) + e^{\frac{ux}{D}} \operatorname{erfc}\left(\frac{x + ut}{2\sqrt{Dt}} \right) \right]. \tag{2.20}$$

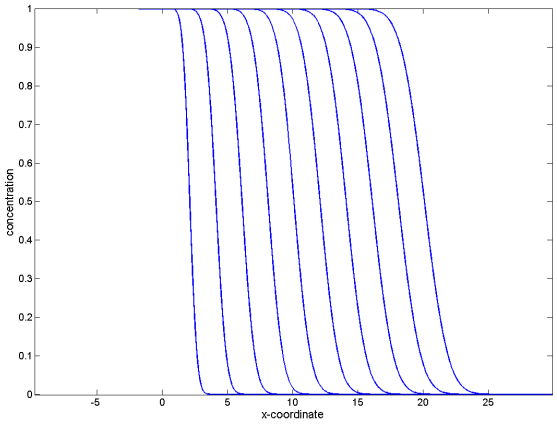

[a]

Figure 2.4: Plot of (2.20) showing the concentration

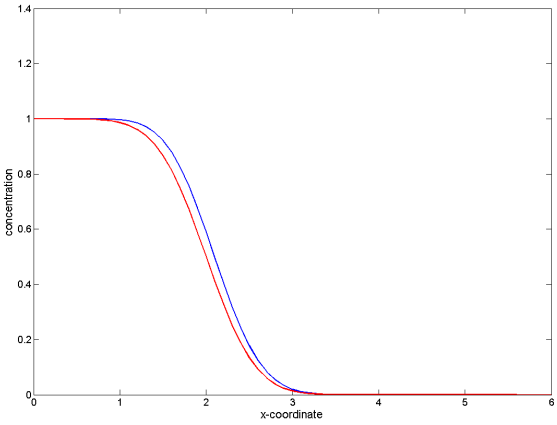

[b]

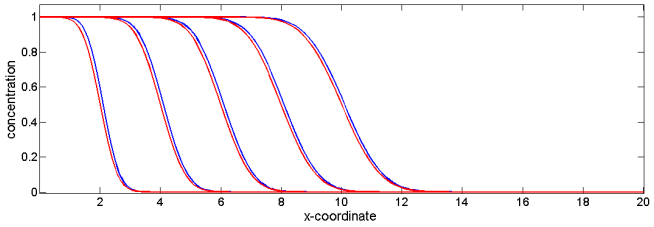

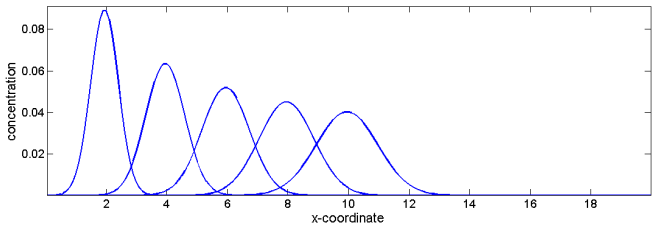

[c]

Figure 2.5: the modification of (2.20) is shown.

In 2.4 and 2.5 the solution of the semi-definite problem and its modification for different time steps is shown. Despite the first five time steps are the same as in figure 2.2 $t = 100$, 200,..,500 the output is different. Velocity v and diffusion coefficient D are also set to the same values, respectively. Due to the fact that the boundary condition differs in the infinite domain and semi-finite domain problem the concentration curves look different. The initial condition is set to $c(0,t) = C_0 = 1, \quad t \geq 0$. Compared to the analytical solutions on infinite domain the source is constantly injecting pollution. The left boundary changes from $x = -\infty$ to $x = 0$. The part left of $x = 0$ can be imagined as a pollution filled area with a blockade at $x = 0$. In other words at $t = 0$ the concentration would look like a mirrored Heaviside function. When diffusion starts the blockade disappears and the pollution spreads into the considered area, the positive x-direction. This behavior also explains that the curve has nearly the same slope at any time. The shape would change if another diffusion coefficient would be used but again not over time.

In the semi-finite case a certain point in time exists where the whole area is filled uniformly with pollution equal to the initial pollution.
In figure 2.4 the red curve represents a modification of the original solution. For this curve the right term in equation (2.20) is neglected. For observation of diffusion in the region of flow the second term can be ignored without major effects. [OB61] In fact the exponential function in this term can be written as $\exp\left(\frac{x \cdot v}{D}\right)$ which leads to the following condition $x(1-v) < 35.5$. If this condition is not fulfilled this term reaches values near ∞ due to the accuracy of MATLAB. In other words the viewable range of solution depends on the flux velocity. Neglecting the second term the concentration at every x-value can be given. As shown in figure 2.4 the uncertainty of the modification is minimal. The maximal error is lower than 10^{-1} and decreases exponentially which shows that at least one of the regarded functions changes minimally over time.

2.2 Numerical Solution

Numerical solutions are very important in cases of mathematical problems which cannot be solved analytically. Especially problems dealing with partial differential equations require numerical methods. There are many numerical approaches regarding ordinary differential equations. Different solver are defined to satisfy all the various needs of the varying mathematical challenges regarding ordinary differential equations. When it comes to partial differential equation there are two mainly used methods. One of them is the finite difference method (FDM) which was invented first. This method is based on using grid points to approximate the solution. In this approximations the derivative of the differential equation is approached by taking the difference quotient of the neighboring grid points. The method is easy to use but slightly weak concerning the accuracy. The second method is called finite element method (FEM) and is based on formulating variations of the differential equation. FEM determines approximated solutions consisting of piecewise defined polynomials on a fine resolution of the domain. The advantage of FEM is the suitability for any geometry. The method is particularly used for elliptic and parabolic partial differential equations.

2.2.1 Finite Difference Method

The finite difference method is a simple technique used for approximating derivations of functions. A function $c(x)$ in an one dimensional domain is considered. Three equidistant different x-values and their function values $c(x)$ are given. The distance between the x-values is written as dx.

The first derivative of the function at point x_i can be calculated in three different ways.

$$
\begin{aligned}
c'(x_i) &= \frac{c_{i+1} - c_{i-1}}{2dx} && \text{central} \\
c'(x_i) &= \frac{c_{i+1} - c_i}{dx} && \text{forward} && dx = x_{i+1} - x_i \\
c'(x_i) &= \frac{c_i - c_{i-1}}{dx} && \text{backward}
\end{aligned}
$$

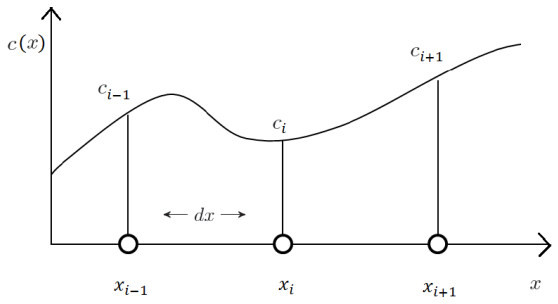

Figure 2.6: Schematic graphic for finite differences.

For the gradient of the concentration according to convection backward differences are used because the flux transports the concentration from left to right. Regarding the convection-diffusion equation also the second derivative is necessary. For this derivative the central finite difference method will be used. The repeated usage of this method on the first derivative gives the approximation of the second.

$$c''(x_i) = \frac{c_{i+1} - 2c_i + c_{i-1}}{dx^2}$$

These two approximations for both the first and the second derivative can now be inserted in convection-diffusion equation (2.1). The partial differential equation ends up in an ordinary differential equation with only the time derivative left.

$$\frac{dc}{dt} = D \cdot \frac{c_{i+1} - 2c_i + c_{i-1}}{x^2} - v \cdot \frac{c_i - c_{i-1}}{dx} \tag{2.21}$$

Therefore the simulation of this approximation can be done with different numerical approaches for ordinary differential equations, e.g. Euler method, Runge-Kutta etc. The first application uses the explicit Euler method. The algorithm starts at a certain point t in time. The value of c at the next time step $t + \Delta t$ is then calculated by

$$c(t + \Delta t) = c(t) + \Delta t \cdot \dot{c}(t). \tag{2.22}$$

To implement the regarded partial differential equation an initial condition is necessary. In the following figures the initial concentration is zero everywhere except the origin. At $x = 0$ the initial concentration is set to c_0. The implementation is ensured in MATLAB.

In figure 2.7 the results of the explicit Euler method are shown. For the numerical methods it is not possible to choose a certain point in time for calculation. In fact the simulation always starts at $t = 0$ and iterates the concentration for every time step until t_{end} is reached. In both figures the simulation time is $t_{end} = 10000$. The ten different lines show the progress after $t = 100, 200, \cdots, 1000$. To visualize the effect of convection two different velocity values

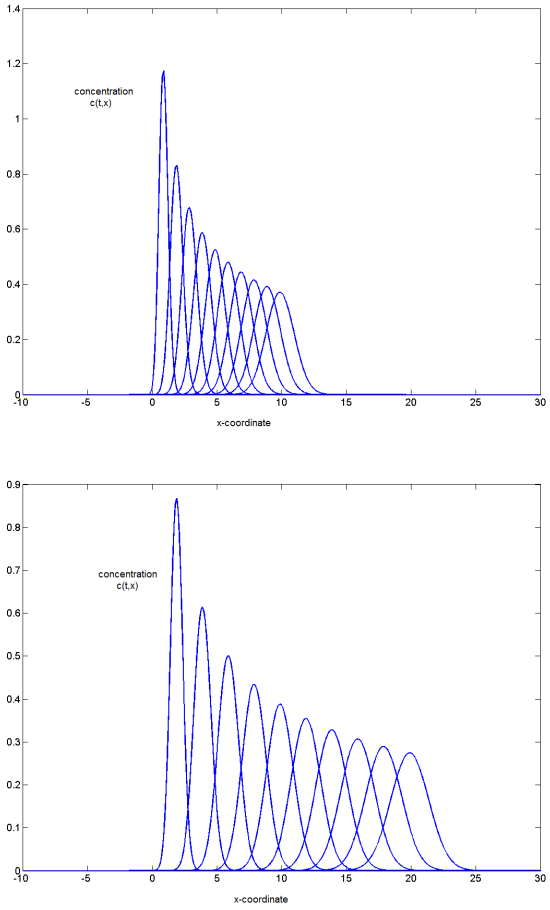

Figure 2.7: Simulation of convection-diffusion using the Explicit Euler.

$v_1 = 0.01$ and $v_2 = 0.02$ are chosen. Due to the increasing velocity $v_1 \cdot 2 = v_2$ one can see that the peak of the last line moves from $x = 10$ to $x = 20$.

The second application uses the implicit Euler method. It is well known that the implicit Euler offers a stability which is not given in the explicit algorithm. To realize the implicit Euler the notation of the finite difference scheme has to be modified. Therefore equation 2.21 is transformed into a matrix vector product.

$$\underbrace{\frac{dc}{dt}}_{\frac{c^{k+1}-c^k}{\Delta t}} = \underbrace{\begin{pmatrix} -\frac{D}{h^2}+\frac{v}{h} & \frac{2D}{h^2}-\frac{v}{h} & 0 & \dots & 0 \\ \frac{D}{h^2}+\frac{v}{h} & \frac{2D}{h^2}-\frac{v}{h} & \frac{D}{h^2} & \dots & 0 \\ 0 & \dots & & & \vdots \\ \vdots & \vdots & \frac{D}{h^2}+\frac{v}{h} & \frac{2D}{h^2}-\frac{v}{h} & \frac{D}{h^2} \\ 0 & \dots & 0 & -\frac{D}{h^2}+\frac{v}{h} & \frac{D}{h^2}-\frac{v}{h} \end{pmatrix}}_{=:S} \cdot \underbrace{\begin{pmatrix} c_1 \\ c_2 \\ c_3 \\ \vdots \\ c_n \end{pmatrix}}_{=:c^k} \tag{2.23}$$

In order to receive the iteration c^{k+1} for the next time step equation 2.23 is rearranged.

$$c^{k+1} = (\Delta t S + I)c^k \tag{2.24}$$

I stands for the identity matrix. Instead of implementing the finite difference method using a for-loop as described in (2.22) the expression 2.24 enables matrix calculations.

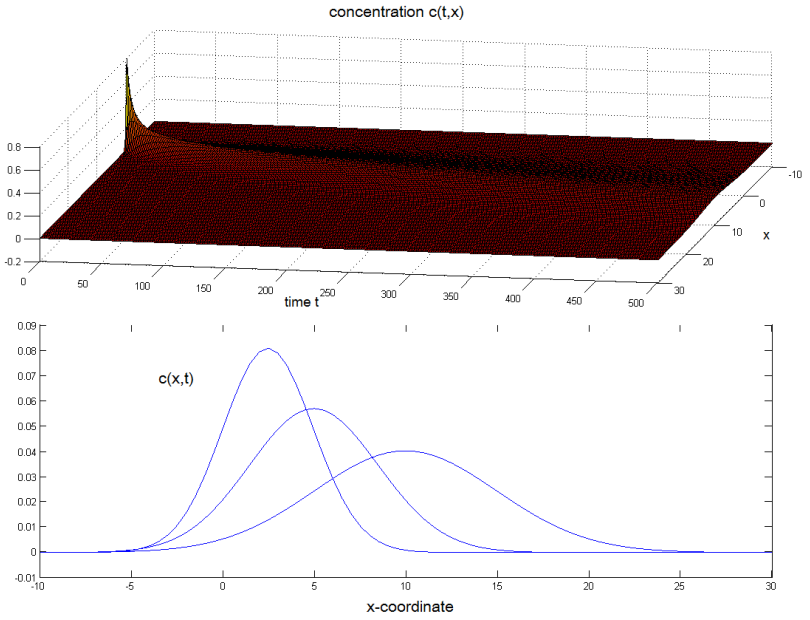

Figure 2.8: Convection diffusion simulation using explicit Euler.

In figures 2.8 velocity and diffusion coefficient are set $v = D = 0.02$. The running time is $t_{end} = 500s$. In figure 2.8 the spatial step size is $\Delta x = \frac{1}{2}$. The upper plot shows the development of concentration over time. The lower graphic presents three concentration lines in a distance of time $t = \frac{t_{end}}{3}$.

In figure 2.9 the step size changes to $\Delta x = \frac{1}{5}$. The other parameters are the same as in figure 2.8. Due to the bad condition of matrix S the explicit Euler algorithm is unstable and causes

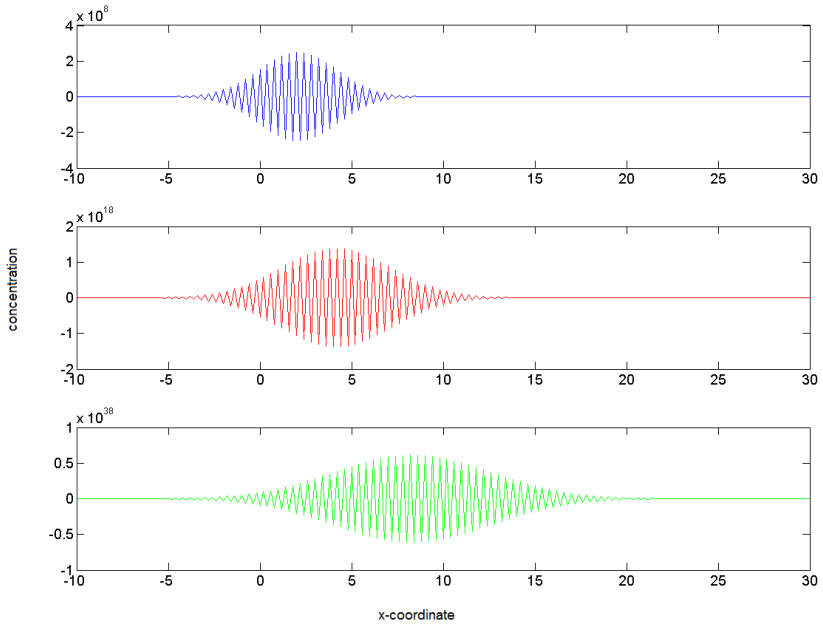

Figure 2.9: Oscillating explicit Euler method for small Δx.

oscillations. For both plots 2.8 and 2.9 the used time step is $\Delta t = 1$. It is well known the the implicit Euler is stable for every choice of Δx and Δt.The new matrix notation (2.23) helps to formulate the implicit Euler algorithm of the finite difference method.

$$c^{k+1} = (I - \Delta t S)^{-1} c^k \tag{2.25}$$

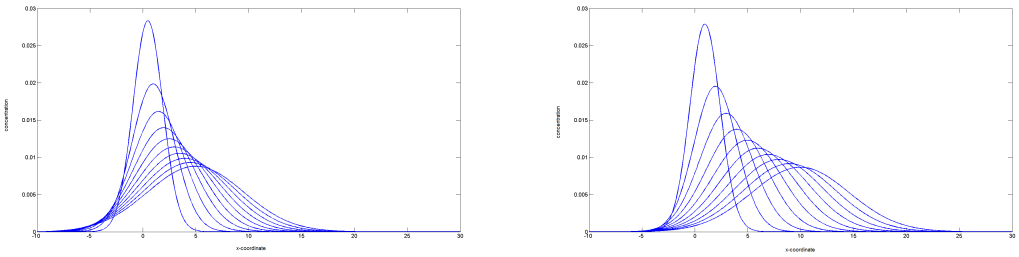

Figure 2.10: Simulation of convection-diffusion using the Implicit Euler.

The implementation of the implicit Euler algorithm in figure 2.10 is stable for all possible choices of step size Δx as shown later on. In this case it is set $\Delta x = \frac{1}{1}0$. In the graphics the used parameter setting is $D = 0.02$, $\Delta t = 1$ and $t_{end} = 500s$. These figures outline the influence of

increasing velocity values, $v_1 = 0.01$ left and $v_2 = 0.02$ right. Regarding stability and efficiency reference is made to chapter 3.

2.2.2 Finite Element Method

The finite element method (FEM) was invented from engineers in the 1960s. Nowadays it is one of the most important numerical methods regarding partial differential equations, in particular for elliptic and parabolic equations. The method is based on the formulation of a variation of the boundary value problem and approximates the solution with piecewise polynomial functions. In contrast to the finite difference method it is much easier to match the FEM to the considered geometry. To use this method some mathematical definitions and methods are summarized. First of all the considered problem and its condition is presented. The condition in (2.26) is again the Dirichlet boundary condition as mentioned in 1.5.

$$\begin{aligned} \frac{\partial c}{\partial t} - D\frac{\partial^2 c}{\partial x^2} + v\frac{\partial c}{\partial x} = 0 \qquad & \text{in} \quad \Omega \\ c = 0 \qquad & \text{on} \quad \partial\Omega \end{aligned} \tag{2.26}$$

Weak Formulation. This formulation was introduced by pure mathematicians to proof the existence and uniqueness of a solution. Several numerical schemes, also FEM, are based on this weak formulation. The Sobolev space H_0^1 as mentioned in 1.5 will be used. By picking a so called test function $\phi \in H_0^1$, multiplying (2.26) with it and integrating all terms over the domain Ω results in

$$\int_\Omega \frac{\partial c}{\partial t}\phi d\Omega - \int_\Omega \left(D\frac{\partial^2 c}{\partial x^2} + v\frac{\partial c}{\partial x} \right) \phi d\Omega = 0. \tag{2.27}$$

In order to get rid of the second derivative in (2.27) the Gauß divergence theorem 1.5 for integrating by parts is used. The resulting equation is the weak formulation of (2.26).

$$\begin{aligned} \int_\Omega \frac{\partial c}{\partial t}\phi d\Omega + \int_\Omega D\nabla c\nabla\phi d\Omega - \underbrace{\int_{\partial\Omega} D\nabla c \cdot n\phi ds}_{=0,\ \phi\in H_0^1} + \int_\Omega v\nabla c\phi d\Omega = 0 \\ \Rightarrow \int_\Omega \frac{\partial c}{\partial t}\phi d\Omega + \int_\Omega \left(D\nabla c\nabla\phi + v\nabla c\phi\right) d\Omega = 0 \end{aligned} \tag{2.28}$$

Galerkin Method. The finite element method uses (2.28) instead of (2.26) for discretization. The Galerkin method names the approximation of the solution using linear combination of base functions. In the following these base functions are named $\varphi_j \in H_0^1$. The Galerkin approximation of the solution can be written as

$$c^n(x) = \sum_{j=1}^{n} c_j\varphi_j(x) + c_0(x) \tag{2.29}$$

whereas c_j are unknown and have to be determined. The basis functions have to be linearly independent. Formulated as conditions for one dimensional problems $\varphi_j(x)$ and $c_0(x)$ have to fulfill the following equations.

$$\begin{aligned} &c_0(x) = 0 \qquad \text{on} \quad \partial\Omega \\ &\varphi_j(x_i) = \delta_{ji} \quad \text{and} \quad \varphi_j(x) \quad \text{linear} \\ &\varphi_j(x) = 0 \qquad \text{on} \quad \partial\Omega \end{aligned} \tag{2.30}$$

These conditions lead to linear base functions used in a one-dimensional domain. Depending on the wanted behavior the solution should have, base functions of other structure are possible also.

$$\varphi_i(x) = \tfrac{x_{i+1}-x}{h_i} \qquad \varphi_{i+1}(x) = \tfrac{x-x_i}{h_i}$$

$$h_i = x_{i+1} - x_i$$

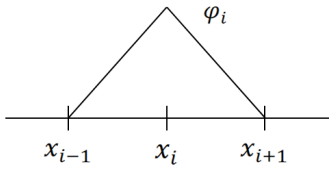

Figure 2.11: Definition of the hat-functions

In the linear case they are usually called 'hat-functions' and are defined in equations 2.11. It is also possible to use quadratic functions instead of linear ones.

$$\phi(x) = \varphi_i(x) \tag{2.31}$$

In order to determine all c_j the test function ϕ is set as a function in space spanned by these base functions (2.31). Using substitution (2.31) for test function ϕ in (2.28) a linear system of n equations with n unknowns, called the Galerkin formulation, results. [Seg12]

$$\sum_{j=1}^{n_e} \frac{\partial c_j}{\partial t} \int_{\Omega^{e_k}} \varphi_j \, \varphi_i d\Omega + \sum_{j=1}^{n_e} c_j \int_{\Omega^{e_k}} \left(D\nabla\varphi_j\nabla\varphi_i + \nabla\varphi_j\varphi_i\right) d\Omega = 0 \tag{2.32}$$

In equation (2.32) n_e is the number of elements in the regarded finite element and Ω^{e_k} is the domain of element e_k. (2.32) can be written in a short form as follows.

$$\begin{aligned} &\dot{c} \cdot M + c \cdot S = 0 \qquad \text{with} \\ &m_{ij} = \int_{\Omega^{e_k}} \varphi_i \, \varphi_j d\Omega \\ &s_{ij} = \int_{\Omega^{e_k}} \left(D\nabla\varphi_i\nabla\varphi_j + \nabla\varphi_i\varphi_j\right) d\Omega \end{aligned} \tag{2.33}$$

The matrices of (2.33) are called mass matrix M and stiffness matrix S. Considering the typical elements shown in figure 2.11 it is clear, that only a few of the possible integrals are unequal to zero. Those basis function which correspond to the corner points of the element will lead to non trivial results. Looking at all non-zero elements of the matrices M and S, a certain profile appears. Because the element i is connected to $i-1$ and $i+1$ the profile is a band matrix with width three. The partial matrices of the mass and stiffness matrix of one single element can be written down in particular. Considering an equidistant grid with distance h the integrals in (2.33) can be calculated.

$$\begin{aligned} M_p &= \begin{pmatrix} m_{jj} & m_{jj+1} \\ m_{j+1j} & m_{j+1j+1} \end{pmatrix} = \begin{pmatrix} \frac{h}{3} & \frac{h}{6} \\ \frac{h}{6} & \frac{h}{3} \end{pmatrix} \\ S_p &= \begin{pmatrix} s_{jj} & s_{jj+1} \\ s_{j+1j} & s_{j+1j+1} \end{pmatrix} = \begin{pmatrix} \frac{D}{h} - \frac{v}{2} & -\frac{D}{h} + \frac{v}{2} \\ -\frac{D}{h} - \frac{v}{2} & \frac{D}{h} + \frac{v}{2} \end{pmatrix} \end{aligned} \tag{2.34}$$

(2.34) presents a system of ordinary differential equations. In order to solve this system well known methods for ordinary differential equation can be used. First of all the time derivative will be replaced by a forward difference discretization:

$$\dot{c} = \frac{c^{k+1} - c^k}{\Delta t} \tag{2.35}$$

where c^k is the concentration at the present time and c^{k+1} the concentration one time step ahead. In all numerical methods a decision regarding explicit or implicit methods has to be made. Explicit methods only use the results of the present time-step to calculate the next. In implicit methods an algebraic equation appears due to the fact of using the future time-step in the calculation part of the equation. The θ-method will be used to present implicit and explicit methods for solving (2.34) [Seg12].

$$\theta\text{-method}: \quad M\frac{c^{k+1} - c^k}{\Delta t} + \theta S c^{k+1} + (1-\theta) S c^k = 0 \qquad , 0 \leq \theta \leq 1 \tag{2.36}$$

The most common values for θ are:

- $\theta = 0$, Explicit Euler
- $\theta = 1$, Implicit Euler
- $\theta = \frac{1}{2}$, Implicit Heun

First the Explicit Euler will be implemented. Setting $\theta = 0$ in 2.36 gives

$$\begin{aligned} M\frac{c^{k+1} - c^k}{\Delta t} + S c^k &= 0 \\ \Rightarrow M c^{k+1} &= (M - \Delta t S) c^k \end{aligned} \tag{2.37}$$

Hence, the coefficients c^{k+1} of the next time step have to be calculated by multiplying with the inverse matrix M^{-1}. Comparing notation (2.37) with FDM formulation (2.25) matrix M has to be set I to gain equivalence. In MATLAB Matrix inverting can be realized by using the 'backslash' operator. It would also be possible to use the Thomas-algorithm which is especially configured to invert band matrices efficiently. The iteration of c^{k+1} is repeated until t_{end} is reached. Then the approximated solution can be determined with (2.29). Due to the fact that linear base functions are used and only two of these functions are non zero on every element equation (2.34) results in the calculated functions c_j.

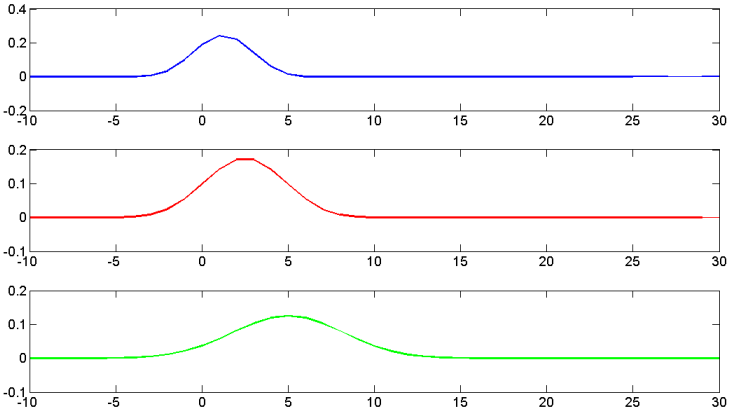

a)

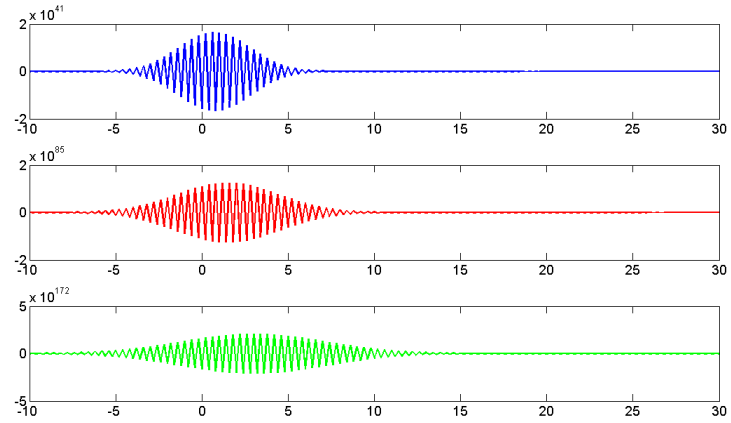

b)

Figure 2.12: The results of FEM using Explicit Euler are shown.

In figure 2.12 the parameter setting for the Explicit Euler is as follows: velocity $v = 0.02$, diffusion coefficient $D = 0.02$ and simulation time $t_{end} = 250s$. In fact both figures are created with the same variable values except one parameter. The reason for the different appearance is the choice of the grid size. In figure a) the element size is $\Delta x = 1$ and in b) $\Delta x = \frac{1}{5}$. Although the scales of the figures changes the diffusive movement is very obvious. Even if it is not a great

shift to the right the convection is also working.
It is well-known that the Explicit Euler method often causes oscillations in results. The smaller the elements the more oscillations appear if step size Δt is not readjusted. To avoid such behavior an implicit method is used, in this case the implicit Euler and Heun method respectively. Therefore θ is set to 1 and $\frac{1}{2}$ in (2.36). $\theta = 1$ results in the following equation.

$$(M + \Delta t S)c^{k+1} = M\ c^k \tag{2.38}$$

As in the explicit case the backslash operator is used to solve this equation numerically.

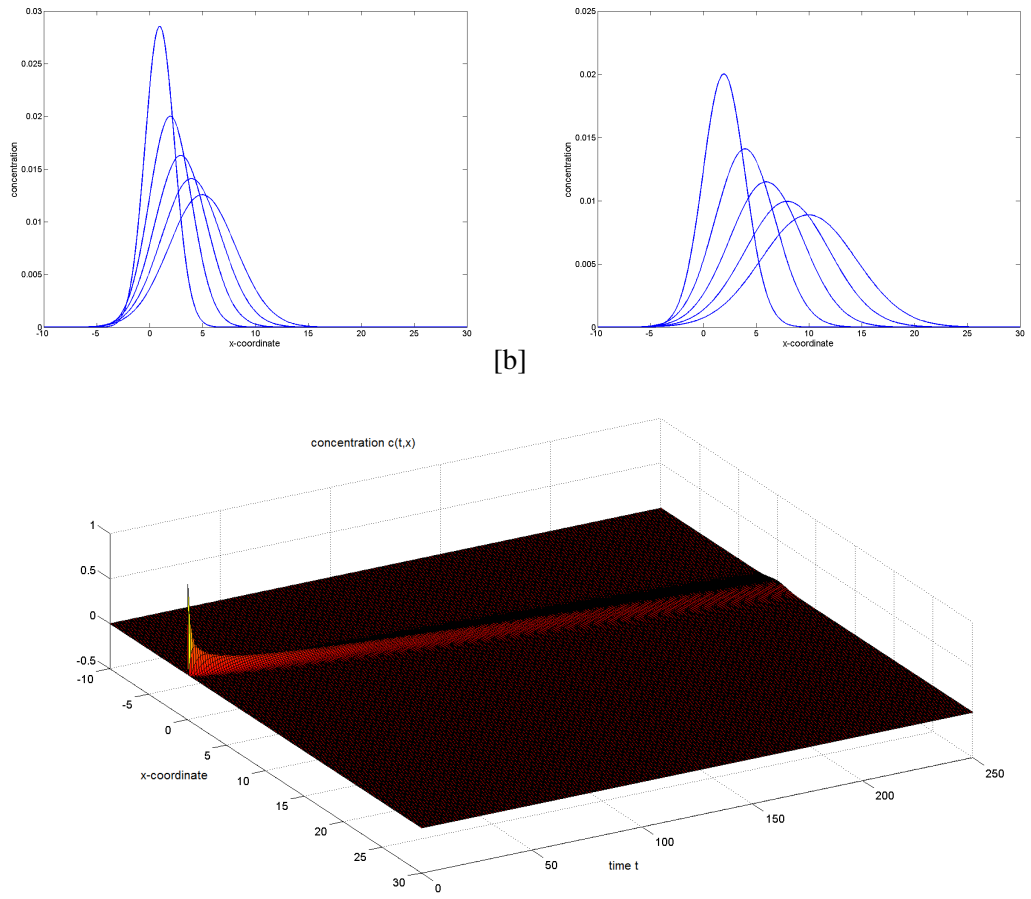

[a] [b] [c]

Figure 2.13: The implicit Euler method is shown.

In figure 2.13 the element size is set $\Delta x = \frac{1}{1}0$ without causing any oscillations. The other parameters including velocity and diffusion are equal to figure 2.12. In graphics [a] and [b] the end time differs, [a] shows $250s$ and [b] $500s$. The five lines show the concentration after every

fifth of t_{end}. In figure 2.13 [c] the progress over time is shown. The convection of the concentration is identifiable. The concentration beam processes not parallel to the time axis but slight diagonal. The influence of the diffusion coefficient is obvious especially in the fist $100s$.

As mentioned before also the implicit Heun algorithm can be used to simulate convective diffusion. Plugging $\theta = \frac{1}{2}$ in (2.36) the necessary equation can be written as

$$c^{k+1} = (M + \frac{\Delta t}{2}S)^{-1}(M - \frac{\Delta t}{2}S)c^k \tag{2.39}$$

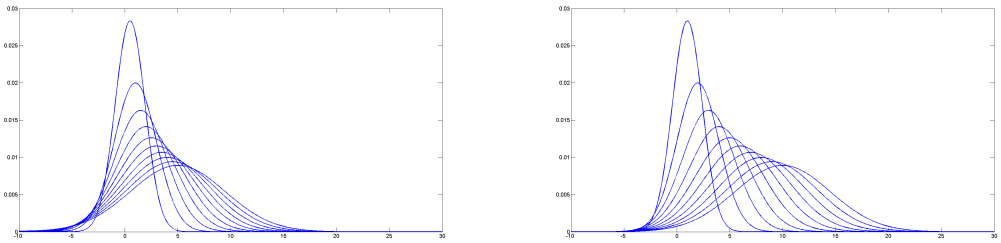

Figure 2.14: The results using the Implicit Heun method are shown.

The implicit Heun method used in figure 2.14 shows the same stability as the implicit Euler. The simulation time $t_{end} = 500s$ is the same for both illustrations. The only difference can be found in the doubled velocity in the right simulation. Due to this increase the coordinate of the fifth peak is also doubled. The different properties of all used methods are discussed in chapter 3.

2.3 Random Walk

Conventional numerical methods need a very high grid resolution and in addition a small time step to generate useable results. This leads to long execution times even with the available computer performance nowadays. This problem also occurs regarding the simulation of diffusion.
All the numerical methods describe the convection-diffusion in a macroscopic way. An alternative for simulating transport is the use of random walk. This approach is contrary to the numerical solutions before. The focus changes to the microscopic behavior of diffusion by analyzing single particles. The term 'random walk' was first introduced by Karl Pearson in 1905. Probability theory is an important basis of random walk. Regarding this theory transition probabilities are focused on. To define a transition it is necessary to put a grid on the regarded domain. In the two-dimensional problem in chapter 4 random walk approaches using a grid will be introduced in detail.
The next two solutions are implemented without using any grid. The velocity field is chosen to be constant. As in the analytical and numerical simulations it is independent from the particle's position.

2.3.1 Intuitive Approach

The intuitive approach describes a model which uses no grid or collision rules. At the beginning $t = 0$ all the particles are placed in the origin presenting a source of pollution. The pollution injection happens only at $t = 0$. The simulation focuses on the convection and diffusion behavior of these initial particles. The domain is one dimensional which, in parricular the whole x-axis. The plotted area is an interval $[-10, 30]$ for x as used before. In this simulation the movement of particles is described through:

$$\begin{aligned} p_{new} &= p_{old} + r + v \cdot dt \\ r &= X \cdot \Delta x \end{aligned} \tag{2.40}$$

The particle motion in (2.40) consists of three parts. In order to get the new position p_{new} at $t + dt$ these three components are added. p_{old} stands for the position at time t. Seconds are used as time unit. The velocity field v is given in $[m/s]$ therefore it has to be multiplied by the step size. The variable r describes the diffusive movement of a particle for one time step and is added to the old particle position p_{old}. The second equation in (2.40) defines the movement r in particular. It consists of the step size in space Δx and a normally distributed random variable X with mean zero and unit variance. In every time step the new position of every particle is calculated with equation (2.40). The simulation ends when the chosen simulation time t_{end} is reached.

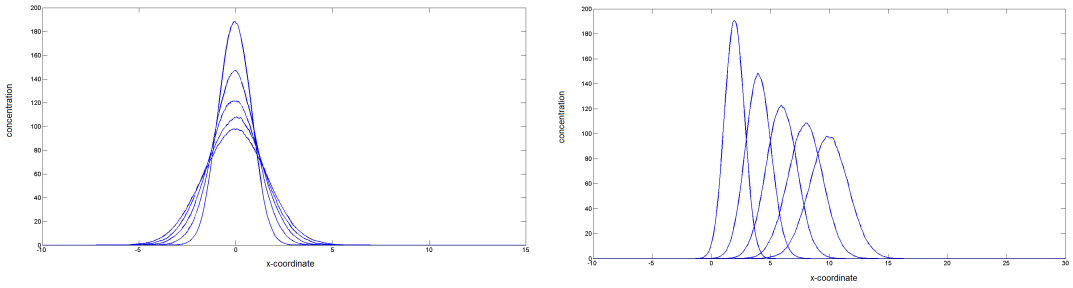

Figure 2.15: Intuitive random walk approach of diffusion

In the left figure in 2.15 the velocity v is neglected to illustrate only the diffusive behavior of the intuitive random walk approach. The right graphic shows the progress of the convection-diffusion equation. In these simulation runs the number of particles is set to $N = 8000$. The other parameters are $\Delta t = \frac{1}{2}$, $\Delta x = \frac{1}{1}5$ left and $\Delta x = \frac{1}{1}0$ right. In order to visualize the development of diffusion over time the duration of simulation is set to $t_{end} = 500s$. Every fifth the concentration curve is plotted.

For the purpose of comparability the parameters used to create figure 2.16 are analog to the figures of analytical and numerical solutions. The influence of the convective part of equation (2.40) is obvious. Only the parameter t_{end} differs in figure 2.16. In the left plot it is $250s$ left and $500s$ in the right. The shift to the right can be risen by using a greater velocity. It influences

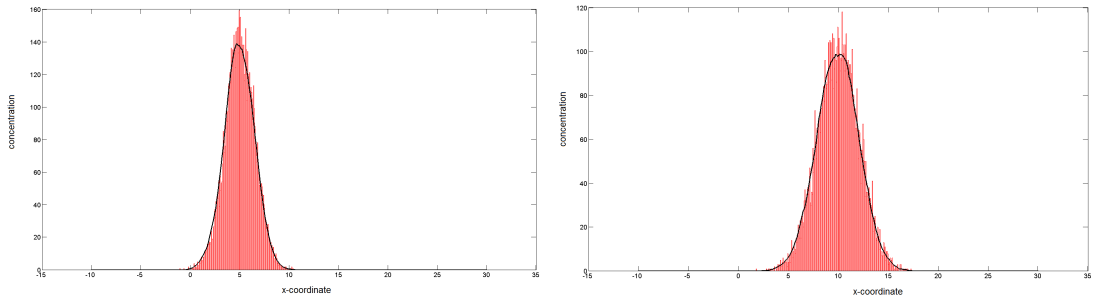

Figure 2.16: Intuitive random walk approach of convection-diffusion

the movement directly, whereas diffusion itself is affected by the value of Δx. The diffusive movement depends on the normally distributed random variable X.

In all figures of the intuitive approach the distribution of the particles are plotted using the histogram function of MATLAB as shown in red. This histogram can be influenced by the choice of step size Δx. The smaller the step size the smoother the curve. The black fitting curve approximates the related bell curve. This curve averages the particle number of each bar using the neighboring particle numbers. This approximation will be used to compare the concentration results with the analytical solution. Due to the minimized randomization of the walking direction compared to two-dimensional random walk, positive or negative x-direction vs. $\alpha = 360\,^\circ$, the intuitive approach for one dimension produces not such regular results regarding diffusion. Whereas the convection can be shown very well by setting v arbitraryly.

2.3.2 Gaussian-based Approach

The second approach is based on an equation whose principle is similar to the intuitive equation but the choice of the coefficient is different. This random walk implementation is connected to the analytical solution of the convection-diffusion equation with the following initial and boundary conditions.

$$\begin{aligned} &\frac{\partial c}{\partial t} = D\frac{\partial^2 c}{\partial x^2} - v\frac{\partial c}{\partial x} \\ &\lim_{x\to+\infty} c(x,t) = 0 \qquad \lim_{x\to-\infty} c(x,t) = 0 \\ &c(x,0) = \delta(x) \end{aligned} \tag{2.41}$$

As already deduced in 2.1.1 the solution of (2.41) is given as

$$c(x,t) = \frac{1}{\sqrt{4\pi D t}} e^{-\frac{(x-vt)^2}{4Dt}}. \tag{2.42}$$

Considering the probability density function of a normal or Gaussian distribution

$$f(x) = \frac{1}{\sqrt{2\pi\sigma^2}} e^{-\frac{(x-\mu)^2}{2\sigma^2}} \tag{2.43}$$

the formal equivalence to (2.42) is obvious. The parameters used in 2.43 stand for the mean value μ and the standard deviation σ which characterize the position and the width of the Gaussian bell curve in a unique way. Therefore the according parameters in (2.42) can be read out. [SFGGH06]

$$\begin{aligned} \mu &= v \cdot t \\ \sigma^2 &= 2 \cdot Dt \end{aligned} \tag{2.44}$$

Due to the properties and meaning of these parameters (2.44) the height and width of the concentration peak dependent on time is given. The corresponding particle movement using (2.44) can now be formulated.

$$p_{new} = p_{old} + v\Delta t + \sqrt{2 \cdot D\Delta t} X \tag{2.45}$$

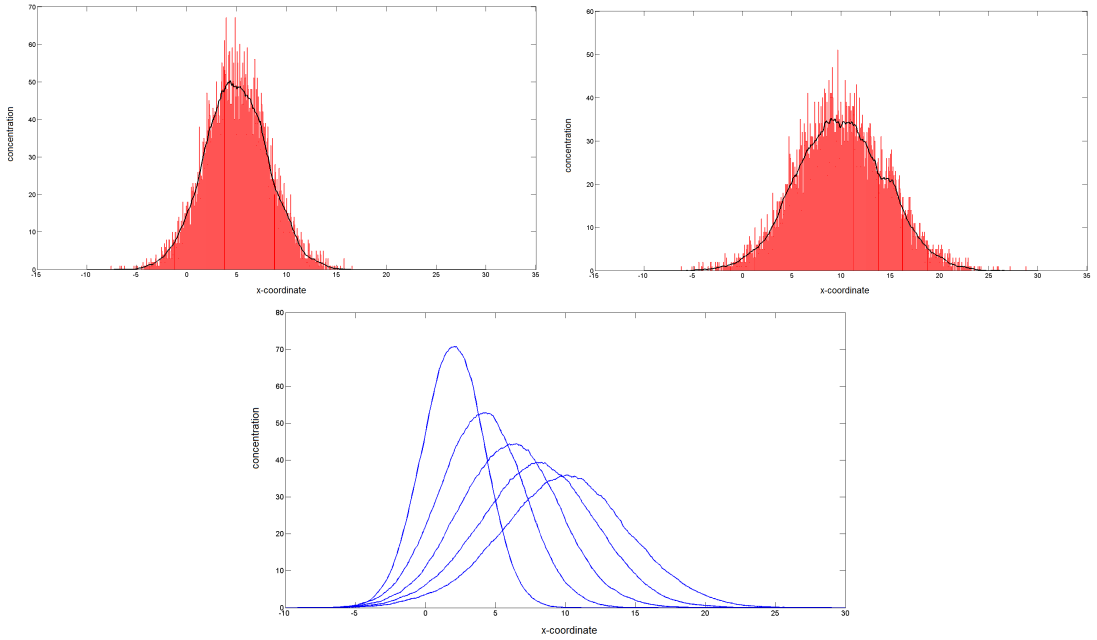

Figure 2.17: Gaussian based random walk for convection-diffusion

Again X symbolizes a normally distributed random number with the same mean and variance as before. X is newly generated in every step for each particle. Identifiable by the velocity

v the second term stands for the convective motion. This term is equal to the term of the intuitive approach. The radical term gives the diffusive motion and is based on the standard derivation.

In figure 2.17 three different results of the implementation are shown. The parameters are similar to the intuitive approach to enable comparability. Therefore the setting is velocity $v = 0.02$, diffusion coefficient $D = 0.02$, number of particles $N = 8000$ and $\Delta t = 0.5$. There is one difference regarding the spatial step size but this parameter is only used for preparing the graphical outputs. Hence, the only change is the precision of the plot. The various durations of simulation in the upper plots are again $250s$ and $500s$. The simulation time in the right plot is twice as long as the left one and therefore the center of the concentration moves twice as far. The increase of width shows the effects of diffusion. The linear relation of velocity and time are detectable. In the third figure the progress in time is shown.

CHAPTER 3

One-dimensional Results

In this chapter the different solutions of the one dimensional convection-diffusion equation are compared. All the approaches have different advantages and disadvantages but the analysis focuses on the certainty and efficiency of the various solutions. Two different error values are inspected. On the one hand the maximal concentration difference of all x-values at the end of simulation is observed. Mathematical speaken the uniform norm $\|.\|_\infty$ is calculated. The second value of interest is the difference of the integral values, the norm $\|.\|_1$. Both results are evaluated for different spatial step sizes Δx and time steps Δt.
In addition a study on the different calculation times is conducted. Comparing the various methods and their performance times is the second focus of this chapter.

3.1 Analytical vs. Numerical

The different numerical implementations and the analytical solution are compared. The numerical solutions are iterative procedures therefore it is not possible to calculate the error at a certain point in time. The simulation always starts at $t = 0$ and iterates every time step until t_{end} is reached.

3.1.1 Finite Difference Method

First of all the results of the finite difference method are considered. In the following all different algorithm are discussed.

In figure 3.1 there are two different plots. The left plot shows the analytical solution colored in blue and the numerical solution using the finite difference method in red. In this comparison the algorithm using the for-loop for iteration is used. The difference in the concentration values is obvious. In fact this difference has a reasoned explanation. In the analytical solution the initial condition of the according partial differential equation is a Dirac-function. In other words this function is equal to ∞ at $t = 0$. Such a value can not be implemented in the numerical solution. The initial value in the numerical implementation at $t = 0$ is $c_0 = 1$ and zero everywhere else.

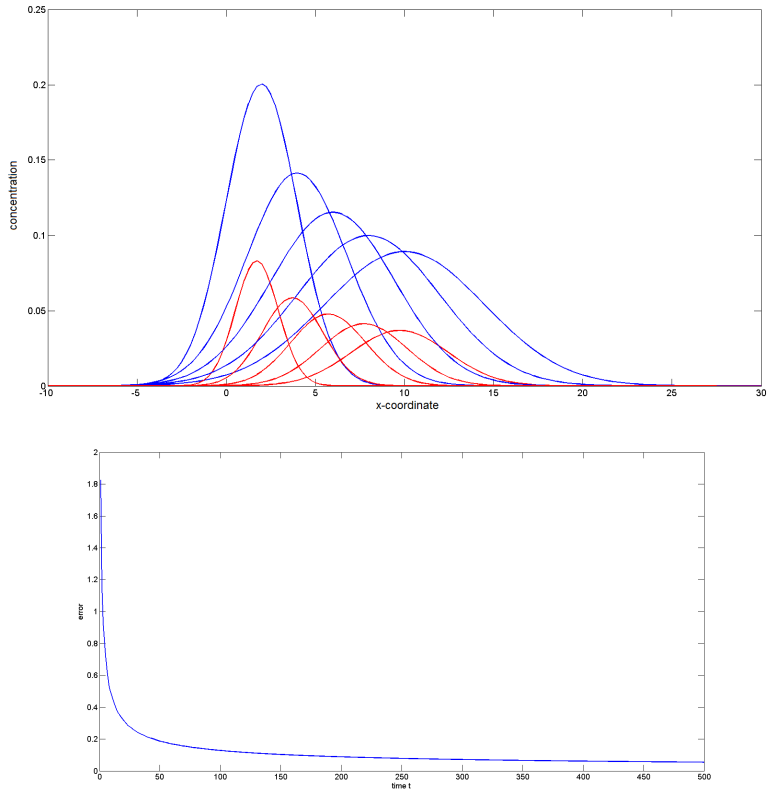

Figure 3.1: Comparing analytical solution and FDM using Explicit Euler.

In the right picture the error value of the numerical solution over time is shown. At every point in time the maximal variation is given. The regarded time interval is $[0, 500]$. Starting with an error value $err < 1.9$ it decreases after $t_{end} = 500s$ to $err < 0.1$. In order to decrease the error the initial condition of the numerical method can be adjusted. One property of the Direac-function is that it has a unit surface area. Due to the fact that the numerical method uses a spatial discretization Δx the value at $x = 0$ has to lead to a unit surface area. The numerical approximation of the acreage uses a linear connection line to the adjoining discretization points. A triangle occurs. Therefore the initial concentration at $x = 0$ has to be $c_0 = \frac{1}{\Delta x}$. Using this values the error concerning the analytical solution decreases.

Figure 3.2 verifies the modified initial condition for the finite difference method. The error decreases from $err < 1.9$ in the beginning and $err < 0.1$ in the end to $err < 0.7$ and $err < 0.01$. In addition to the modified initial condition the Explicit Euler using matrix calculation is used. The based equation and principle are the same but the implementation facilitates. As already shown in chapter 2 the Explicit Euler algorithm has to fulfill a certain condition to produce stable results. Using matrix calculation instead of for-loops the stability condition restricts the choice of parameter even more as shown in a tabular later on.

The ultra stable Implicit Euler algorithm is used to produce figure 3.3. All these figures com-

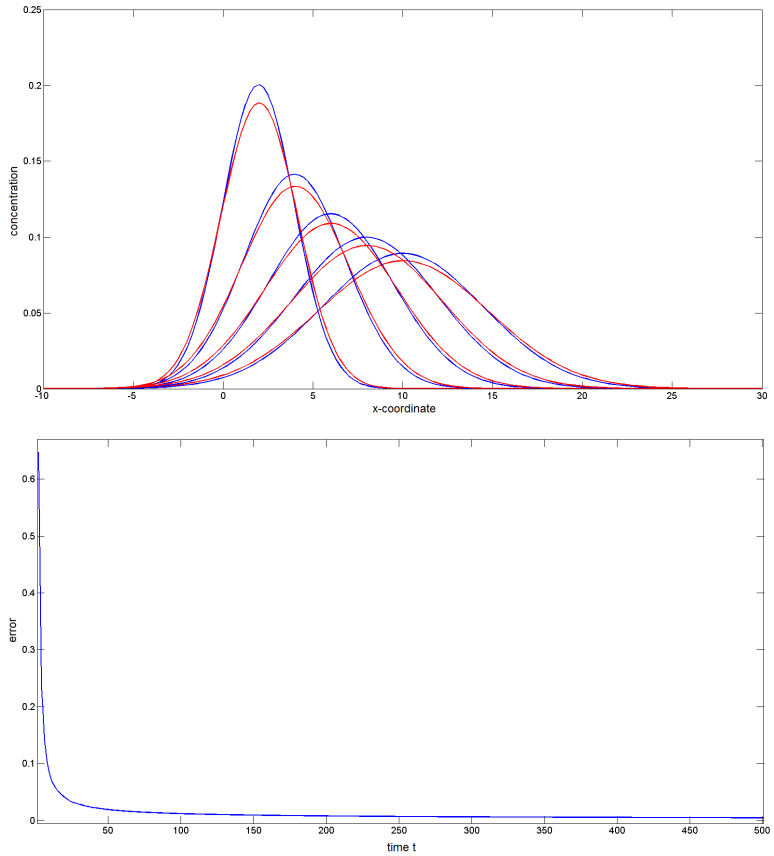

Figure 3.2: Comparing analytical solution and FDM with adapted initial conditions.

paring analytical solution and FDM use the same parameter setting: simulation time $t = 500$, diffusion coefficient $D = 0.02$, velocity $v = 0.02$ and $\Delta t = 1$. The spatial step size is chosen $\Delta x = \frac{1}{4}$ to assure stability of the Explicit Euler. Compared to the error of the Explicit Euler above the right plot shows the new error range $err \in [0.005, 0.2]$.

Δt	Δx	Explicit Euler	Explicit Euler*	Implicit Euler*
1	$\frac{1}{2}$	0.12183	0.01254	0.025233
1	$\frac{1}{4}$	0.23165	0.04048	0.07208
$\frac{1}{2}$	$\frac{1}{2}$	0.23465	0.03641	0.06059
$\frac{1}{2}$	$\frac{1}{4}$	0.46153	0.10132	0.16312
$\frac{1}{4}$	$\frac{1}{4}$	0.91544	0.29568	0.41167

Table 3.1: Simulation times for FDM using Explicit and Implicit Euler are shown.

Table 3.1 shows the different calculation times for various parameter. The values for the Ex-

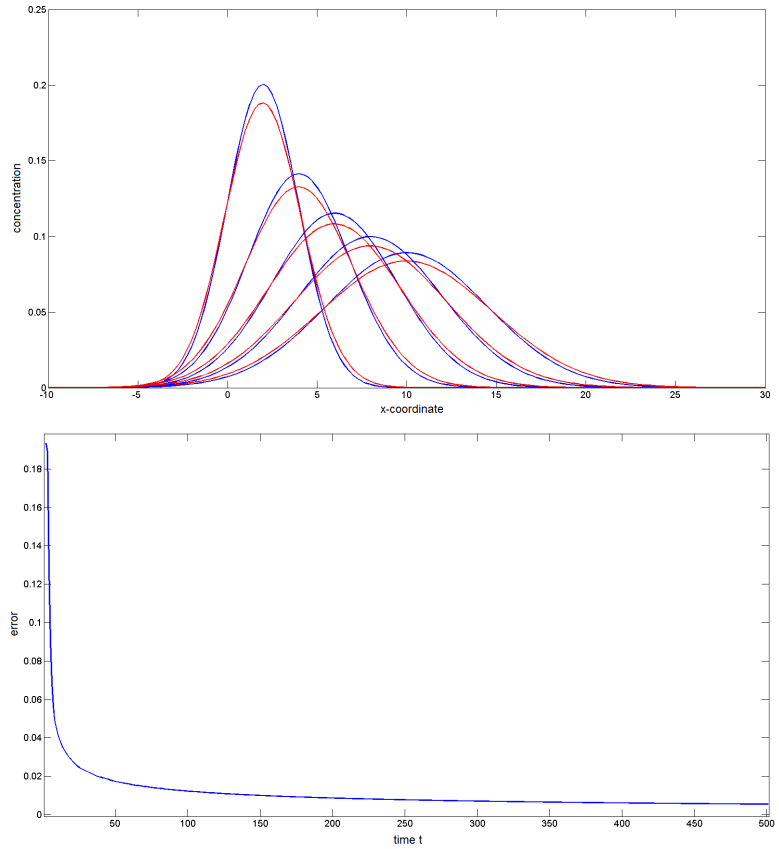

Figure 3.3: Comparison of the analytical solution and FDM using matrix notation.

plicit Euler approximation using loops for implementation show the linear behavior in time and space. If any of the step size halves the CPU-time increases to the double. A inversely proportional relation is described. In case of the explicit and Implicit Euler using matrix calculations no linear or other relation can be found. Due to the fact that the algorithm needs to invert the stiffness matrix the values increase more than doubled.

		Explicit Euler		Explicit Euler*		Implicit Euler*	
Δt	Δx	$\|.\|_\infty$	$\|.\|_1$	$\|.\|_\infty$	$\|.\|_1$	$\|.\|_\infty$	$\|.\|_1$
1	1	0.0231	$7.0381E^{-6}$	0.016	$4.2305E^{-4}$	0.0164	$4.7529E^{-4}$
1	$\frac{1}{2}$	0.0396	$5.8884E^{-6}$	0.0091	$1.4039E^{-4}$	0.0097	$1.6002E^{-4}$
$\frac{1}{2}$	$\frac{1}{4}$	0.0577	$6.7739E^{-6}$	0.005	$0.831E^{-5}$	0.0053	$7.3229E^{-5}$
$\frac{1}{2}$	$\frac{1}{16}$	$.E^{173}$	$.E^{172}$	NaN	NaN	0.0016	$3.5306E^{-5}$

Table 3.2: Depending on the used FDM two different error values are shown.

After readjusting the initial condition the FDM approximates the analytical solution in an

appropriate way. As mentioned in the beginning there are two values of interest. The left value is the maximal error of the concentration value for $t = 500$ and the right one represents the surface area at that time. All parameters which are not mentioned in the table are set as in the figures above. In table 3.2 some error values are noted. In the last row the instability of the Explicit Euler is shown. The Explicit Euler using matrix inverting is more unstable than the step implementation. The Implicit Euler is stable for all chosen values. In order to receive useable results for Explicit Euler the fineness of Δt and Δx and their relation have to be chosen carefully. If spatial step size is halved the step size size in time should be minimized too.

3.1.2 Finite Element Method

The same analysis can be made with the numerical solutions using different FEM approaches. Due to the fact that the Explicit Euler causes oscillations as mentioned in 2.2.2 the error study for Implicit Euler is neglected. Because of the oscillations the error plot would jump as well. Therefore the FEM solution using Implicit Euler method is analyzed.

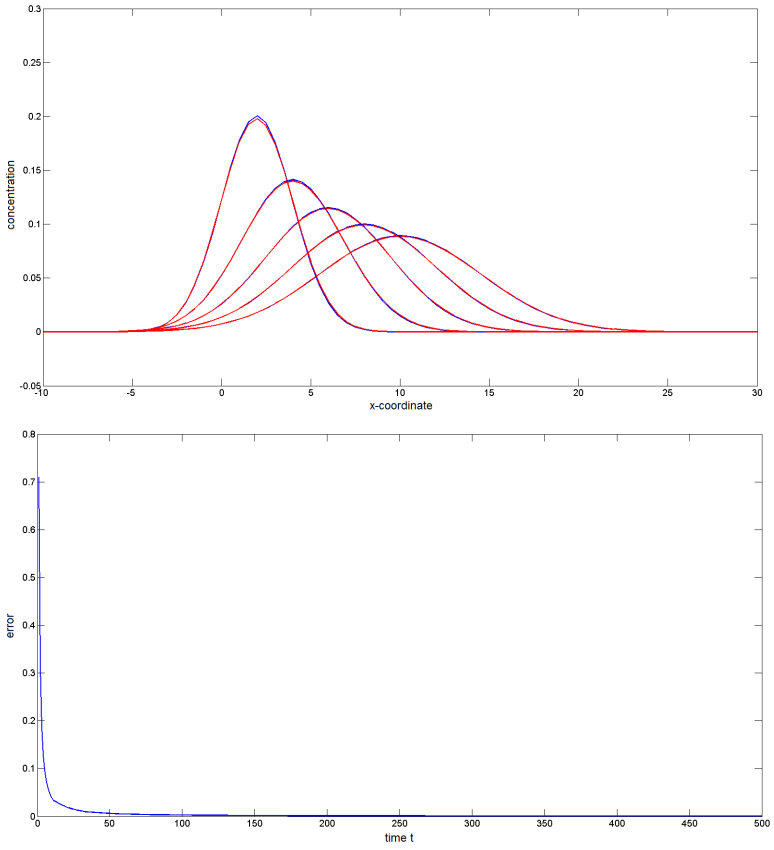

Figure 3.4: The error for the Implicit Euler algorithm of the FEM is shown.

The two figures 3.4 and 3.5 are generated using the Implicit Euler method to solve the finite element equation. In the left graphic the concentration at five different points in time

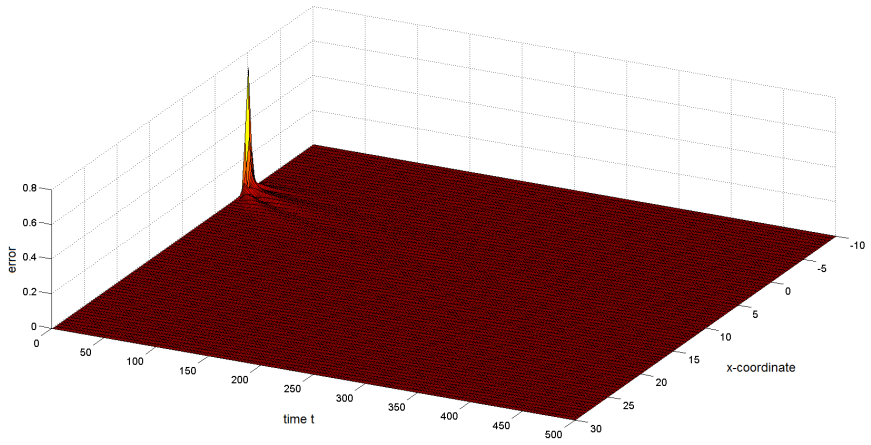

Figure 3.5: Error surface plot of FEM using Implicit Euler over time is outlined.

is plotted. The difference is hard to see but there is still a small one. Compared to the FDM an improvement is measurable. In the right plot the maximal error values for every single time step are sketched. The certainty of this graphic results in an error value $err = 0$ after approximately $t = 270$. In figure 3.5 the progress of the concentration error is shown. It looks similar to the convection-diffusion simulation of chapter 2. Due to the Dirac-function there is a greater error at the beginning. The velocity field moves the concentration to the right and therefore the error moves slightly to the right as well. The approximation of convection-diffusion using FEM is very exactly.

Another approximation is given using the Implicit Heun algorithm. In the right graphic the blue line shows the analytical solution. The approximation is very close to the analytical solution. Compared to FEM using Implicit Euler the error plot right starts at a lower value. Again after a certain time the error value is not distinguishable and seems to be zero. The exact values are shown in a table later on. The necessary parameter used for both studies (FDM, FEM) are the same as in most of the graphics of chapter 2. The velocity and diffusion coefficient are $v = 0.02$ and $D = 0.02$. This enables steeper curves and a better illustration of the error. The time step size is $t = 1$ and the step in space $\Delta x = 0.5$. In order to look closer to the convergence of the error the simulation duration is $t_{end} = 500s$.

Table 3.3 shows the different calculation times for various parameter. The values of all algorithm show a linear behavior regarding time. If any of the step size in time halves the CPU-time increases to the double. A inversely proportional relation is described. Regarding the spatial step size no linear relation is described. The values increase more than doubled. The Implicit Euler method is the fastest algorithm independent of time and space. The star in the second row marks an unstable Explicit Euler solution. The condition for a stable Explicit Euler algorithm used for finite element method restricts the useable combination of step sizes to a minimum.

The parameter setting and the description of the shown values in 3.4 are the same as in the analysis of the finite difference method. Left the maximal error of the concentration value and

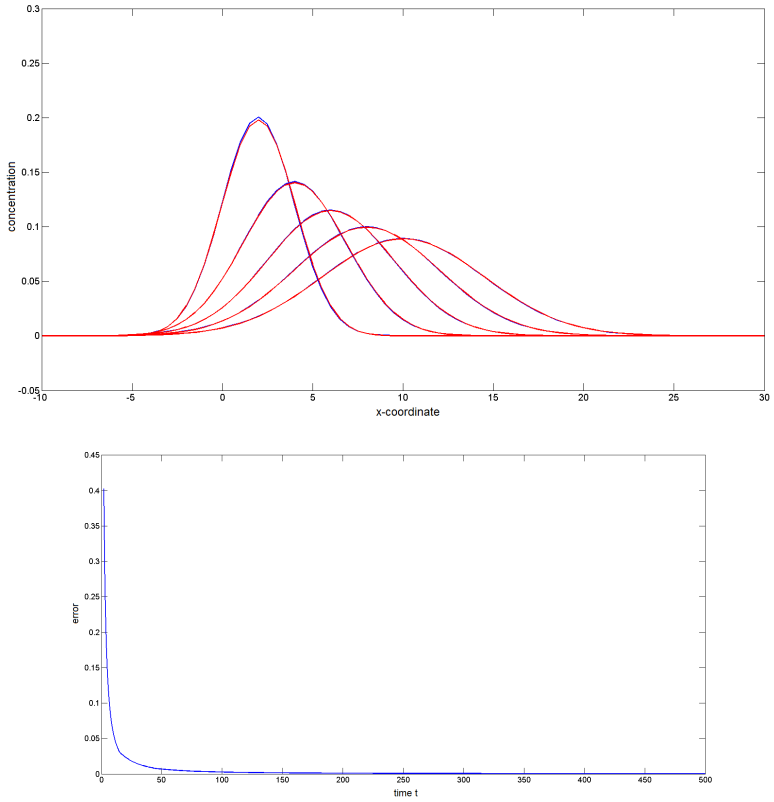

Figure 3.6: The error of the Implicit Heun algorithm is shown.

Δt	Δx	Explicit Euler	Implicit Euler	Implicit Heun
1	$\frac{1}{2}$	0.05850	0.02389	0.02781
1	$\frac{1}{4}$	0.19921*	0.10158	0.11113
$\frac{1}{2}$	$\frac{1}{2}$	0.10152	0.04469	0.05162
$\frac{1}{2}$	$\frac{1}{4}$	0.33960	0.15108	0.21392
$\frac{1}{4}$	$\frac{1}{2}$	0.20158	0.08706	0.10085
$\frac{1}{4}$	$\frac{1}{4}$	0.68343	0.31987	0.41167

Table 3.3: In this table the different calculation times for FEM using different algorithm are shown.

right the error of surface area for $t = 500$ are shown. In the last row an unstable example of the Explicit Euler is given. Again the high sensibility of this algorithm regarding FEM is emphasized. Concerning the first error value the Implicit Heun yields the best results but takes more time then the Implicit Euler. In general the approximation of the convection-diffusion equation using any of these FEM algorithm works very well. Due to oscillation implicit methods are preferred.

		Explicit Euler		Implicit Euler		Implicit Heun	
Δt	Δx	$\|.\|_\infty$	$\|.\|_1$	$\|.\|_\infty$	$\|.\|_1$	$\|.\|_\infty$	$\|.\|_1$
1	1	$7.1787E^{-4}$	$3.1557E^{-5}$	$9.9512E^{-4}$	$3.0271E^{-5}$	$6.3571E^{-4}$	$3.1862E^{-5}$
1	$\frac{1}{2}$	$6.23E^{-4}$	$8.6035E^{-5}$	$6.0942E^{-4}$	$8.5411E^{-5}$	$3.3217E^{-4}$	$8.5838E^{-5}$
$\frac{1}{2}$	$\frac{1}{4}$	$3.1307E^{-4}$	$1.0201E^{-4}$	$2.7349E^{-4}$	$1.0143E^{-4}$	$1.4622E^{-4}$	$1.0174E^{-4}$
$\frac{1}{2}$	$\frac{1}{8}$	NaN	NaN	$2.4876E^{-4}$	$1.0468E^{-4}$	$1.3088E^{-4}$	$1.0507E^{-4}$

Table 3.4: Depending on the used FEM the error values are shown.

3.2 FDM vs. FEM

In this section a direct comparison of the two different numerical approaches is done. Regarding certainty an intuitive assumption favors the finite element over the finite difference method.

In figure 3.7 the red line marks the approximation using FEM and blue using FDM. The used parameter setting is velocity $v = 0.02$, diffusion coefficient $D = 0.02$ and simulation time $t_{end} = 500s$. To justify the comparison in both methods the Implicit Euler algorithm is used. Using different step sizes the error can be minimized. In the left plot the time step size is $\Delta t = 1$ and $\Delta t = \frac{1}{8}$ right. Also the spatial step is changed from $\Delta x = \frac{1}{4}$ to $\Delta x = \frac{1}{16}$. Comparing the two tables 3.1 and 3.3 concerning various calculation times excluding the Explicit Euler using loops the FDM is faster than the FEM.
It is well known that the Explicit Euler algorithm is not as stable as any implicit algorithm. Therefore a stability criterion for Explicit Euler can be formulated.

$$\Delta t \leq C\Delta x^2 \tag{3.1}$$

Dependent on, C an arbitrary but positive constant, the Explicit Euler is stable. On the contrary the Implicit Euler belongs to the class of ultra-stable methods. Generally speaking implicit methods are more stable than explicit ones.

		Implicit Euler				Implicit Euler	
Δt	Δx	$\|.\|_\infty$	$\|.\|_1$	Δt	Δx	$\|.\|_\infty$	$\|.\|_1$
1	$\frac{1}{4}$	0.005	$1.7781E^{-4}$	$\frac{1}{2}$	$\frac{1}{8}$	0.026	$1.5083E^{-4}$
$\frac{1}{2}$	$\frac{1}{4}$	0.005	$1.7466E^{-4}$	1	$\frac{1}{16}$	0.013	$1.4193E^{-4}$
1	$\frac{1}{8}$	0.026	$1.5288E^{-4}$	$\frac{1}{2}$	$\frac{1}{16}$	0.013	$1.0433E^{-4}$

Table 3.5: Error values of FDM to FEM are given.

In table 3.5 the maximum according to amount of error at $t = 500$ is shown. The pattern in this table is remarkable. The left error value changes only if the spatial step size halves. There is a linear relation between Δx and the error value, both are halved. It seems as if the error is

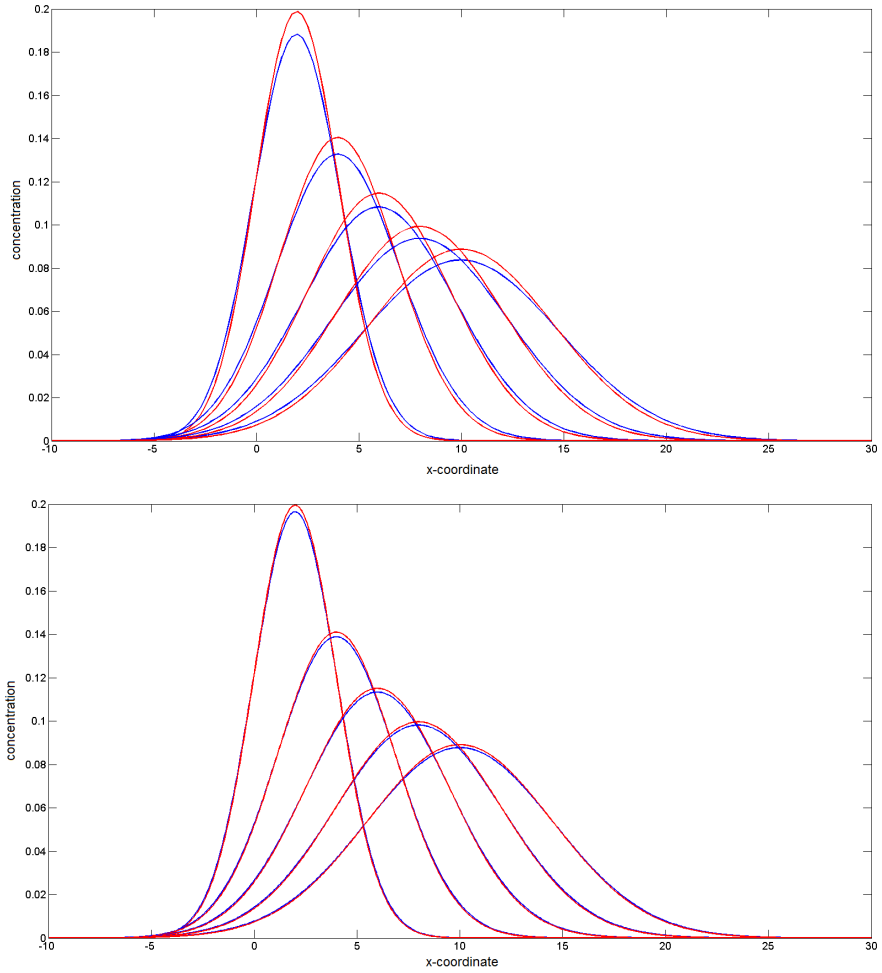

Figure 3.7: Comparison of FDM and FEM

independent of the time modifications. Concerning the surface area a small decreasing can be noticed. Although the finite element method, using any implicit algorithm for solving, is slower than finite difference methods it is the best approximation for the convection diffusion equation.

3.3 Random Walk

Before the comparison with the analytical solution can be done the two random walk approaches are analyzed.

Figure 3.8 shows both applications. The used particle number is $N = 3000$. In the intuitive approach the velocity is set to $v = 0.02$. After $t = 250s$ the finial concentration is given. As explained in Chapter 2 only the stochastic approach uses the diffusion coefficient set $D = 0.02$.

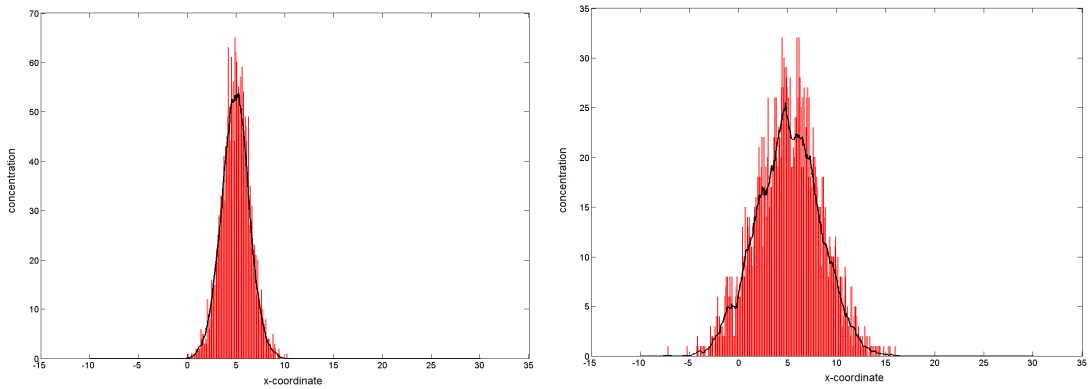

Figure 3.8: Comparison of intuitive and stochastic based random walk are shown.

The two step sizes are chosen $\Delta t = 0.5$ and $\Delta x = \frac{1}{16}$. In both implementation the center of the peak moves to $x = 5$ at $t = 250$. There is a difference in the diffusive distribution differs. Due to the fact that the diffusion in the intuitive approach depends on the spatial step size and the stochastic approach uses Δt and D for calculation a the parameter D has to be adjusted.

$$\begin{aligned} \Delta x X &= \sqrt{2d\Delta t} X \\ \Rightarrow D &= \frac{\Delta x^2}{2\Delta t} \end{aligned} \tag{3.2}$$

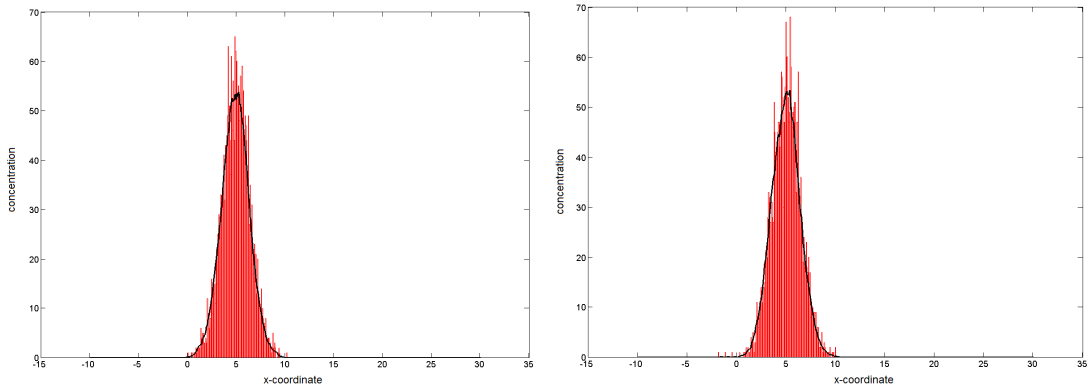

Figure 3.9: stochastic based and intuitive random walk with modified diffusion coefficient are shown.

In 3.9 the adjusted diffusion coefficient introduced in (3.2) is used. The resemblance of the two random walk approaches is now obvious.

In table 3.6 the calculation time of different parameter settings is analyzed. The CPU-time of both approaches is approximately the same. The linear relation in all the parameters is obvious.

Δt	Δx	t_{end}	N	intuitive RW	stochastical RW
1	$\frac{1}{10}$	500	4000	30.61838	29.55086
1	$\frac{1}{10}$	500	8000	60.28040	59.58526
$\frac{1}{2}$	$\frac{1}{10}$	500	8000	119.1364	119.480
$\frac{1}{2}$	$\frac{1}{15}$	250	8000	59.3995	61.18594
$\frac{1}{2}$	$\frac{1}{20}$	500	8000	120.8230	119.6362

Table 3.6: In this table the different simluation durations for the two random walk approaches are shown.

If the particle number doubles or the step size in time or space halves the needed calculation time doubles as well. Also a change regarding duration shows the same behavior. Compared to the numerical methods the calculation time of the random walk, influenced by the great number of particles, ascends extremely.

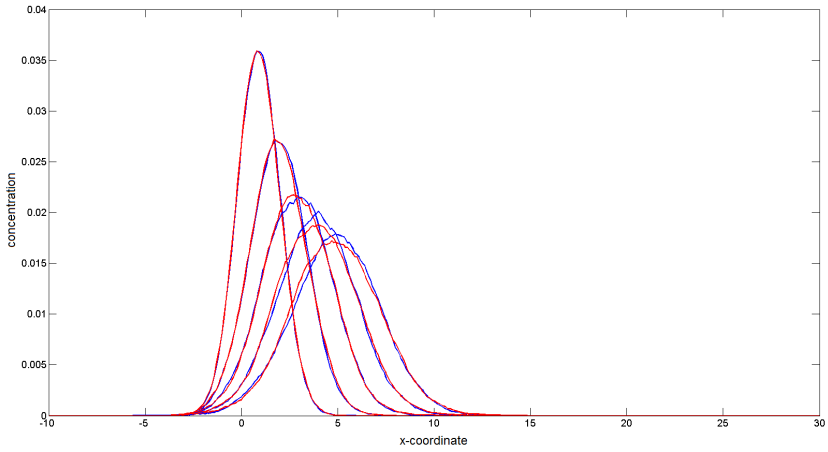

Figure 3.10: Comparison of the two random walk approaches are shown.

In figure 3.10 both random walk approaches are sketched. The red line shows the intuitive and the blue line the Gaussian-based approach. To receive this results the diffusion coefficient is determined as introduced before (3.2). The other parameter are set to velocity $v = 0.02$, simulation time $t_{end} = 250s$ and the step sizes $\Delta t = 0.5$ and $\Delta x = \frac{1}{10}$.

In table 3.7 the error values dependent on different parameter settings are shown. A great number of particles is necessary to create a good approximation. Therefore a long execution time follows. Due to the fact that both random walk approaches use normally distributed numbers the results of one simulation can not be reproduced exactly. Using more particles not necessarily leads to a better result. However the fineness of the step sizes impacts the result of the maximal occurring error positively. The values of the surface area are behaving contrary.

Δt	Δx	N	random walk $\|.\|_\infty$	random walk $\|.\|_1$
1	$\frac{1}{5}$	6000	$8.75E^{-4}$	$8.3267E^{-17}$
1	$\frac{1}{10}$	6000	0.0011	$3.9583E^{-5}$
$\frac{1}{2}$	$\frac{1}{5}$	6000	0.0011	$3.9583E^{-5}$
$\frac{1}{2}$	$\frac{1}{10}$	6000	$8.5417E^{-4}$	$4.1633E^{-17}$
$\frac{1}{2}$	$\frac{1}{15}$	6000	$8.3333E^{-4}$	$6.9389E^{-17}$
1	$\frac{1}{5}$	8000	0.0013	$2.7756E^{-17}$
1	$\frac{1}{10}$	8000	$7.9688E^{-4}$	$5.5511E^{-17}$

Table 3.7: In this table the comparison of the two random walk approaches are shown.

3.4 Analytical vs. Random

In the following section the two random walk implementations are compared to the analytical solution.

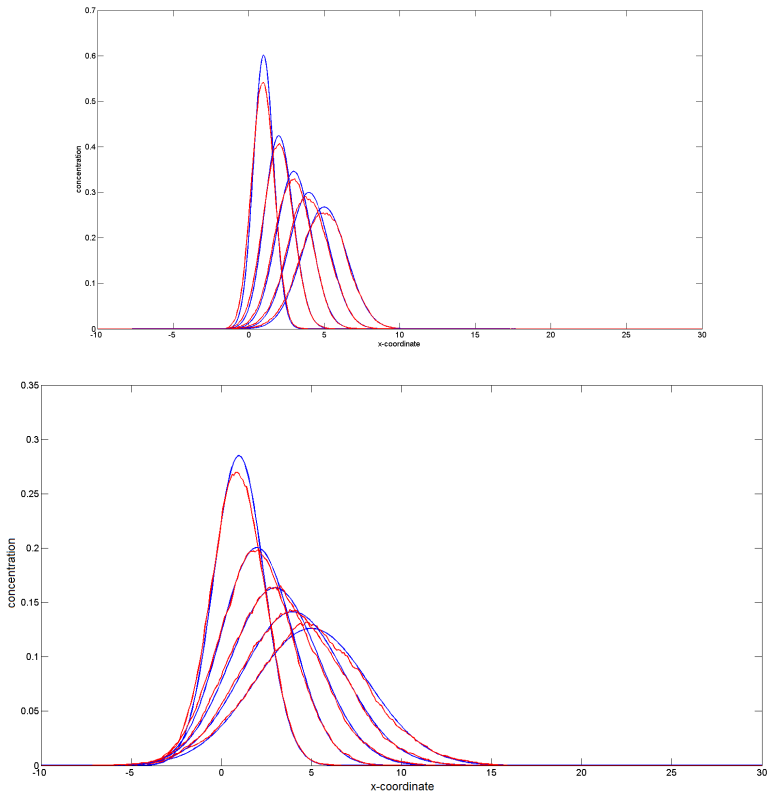

Figure 3.11: Comparison of intuitive and stochastic based random walk are shown.

The two graphics in figure 3.11 show both random walk approaches in red and the analytical solution in blue. In the left plot the intuitive implementation is shown. The right plot sketches the Gaussian-based version of random walk. Due to the In the two plots the number of particles is set to $N = 6000$. In the left plot the step sizes are not the same as in the right one. The spatial step size is $\Delta x = \frac{1}{15}$ and $\Delta t = 0.5$. The other parameters for the right plot are $v = 0.02$, $\Delta x = \frac{1}{10}$ and $\Delta t = 1$. In the numerical comparisons the simulation time is $t_{end} = 500s$. Due to long execution times for the particle movement this parameter is reduced to $t_{end} = 250s$. The diffusion coefficient is usually set to $D = 0.02$ but modifies if the intuitive approach is used.

				intuitive random walk		Gaussian random walk	
Δt	Δx	N	D^*	$\|.\|_\infty$	$\|.\|_1$	$\|.\|_\infty$	$\|.\|_1$
1	$\frac{1}{5}$	6000	0.01	0.0071	$8.9482E^{-7}$	0.0121	$8.9482E^{-7}$
1	$\frac{1}{10}$	6000	0.005	0.0142	$4.4409E^{-16}$	0.0084	$9.7072E^{-7}$
$\frac{1}{2}$	$\frac{1}{5}$	6000	0.04	0.0057	$3.3423E^{-5}$	0.0074	$8.9482E^{-7}$
$\frac{1}{2}$	$\frac{1}{10}$	6000	0.01	0.0094	$8.4185E^{-12}$	0.0103	$9.7072E^{-7}$
$\frac{1}{2}$	$\frac{1}{15}$	6000	0.0045	0.0156	$8.8818E^{-16}$	0.0090	$9.9693E^{-7}$
1	$\frac{1}{5}$	8000	0.01	0.0100	$0.9482E^{-7}$	0.0068	$8.9482E^{-7}$
1	$\frac{1}{10}$	8000	0.005	0.0153	$6.6613E^{-16}$	0.0053	$9.7072E^{-7}$

Table 3.8: Comparison of the random walk approaches and the analytical solution.

The table 3.8 shows all the error results of the parameter study comparing the analytical solution and both random walk approaches. Adapting the diffusion coefficient both approaches fues into one single random walk implementation. The diffusion coefficient for the Gaussian-based algorithm is set to $D = 0.02$. Using the intuitive approach the diffusion coefficient of the analytical solution changes to D^* to enables comparability. Due to the dependency on Δx and Δt the intuitive random walk cannot reach its performance. On contrary a parameter study would be necessary to find for all step size combinations the perfect variable value to perform this algorithm. Therefore for the simulation of the convection-diffusion equation the implementation of the Gaussian-based random walk fits better.

CHAPTER 4

Convective Diffusion in two Dimensions

This chapter deals with an enlarged problem. The convection-diffusion on a two dimensional domain will be discussed. Similar to chapter 1 two different initial conditions are used. As from now the considered equation is the following.

$$\frac{\partial c}{\partial t} = \frac{\alpha u}{R-u} \cdot \left(\frac{\partial^2 c}{\partial x^2} + \frac{\partial^2 c}{\partial y^2} \right) - u \cdot \frac{\partial c}{\partial x} \tag{4.1}$$

In this chapter different approaches to simulate and analyze the convection-diffusion equation are introduced. The structure will be related to chapter 2. First the analytical solution in two dimensions is discussed. This chapter also contains the two frequently used numerical approximations FDM and FEM. The last section covers different implementations and interpretations of the random walk.

4.1 Analytical Solution

In this section two different analytical solutions will be given. The difference between these solutions is not a different boundary condition like in 2.1 but various initial conditions. As mentioned in chapter 2 the scenario can either be an instantaneous release of all pollution or a steady source. The first solution will focus on the instantaneous release of pollution in the origin. The regarded equation and the according conditions are given in the following equation.

$$\frac{\partial c}{\partial t} = D \cdot \frac{\partial^2 c}{\partial x^2} + D \cdot \frac{\partial^2 c}{\partial y^2} - v \cdot \frac{\partial c}{\partial x} \qquad \text{with} c(x_0, y_0, 0) = \delta(x)\delta(y) \quad \lim_{x,y\to\infty} c(x, y, t) = 0 \quad \lim_{x,y\to-\infty} c(x, y, t) = 0. \tag{4.2}$$

The initial condition in (4.2) stands for an instantaneous release at (x_0, y_0). In order to solve (4.2) a solution of the following form is assumed. [ZK99]

$$c(x, y, t) = g_1(x, x_0, t)g_2(y, y_0, t) \tag{4.3}$$

where g_1 and g_2 are solution of the one-dimensional convection-diffusion equation with constant coefficient. Therefore g_1 and g_2 can be taken from the section of one-dimensional analytical solutions 2.1.1.

$$g_1(x, x_0, t) = \frac{A_1}{2\sqrt{D\pi t}} \exp\left(\frac{-(x - x_0 - vt)^2}{4Dt}\right) \tag{4.4}$$

$$g_2(y, y_0, t) = \frac{A_2}{2\sqrt{D\pi t}} \exp\left(\frac{-(y - y_0)^2}{4Dt}\right) \tag{4.5}$$

In (4.5) g_2 has no velocity term because the flux is only along x-direction. Function g_1 is the known solution of the convection-diffustion equation in one dimension. In the next step the coefficient A_1 and A_2 are determined. Due to the fact that the source has unit mass A_1 and A_2 can be reckoned.

$$\int_{-\infty}^{\infty}\int_{-\infty}^{\infty} c(x, y, t)dxdy = 1$$
$$\Rightarrow \int_{-\infty}^{\infty} g_1(x, x_0, t)dx \int_{-\infty}^{\infty} g_2(y, y_0, t)dy = 1$$

The source of pollution is placed at the origin so x_0 and y_0 can be set to zero.

$$\int_{-\infty}^{\infty} \frac{A_1}{2\sqrt{D\pi t}} \exp\left(\frac{-(x - vt)^2}{4Dt}\right) dx \int_{-\infty}^{\infty} \frac{A_2}{2\sqrt{D\pi t}} \exp\left(\frac{-y^2}{4Dt}\right) dy = 1 \tag{4.6}$$

The coefficients in (4.6) can be rearranged. Formally these two integrals are Gaussian bell curves. Due to the fact the every normal distribution is normalized the result of these integrals is 1. Using the following substitution and the integral result

$$z = \frac{x - vt}{\sqrt{2Dt}} \qquad \left(z = \frac{y}{\sqrt{2Dt}}\right)$$
$$\int_{-\infty}^{\infty} e^{-\frac{1}{2}x^2} dx = \sqrt{2\pi}$$

for both integrals the normalizing statement can be proved.

$$\int_{-\infty}^{\infty} \frac{1}{2\sqrt{D\pi t}} \exp\left(\frac{-(x-vt)^2}{4Dt}\right) dx = \int_{-\infty}^{\infty} \frac{1}{2\sqrt{D\pi t}} \exp\left(\frac{-z^2}{2}\right) dz \cdot \sqrt{2Dt} = 1$$

The solution of (4.2) can be given.

$$\begin{aligned} & A_1 A_2 = 1 \\ \Rightarrow & c(x,y,t) = \frac{1}{4D\pi t} \frac{1}{\operatorname{erfc}\left(\frac{-vt}{2\sqrt{Dt}}\right)} \exp\left(\frac{-(x-vt)^2 - y^2}{4Dt}\right) \end{aligned} \tag{4.7}$$

In order to analyize the behavior for positive x-values another approach can be applied.

$$\int_0^{\infty} \frac{A_1}{2\sqrt{D\pi t}} \exp\left(\frac{-(x-vt)^2}{4Dt}\right) dx \int_{-\infty}^{\infty} \frac{A_2}{2\sqrt{D\pi t}} \exp\left(\frac{-y^2}{4Dt}\right) dy = 1 \tag{4.8}$$

According to the proof above the second integral is again 1. In order to solve (4.8) a new parameter is introduced.

$$\begin{aligned} \eta &= \frac{x - vt}{2\sqrt{Dt}} \\ d\eta &= dx \frac{1}{2\sqrt{Dt}} \end{aligned} \tag{4.9}$$

Using (4.9) equation (4.8) can be written as

$$\begin{aligned} & \frac{A_1}{2\sqrt{D\pi t}} \int_{-\frac{vt}{2\sqrt{Dt}}}^{\infty} \mathrm{e}^{\eta^2}\, d\eta 2\sqrt{Dt} \int_{-\infty}^{\infty} \frac{A_2}{2\sqrt{D\pi t}} \exp\left(\frac{-y^2}{4Dt}\right) dy = \\ & \frac{A_1 A_2}{\sqrt{\pi}} \int_{-\frac{vt}{2\sqrt{Dt}}}^{\infty} \mathrm{e}^{\eta^2}\, d\eta = 1 \end{aligned} \tag{4.10}$$

The complementary error function is defined as $\operatorname{erfc}(x) = \frac{2}{\sqrt{\pi}} \int_x^{\infty} \mathrm{e}^{-t^2}\, dt$. Inserting this definition into (4.10) gives

$$\begin{aligned} & A_1 A_2 \cdot \operatorname{erfc}\left(\frac{-vt}{2\sqrt{Dt}}\right) = 2 \\ \Rightarrow\ & c(x,y,t) = \frac{1}{2D\pi t} \frac{1}{\operatorname{erfc}\left(\frac{-vt}{2\sqrt{Dt}}\right)} \exp\left(\frac{-(x-vt)^2 - y^2}{4Dt}\right) \end{aligned} \tag{4.11}$$

Under certain conditions this equation can be simplified. Within the accuracy of MATLAB $\mathrm{erfc}(z) = 2$ if $z < -3$ and approximately zero if $z > 27$. Regarding the argument of the complementary error function in (4.7) one gets

$$\begin{aligned}
\frac{v\sqrt{t}}{D} > 6 \;:\quad & c(x,y,t) = \frac{1}{4D\pi t}\,\exp\left(\frac{-(x-vt)^2-y^2}{4Dt}\right) \\
-54 < \frac{v\sqrt{t}}{D} < 6 \;:\quad & c(x,y,t) = \frac{1}{2D\pi t}\,\frac{1}{\mathrm{erfc}\left(\frac{-vt}{2\sqrt{Dt}}\right)}\,\exp\left(\frac{-(x-vt)^2-y^2}{4Dt}\right) \\
\frac{v\sqrt{t}}{D} < -54 \;:\quad & c(x,y,t) \to \infty.
\end{aligned}$$

The analysis of the part with positive x-values results in the same equation validated for the whole regarded domain. An explanation for this behavior is the development of concentration due to the convection-diffusion equation. After a certain point in time nearly all pollution reaches the positive half of the domain and there the results of both calculation have to agree.

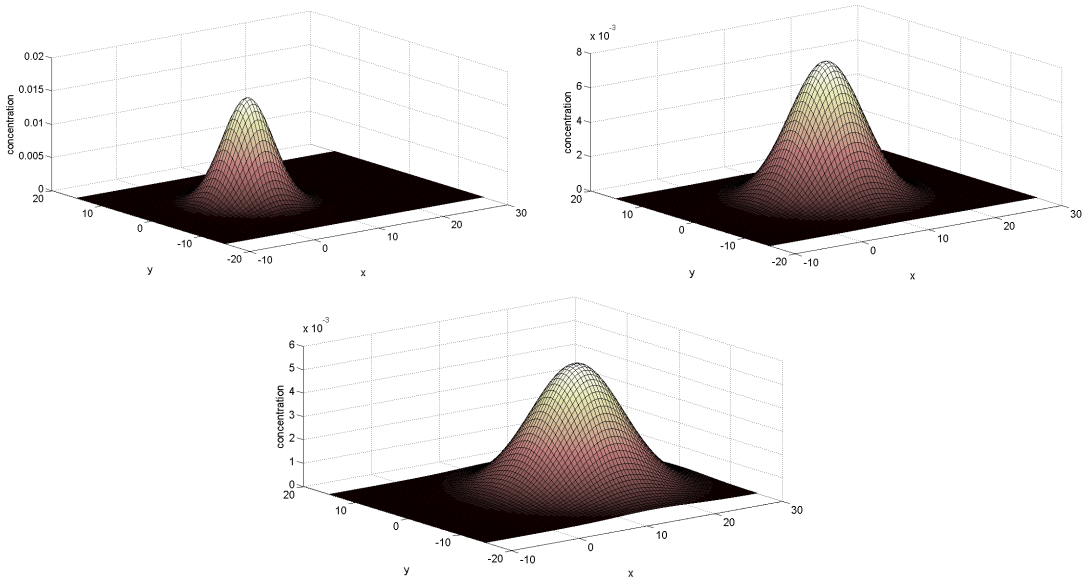

Figure 4.1: Two dimensional diffusion using (4.7) for different time steps

In figure 4.1 the analytical solution for the convection-diffusion equation in case of an instantaneous release of all pollution is shown. The parameter setting is similar to the simulation in one dimension. For velocity $v = 0.02$, for diffusion $D = 0.02$ and for simulation time the following values are chosen from left to right $t = 250s$, $t = 500s$ and $t = 750s$. These three graphics show the concentration as a function of x and y. The effect caused by the diffusion coefficient is clearly visible. In the first plot the diameter of the bell curve is approximately 15 units of length which changes to more than 20 in the second and out of boundaries in the third.

Without measuring the flattening of the curve's peak is obvious. The height starts at 0.035, goes to 0.016 and ends at 0.012. The convective movement can be measured with the position of the peak which switches from 5 and then 10 to 15. The choice of the parameter shows a good balance between convective and diffusive transport.

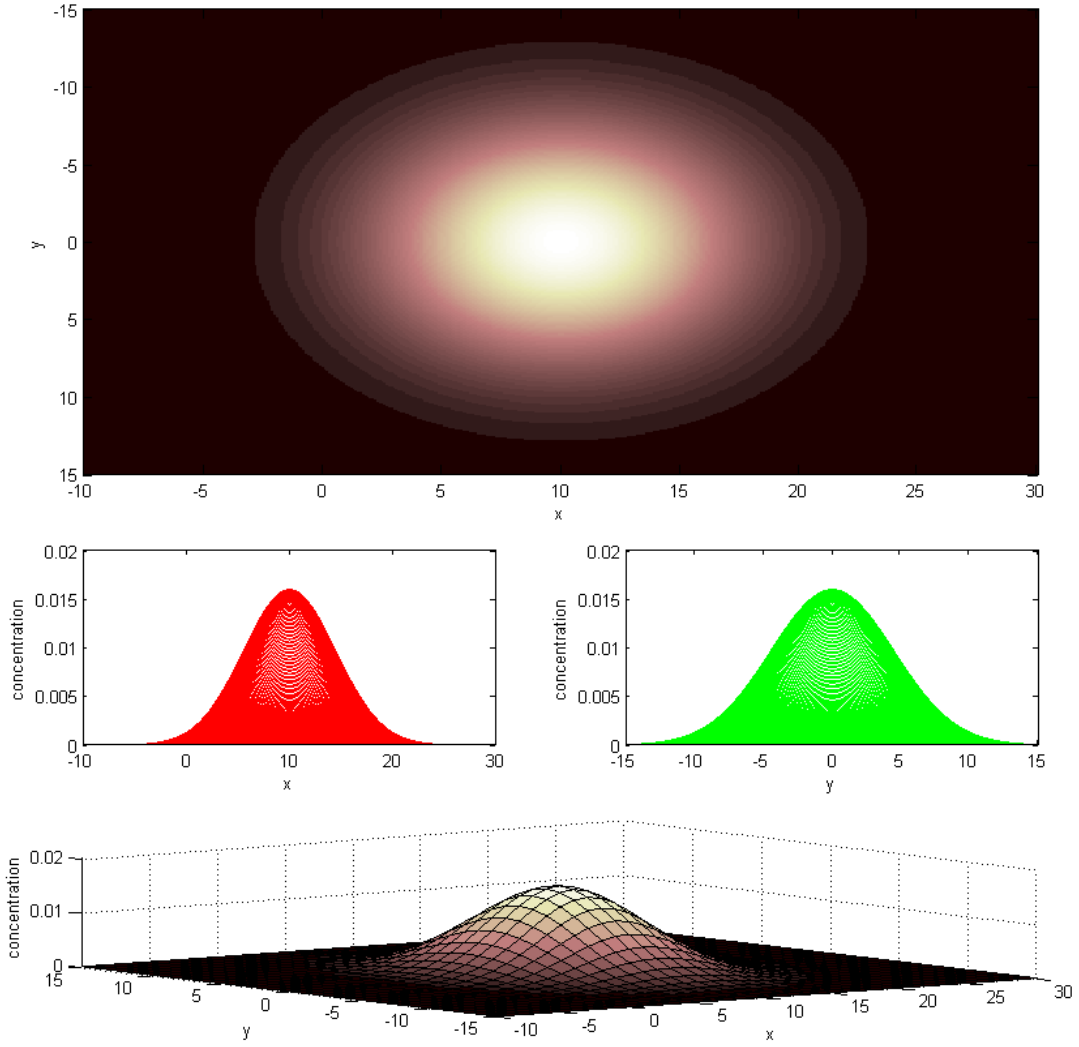

Figure 4.2: Analytical solution on the rectangle.

Figure 4.2 shows three different aspects of the analytical solution. The two Gaussian curves sketch the diffusive progress from the x- and y-axis point of view. The red one shows the convection of the concentration peak moving from $x = 0$ at the beginning to $x = 10$ in the end. In the right plot the peak of the green bell curve is still at $y = 0$ because there is no velocity along the y-direction. The third plot shows the concentration dependent on x and y as in figure 4.1, which offers a three dimensional view of the red and green curves. The first illustration

can be seen as the aerial perspective of the third graphic. The different colors mark the grade of pollution. The duration of this simulation is $t = 500s$. All other parameters are the same as in figure 4.1, velocity $v = 0.02$ and the diffusion coefficient $D = 0.02$.

4.2 Numerical Solution

In the following sections the numerical methods used in chapter 2 will be modified for the two dimensional problem.

4.2.1 Finite Difference Method

The finite difference method for one dimension was introduced in 2.2.1. The same principle will be used to apply the FDM for a two dimensional domain. Consider the finite domain from the introduction 1.2 covered with an equidistant grid.

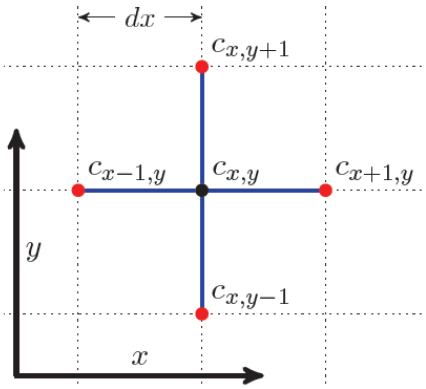

Figure 4.3: Equidistant grid in the two dimensional domain.

Remembering the FDM in one dimension one can imagine how the first partial derivatives of the function $c(x, y)$ look like 4.12. To establish second derivatives again the central finite difference method is used.

$$\begin{aligned} \frac{\partial c}{\partial x} &= \frac{c_{x+1,y} - c_{x-1,y}}{2dx} \\ \frac{\partial c}{\partial y} &= \frac{c_{x,y+1} - c_{x,y-1}}{2dy} \end{aligned} \tag{4.12}$$

Repeating FDM for the first derivative of two neighboring points leads to the second derivative for variable x of $c(x, y)$. The partial derivatives for y can be defined analog. Combining these two equations and assuming using a grid of equal-sized squares, $dx = dy$, one receives the needed form.

$$\begin{aligned}\frac{\partial^2 c}{\partial x^2} &= \frac{c_{x+1,y} - 2c_{x,y} + c_{x-1,y}}{dx^2} \\ \frac{\partial^2 c}{\partial y^2} &= \frac{c_{x,y+1} - 2c_{x,y} + c_{x,y-1}}{dx^2}\end{aligned} \tag{4.13}$$

$$\Rightarrow \Delta c = \frac{c_{x+1,y} + c_{x-1,y} - 4c_{x,y} + c_{x,y+1} + c_{x,y-1}}{dx^2}$$

For simulating the convection-diffusion equation an approximation of the convection is necessary. Due to the fact that the the velocity field is still only parallel to the x-axis the convection consists of the first derivative in x as explained and defined in equation (4.12). The concentration c depends on the spatial coordinates as well as time. Hence, the equation (4.1) using FDM can be written as:

$$c_t = \frac{dc}{dt} = D \cdot \frac{c_{x+1,y} + c_{x-1,y} - 4c_{x,y} + c_{x,y+1} + c_{x,y-1}}{dx^2} - v\frac{c_{x,y} - c_{x-1,y}}{dx} \tag{4.14}$$

In (4.14) the time derivative can be written with dt instead of ∂t because FDM transforms the equation into an ordinary differential equation. The numerical method which is used to calculate the next time step is called Euler method. This method calculates the next time step by using the last one and adding the derivative of the function times step size h.

$$c_{x,y}(t + \Delta t) = c_{x,y}(t) + h \cdot \frac{dc}{dt} \tag{4.15}$$

The equation (4.14) is implemented in MATLAB using the explicit Euler method (4.15).

For Figure 4.4 the parameter setting is: velocity $v = 0.02$, diffusion coefficient $D = 0.02$ and the duration time is $t = 250s$ left and $t = 500s$ right. Except the simulation time the same parameters are used to enable comparability. The center of pollution after $250s$ is at $(x, y) = (5, 0)$ and the height is approximately $c(5, 0) = 1.8$. The right figure shows the same parameter set running for $500s$. The height decreases and the center of peak changes to $(x, y) = (10, 0)$.

As mentioned at the beginning different initial scenarios are simulated. In the following a change from an instantaneously to a steady releasing source take place. The steady source of pollution is realized by adding partial pollution to the concentration value at $(0, 0)$ which leads to $c_{0,0} = c_{0,0} + p_{rate} \cdot \Delta t$ in every time step, whereas p_{rate} stands for the added constantly pollution rate.

The velocity and diffusion coefficient in figure 4.5 are $v = 0.02$ and $D = 0.02$. They are equal to the parameters in figure 4.1. The pollution rate was set to $p_{rate} = \frac{1}{t_{end}}$. In doing so the same amount of pollution as in the simulations with in instantaneous source is distributed. In the left image the running time is $t_{end} = 500s$ and in the right $t_{end} = 1000s$. Regardless of how long the simulation runs the maximum of pollution is always at the source itself. The influence of the flux is obvious. As mentioned in the introduction the absence of flow in y-direction causes

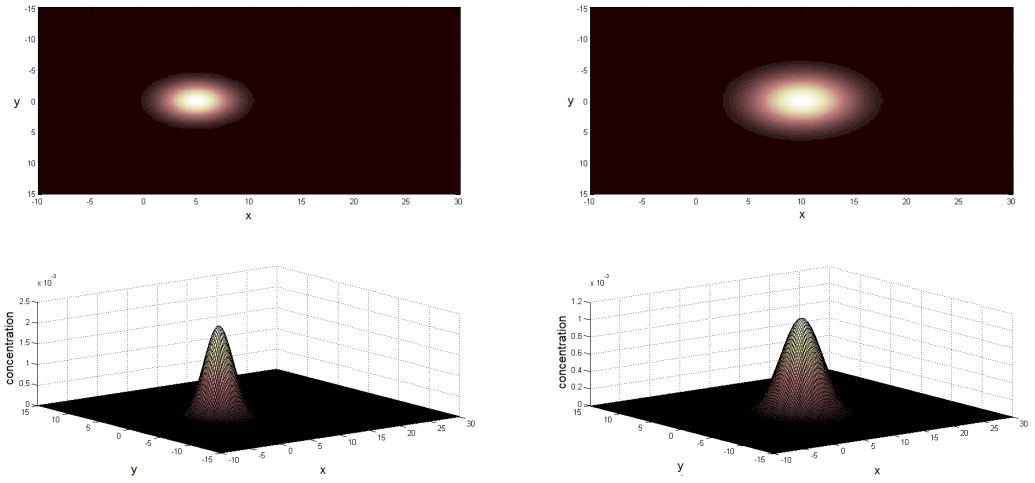

Figure 4.4: Numerical solution using FDM for a two-dimensional domain with instantaneous source.

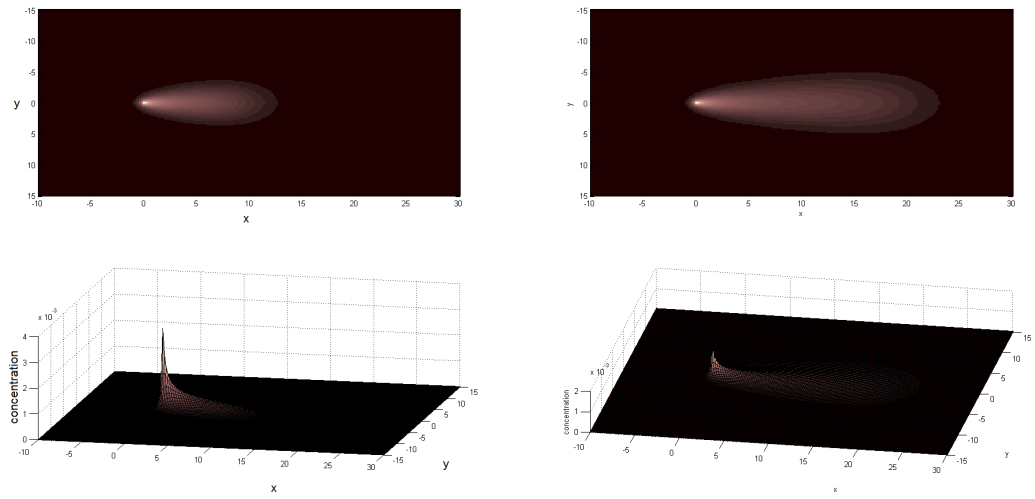

Figure 4.5: Numerical solution using FDM for a two-dimensional domain with steady source.

a cone-shaped pollution in x-direction. The upper graphic shows again a color map of the grade of pollution. The steep peak in the lower illustration pictures that the pollution rate added every time step is bigger than the moved pollution. Therefore some pollution stays near the source for minimal one more time step which causes this peak.

4.2.2 Finite Element Method

Numerical approaches need much computing time due to high accuracy needed to generate useable outputs. The finite element method for two-dimensional regions is more complicated than for one dimension. Putting a grid on the domain expanses the number of elements to the power of two. For the basis function a linear or quadratic approximation can be used. An direct implementation of the algorithms in MATLAB would be very time-consuming. Instead the software called COMSOL, formerly FEMLAB, is used. It is qualified for physical simulations and is based on the interaction of differential equations. The actual solving algorithm of COMSOL uses the finite element method. COMSOL is a widespread language which is used in education, research and development. It is a software that eases the linking of different physical problems. Coupled equations can be solved simultaneously.
The simulation software contains different packages for various fields of natural sciences. COMSOL was originally a toolbox of MATLAB dealing with partial differential equations. The current version offers points of interactions with MATLAB as well as Simulink, software for designing electric systems, reaction and electric circuit simulators. Connections to graphical design programs for creating difficult geometries as well as statistical programs to analyze output data are given.

After opening COMSOL the dimension of the problem is asked. As already mentioned COMSOL offers many different toolboxes. In this case the mathematical package without any additional physical specification is used. In the next step the obtained geometry has to be designed. In this study it is only rectangular but in case of an natural application it can be necessary to include a difficult shape. Therefore the connection to graphical design programs can be used and to import the exact geometry. The global variables are defined next.

$$\frac{\partial u}{\partial t} + \nabla(-D\nabla u) + v\nabla u = f \tag{4.16}$$

The mathematical toolbox offers some prepared equations. The convection-diffusion equation in the following form (4.16) is one of them. The missing point source is located at $(0, 0)$. For the following simulations the function f is set to zero. The simulation time for all parameter choices is $t_{end} = 500$ and the concerning $\Delta t = \frac{1}{4}$.

Before the simulation starts the regarded domain is covered with a fine grid. This grid adapts to the certain conditions. The element size is chosen very small to avoid mathematical errors at critical points. Due to the fact that a point source is used the grid refines at its location.

Figure 4.7 shows the simulation of the convection-diffusion equation using the software COMSOL. The based method is FEM. In the first plot the parameters are set $D = 0.02$ and $v = 2$. The velocity dominates the diffusive motion. Therefore the concentration distribution shape is only a beam. Comparing these values to the usual variable values a difference is recognizable. Due to the fact that COMSOL can distinguish different physical meanings of the equation the same variables have another effect to the visualization. In the second graphic the diffusion coefficient is changed to $D = 0.2$. The results looks more like the numerical solution outputs. The convection is still dominating but also the diffusive effect can be found. In the third plot the

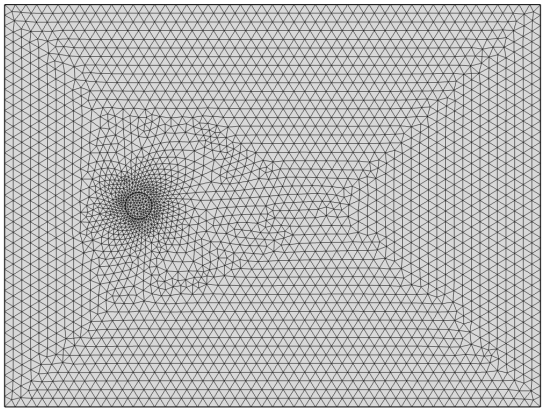

Figure 4.6: Grid used in the FEM calculations.

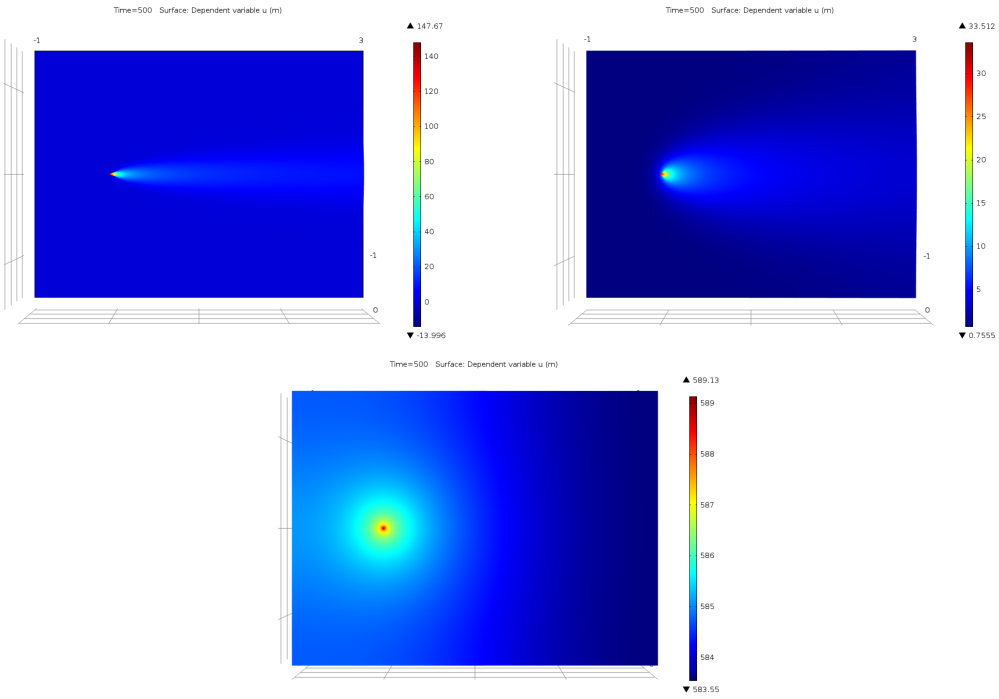

Figure 4.7: FEM solution realized using COMSOL.

relation between diffusion and convection is completely different. The parameter are set $D = 2$ and $v = 1$. This parameter choice already shows the domination of diffusion. In the graphic the effects of convection disappears.

Figure 4.8 shows the second plot of firgue 4.7 from another angle. The pollution distribution from the x point of view is presented. Due to the different physical interpretation this solution is not compared to any other approach. For prospective studies COMSOL can play a big role.

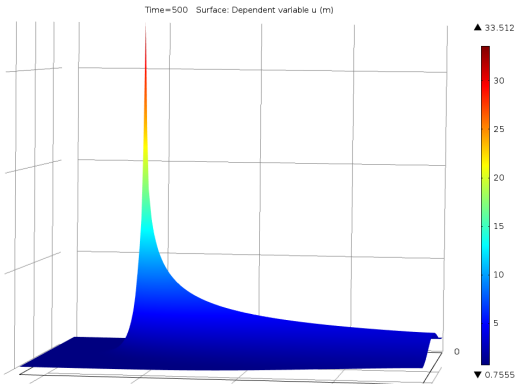

Figure 4.8: A surface plot of the COMSOL results is shown.

Especially for complex geometries it is a very comforting application.

4.3 Random Walk

The introduction concerning random walk can be found in section 2.3. The simulation of diffusion using random walk is based on particle tracking. These particles are moving minimally and randomly but by taking account of all particles a diffusive movement appears. In the following sections different random walk approaches are discussed. In contrast to the random walk in section 2.3 a two dimensional domain is considered. This leads unavoidably to the question how to deal with the second dimension.
An important difference regarding analytical simulations are the boundary conditions. In the following models a Neumann boundary of kind $-\frac{\partial c}{\partial x}n = 0$ is used. This means that there is no flow through the boundaries. All particles remain in the domain the whole simulation. Due to the fluid flow the worst scenario would be a reflection of all particles at the right boundary and their gathering there. In the following during the simulation time there won't occur reflections at all.
One suggestion for the realization of the two dimensional random walk is to use a grid with high resolution. This approach is closely connected to the numerical approach FEM. A disadvantage of using a grid is the restricted movement from one node to another. On the other hand it is very easy to realize complex structures using collision and other motion rules. Implementations dealing with random walk on a grid are introduced later on. The first two approaches are technically expansions of the implementations in section 2.3.1 and 2.3.2.

4.3.1 Intuitive Approach

This first implementation of random walk follows intuitive gestures. The problem domain is given as shown in the motivation 1.2.

As pictured in figure 4.9 a finite domain with a source of pollution at its origin is given. The convection-diffusion equation consists of the oriented transport caused by the flux and

Figure 4.9: A schematic illustration of the described area.

the chaotic transport of diffusion. The velocity field v is constant and only nonzero along x-direction. The movement of the particles especially the tracking of the movement is realized without using a grid. In this implementation the possibility of collisions is neglected. The model contains three important steps:

· initialization of particles

· random movement of diffusion

· x oriented movement due to flux

The number of particles joined to the system is N. Initially all the particles are set at the origin $(x, y) = (0, 0)$ where the source of pollution is located. There is no initial velocity but there is an initial direction d_0 to start the random walk algorithm. The next step concerns the diffusive motion. The chaotic transport is realized by using a normally distributed random variable X and a uniformly distributed random number U. X is used to generate a random length and U chooses a coincidental direction.

$$\begin{aligned} r &= X \cdot \Delta x \qquad & \alpha &= U \cdot 2\pi \\ d_0 &= \begin{pmatrix} 1 \\ 0 \end{pmatrix} \qquad & d_{n+1} &= \begin{pmatrix} \cos\alpha & -\sin\alpha \\ \sin\alpha & \cos\alpha \end{pmatrix} \cdot d_n \end{aligned} \tag{4.17}$$

In (4.17) r stands for the distance the particle moves in a certain time step. The influence of this parameter is similar to the diffusion coefficient. X is the mentioned normally distributed random variable and Δx describes the step size in space. The second equation of (4.17) sets the direction for the particle's next move. The initial direction d_0 is only necessary for the recursive definition. During simulation the direction of the last movement is used to calculate the next one. The convection is realized by a move in direction of the flow. The final formula for the random walk movement can be given as follows

$$p_{new} = p_{old} + d \cdot r + vdt. \tag{4.18}$$

Starting with the actual position of the particle p_{old} the new position p_{new} contains the direction multiplied by the distance the particle will move. Then the move regarding flux velocity is added. The random variables X and U are newly created in every time step for each particle. These movement steps are repeated for all particles in every step.

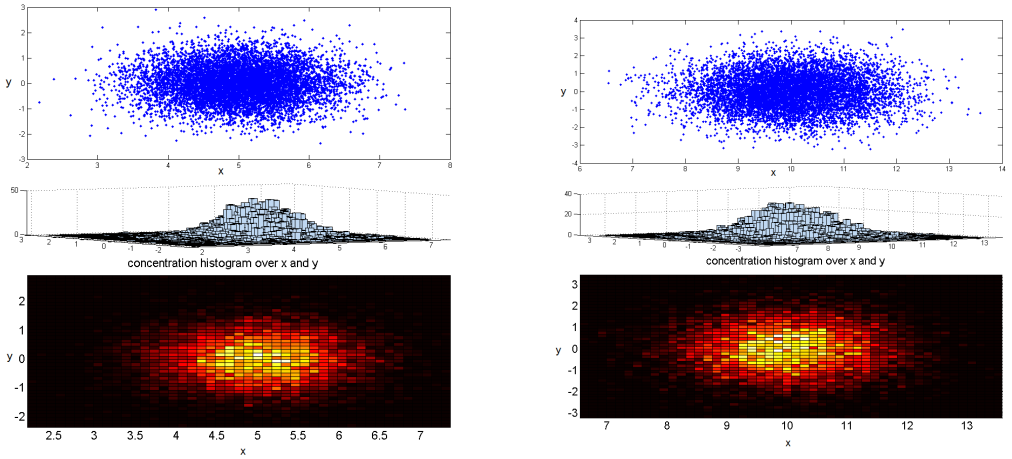

Figure 4.10: Gaussian random walk for convection-diffusion with instantaneous source

In figure 4.10 the parameters are set to $v = 0.02$, $\Delta x = \frac{1}{16}$ and the number of particles are $N = 8000$. The simulation times are $t = 250s$ and $500s$. The upper plot places every single particle at its position. In the middle a histogram of the concentration is given. Every pillar of the histogram presents the amount of the particles in each square of a chosen size. In the lower plot the aerial perspective of the histogram is shown. The brighter the higher is the pollution in this area. Comparing the centers of pollution in these two illustrations with the outputs of the numerical solutions using the finite difference method a correlation can be found. After $250s$ the peak moves from $x = 0$ to $x = 5$ and at $t = 500$ the final position $x = 10$ is reached.

The steady source used in the numerical approaches can be realized with random walk as well. Instead of placing all the particles at $x = 0$ in the beginning the amount of particles is divided over the regarded time span.

The figure 4.11 uses the same parameter setting as in figure 4.10. The difference is the choice of initial condition. The steady source of pollution is obvious. The maximum of solid is at the source itself. The maximal reached x-values are related to the peak location in the instantaneous release figures above.

4.3.2 Gaussian-based Approach

The second approach can be seen as expansion of the model in one dimension, see section 2.3.2. The random walk implementation is connected to the two-dimensional analytical solution (4.7) of the diffusion equation with the following initial and boundary conditions.

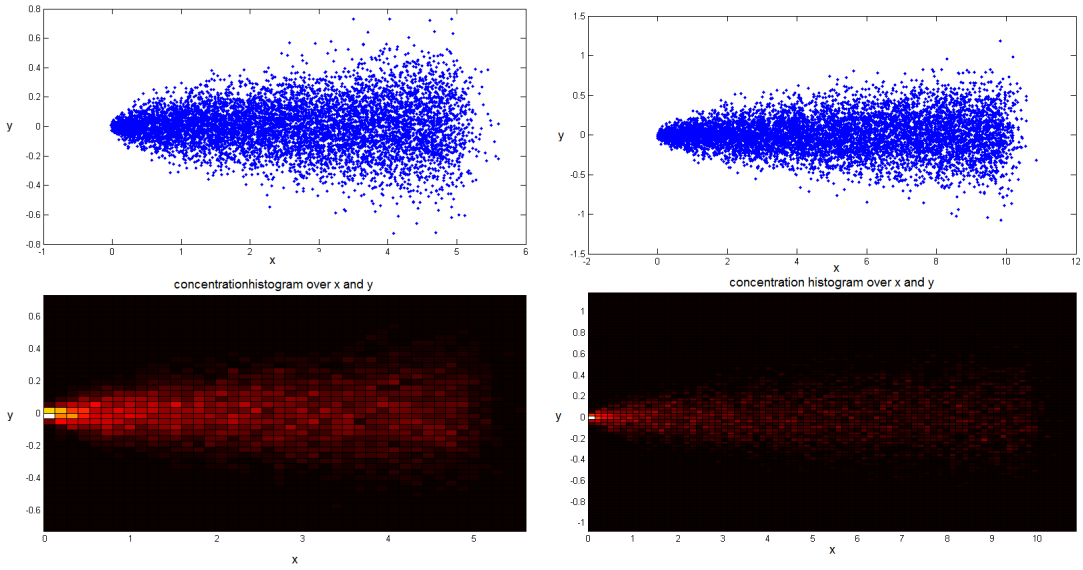

Figure 4.11: Intuitive random walk for convection-diffusion with instantaneous source

$$\frac{\partial c}{\partial t} = D\frac{\partial^2 c}{\partial x^2} - v\frac{\partial c}{\partial x} \qquad \text{with} \quad c(x,0) = \delta(x) \tag{4.19}$$

$$\lim_{x,y\to\pm\infty} c(x,y,t) = 0 \tag{4.20}$$

$$\lim_{x\to\infty}\lim_{y\to-\infty} c(x,y,t) = 0 \tag{4.21}$$

$$\lim_{x\to-\infty}\lim_{y\to+\infty} c(x,y,t) = 0 \tag{4.22}$$

Looking at the simplified but differently arranged analytical solution (4.7)

$$c(x,y,t) = \frac{1}{2\sqrt{D\pi t}}\exp\left(\frac{-(x-vt)^2}{4Dt}\right)\ \frac{1}{2\sqrt{D\pi t}}\exp\left(\frac{-y^2}{4Dt}\right) \tag{4.23}$$

the equation parts belonging to the movement along x on the one hand and y on the other hand become visible. Once more the connection to the Gaussian distribution is obvious.

$$f(x) = \frac{1}{\sqrt{2\pi\sigma^2}}e^{-\frac{(x-\mu)^2}{2\sigma^2}}$$

There is a formal equivalence to parts of equation (4.23). The parameters for mean value μ and standard deviation σ are the same as in the one dimensional case.

$$\mu = v \cdot t$$
$$\sigma^2 = 2 \cdot Dt$$

Therefore the concentration can be approximated using the information of height and width given by the Gaussian parameter. The corresponding particle movement in x and y-direction can be defined.

$$\begin{aligned} p_x^{new} &= p_x^{old} + v\Delta t + \sqrt{2 \cdot D\Delta t} X_x \\ p_y^{new} &= p_y^{old} + \sqrt{2 \cdot D\Delta t} X_y \end{aligned} \tag{4.24}$$

X_x and X_y stand for independent normally distributed random numbers which are newly generated in every step for each particle. The term $v\Delta t$ describes the convective transport parallel to x. Due to the fact that the diffusion coefficient is equal for the x- and y-direction the diffusive movement $\sqrt{2 \cdot D\Delta t}$ in the random walk definition (4.24) is also the same.

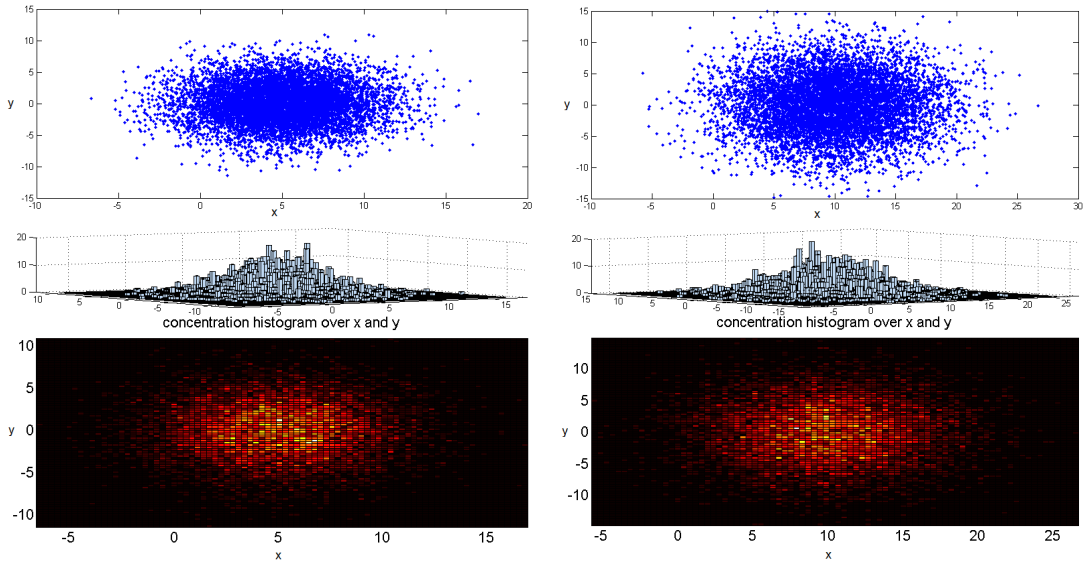

Figure 4.12: Gaussian random walk for convection-diffusion with instantaneous source

In figure 4.12 two results of the implementation are shown. The parameters are similar to the intuitive approach to enable comparability. Therefore the setting is velocity $v = 0.02$, diffusion coefficient $D = 0.02$, number of particles $N = 8000$ and time step $\Delta t = 1$. The spatial step size $\Delta x = 1$ is used to calculate the velocity part for every time step. The simulation time differs, $t = 250$ left and $t = 500$ right.

This approach is also used to approximate the convection-diffusion equation in case of a steady polluting source. This is realized by releasing $\frac{N}{t_{end}\frac{1}{dt}}$ particles every time step.

Figure 4.13 shows the Gaussian random walk approach with a steady source. The parameter setting is similar to figure 4.12. Comparing figure 4.12 and 4.13 the difference using various sources is clear. In spite of all distinctions a correlation in the range of particles can be found. The choice of source influences the maximal x-value of a bunch of particles in a nonlinear way. The longer the duration of the simulations the more these maximums diverge.

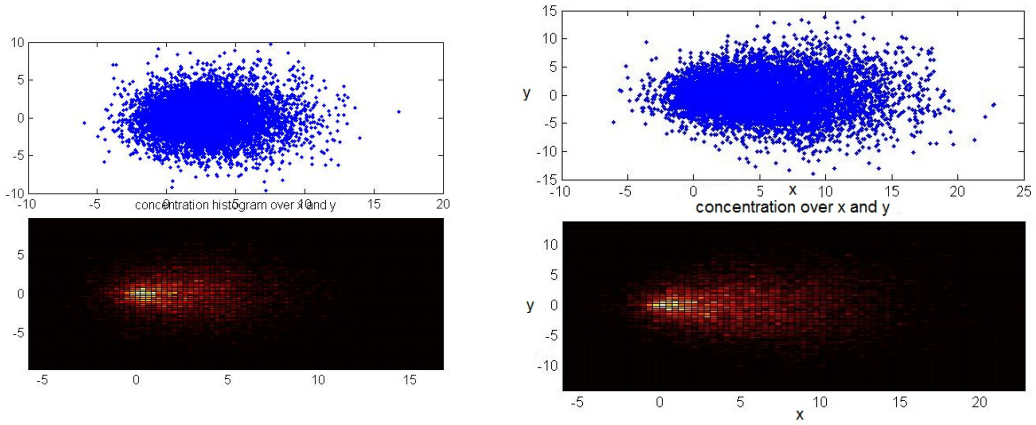

Figure 4.13: Gaussian random walk for convection-diffusion with steady source

4.3.3 Stochastic approach

Based on [SFGGH06] the results of the Gaussian-based approach 4.3.2 can be explained in a more general way. The underlying theory is the stochastic analysis. At first the regarded transport equation is given.

$$\frac{\partial c}{\partial t} = \nabla(\mathbf{D}\nabla c) - \nabla(\mathbf{v}c) \tag{4.25}$$

The diffusion coefficient is usually defined as

$$\mathbf{D} = (\alpha_T|\mathbf{v}| + D_m)\mathbf{I} + (\alpha_L - \alpha_T)\frac{vv^T}{|v|} \tag{4.26}$$

where α_L and α_T are the dispersion in x-direction (longitudinal) and y-direction (transverse). As mentioned in 1.2 they are equal. v is the velocity vector and D_m the diffusion coefficient known as D. Therefore (4.26) is reduced to

$$\mathbf{D} = (\alpha|\mathbf{v}| + D)\mathbf{I}. \tag{4.27}$$

Due to the fact that $\mathbf{v}$ is a two dimensional matrix with only one nonzero entry at $\mathbf{v}(1,1)$, defining the velocity along x-direction, the determinant of this matrix is zero. Hence equation (4.27) can be written as

$$\mathbf{D} = D.$$

The Îto-Taylor integration scheme describes the displacement of a particle in the following way [SFGGH06]:

$$\mathbf{X}_p(t+\Delta t) = \mathbf{X}_p(t) + \mathbf{A}(\mathbf{X}_p, t)\Delta t + \mathbf{B}(\mathbf{X}_p, t)\xi(t)\sqrt{\Delta t}. \tag{4.28}$$

The 'drift' vector $\mathbf{A}$ and the displacement matrix $\mathbf{B}$ are depending on the point in time t and the position of the particle $\mathbf{X}_p(t)$. There is also a normally distributed random variable named $\xi(t)$ with mean zero and unit variance. In order to determine the displacement matrix B a connection to the Fokker-Planck equation is established. In 1951 Îto demonstrated that the particle density distribution obtained from equation (4.28) converges to the Fokker-Planck equation assuming an infinite number of particles and an infinitesimal step size. The particle density distribution stands for the probability to find a particle in the interval $[\mathbf{X}_p, \mathbf{X}_p + d\mathbf{X}_p]$ at a certain time t. The Fokker-Planck equation describes the motion of the particle density distribution f defined as

$$\frac{\partial f}{\partial t} + \nabla(\mathbf{v}f) = \nabla\nabla : (\mathbf{D}f) \tag{4.29}$$

Equation (4.25) and (4.29) both consist of a convection and and diffusion part. To realize this equality an adapted velocity is inserted into a modified version of equation (4.25).

$$\begin{aligned} &\frac{\partial c}{\partial t} + \nabla(\mathbf{v}c) + \nabla\cdot(c\nabla\mathbf{D}) = \nabla\nabla : (\mathbf{D}f) \\ &\mathbf{v}^* = \mathbf{v} + \nabla\cdot\mathbf{D} \\ &\Rightarrow \frac{\partial c}{\partial t} + \nabla(\mathbf{v}^* c) = \nabla\nabla : (\mathbf{D}f) \end{aligned} \tag{4.30}$$

Substituting the drift vector with velocity $\mathbf{v}^*$ leads to

$$\mathbf{X}_p(t+\Delta t) = \mathbf{X}_p(t) + \left(\mathbf{v}(\mathbf{X}_p, t) + \nabla\cdot\mathbf{D}(\mathbf{X}_p, t)\right)\Delta t + \mathbf{B}(\mathbf{X}_p, t)\xi(t)\sqrt{\Delta t}. \tag{4.31}$$

Due to the constant diffusion $\mathbf{D}$ the final notation of equation (4.31) can be written as

$$\mathbf{X}_p(t+\Delta t) = \mathbf{X}_p(t) + \mathbf{v}(\mathbf{X}_p, t)\Delta t + \mathbf{B}(\mathbf{X}_p, t)\xi(t)\sqrt{\Delta t}. \tag{4.32}$$

where the displacement matrix B is a related to the diffusion according to the following relationship

$$2\mathbf{D} = \mathbf{B}\cdot\mathbf{B}^T$$

The matrix $\mathbf{D}$ is diagonal matrix therefore the matrix $\mathbf{B}$ is unitary. The displacement matrix can be given as follows

$$B = \begin{pmatrix} \sqrt{2D} & 0 \\ 0 & \sqrt{2D} \end{pmatrix} \tag{4.33}$$

Equation (4.32) can be split into the x and y-coordinate of the movement using the determined matrix **B** of (4.33).

$$\begin{aligned} x_p(t + \Delta t) &= x_p(t) + v\Delta t + \sqrt{2 \cdot D\Delta t}\xi_x(t) \\ y_p(t + \Delta t) &= y_p(t) + \sqrt{2 \cdot D\Delta t}\xi_y(t) \end{aligned} \tag{4.34}$$

Comparing this equation system with (4.24) the equivalence is obvious.

4.3.4 Lattice Random Walk

The next two approaches are focusing on random walk simulations using a regular grid. The already known two dimensional area is covered with an individual fine grid. This solution is based on the principles of a cellular automaton. Every cell of the grid can have two different states. The cell can be filled with particles or not. According to the initial condition of the connected mathematical problem all particles start in the cell located at the origin of the coordinate system. The movement of the particles is defined by transmission probabilities to the neighboring cells. This mechanism should simulate the movement from regions with higher to regions with lower concentration.

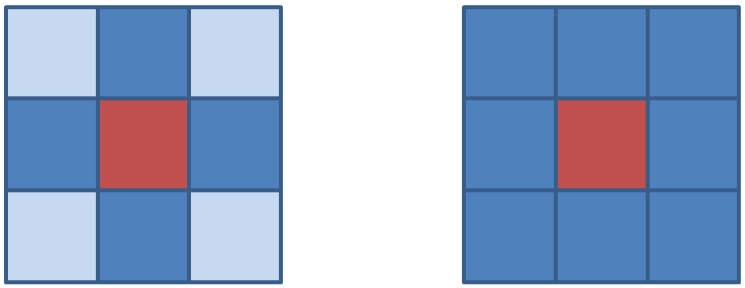

Figure 4.14: The Neumann and Moore neighborhoods are shown.

Regarding the possible neighborhoods two very common structures are used in the following. The first one is the Neumann neighborhood which has nothing to do with the identically named boundary condition. The particle can only move in one of the four cardinal directions as shown in figure 4.14. The second solution will use the Moore neighborhood. The definition enables a particle to move into any touching cell.

The question is how to realize the diffusive and convective motion using this grid. As already mentioned transmission probabilities are used controlled by a random variable. This principle is reminiscent of a Markov models. Every particle is described by a markov process and can have one of $n \times m$ states.

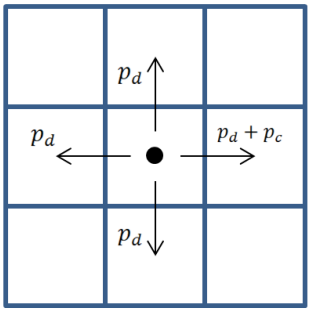

Figure 4.15: The Neumann neighboorhood and the transmission probabilities are shown.

For the Neumann neighborhood only 2 different probabilities are chosen as shown in figure 4.15. The variable p_d stands for the diffusive motion and p_c for the convective. This probabilities are not changing during the simulation. The stochastic behavior of the particles is realized using a random variable. This variable decides if a particle leaves the cell and in which direction. This decision is individual made for each particle in every time step. Due to the fact that a particle can move maximal one cell forward in every time step a fine resolution should be used. In this simulations the convective movement is not only influenced by the probability p_c but also by the spatial step size Δx.

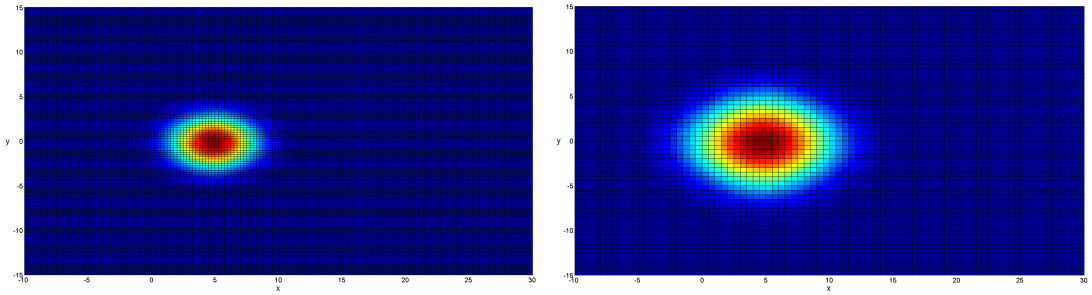

Figure 4.16: Simulating Convection diffusion using lattice random walk with Neumann neighborhoods.

In figure 4.16 two different results are shown. The number of particles is $N = 8000$. The probabilities are set to $p_d = p_c = 0.02$. In both graphics the center of concentration is at $x = 5$ but the used parameter Δt and Δx are chosen different. To reach $x = 5$ the relation between these two values has to be $\frac{dx}{dt} = \frac{1}{2}$ for $t = 500$. The finer the spatial steps the subtler the time steps. Using this knowledge the influence of p_c can be studied.

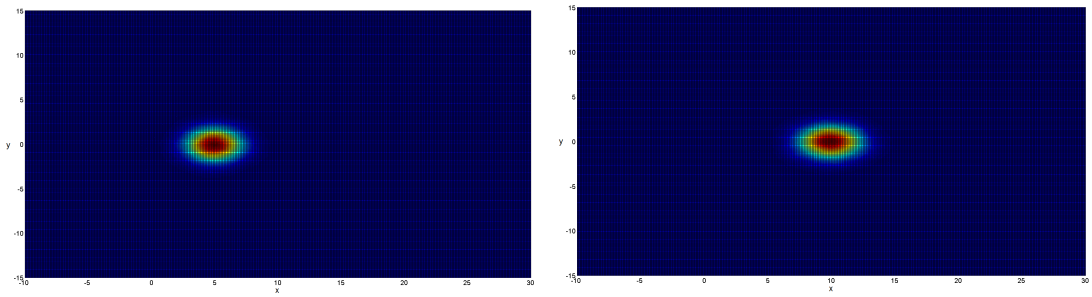

Figure 4.17: The influence of the convection is shown.

Due to the certain used neighborhood a slight rectangle can be found in all three pictures. To avoid this shape the spatial step size has to be chosen small. In the next implementation the Moore neighborhood is used.

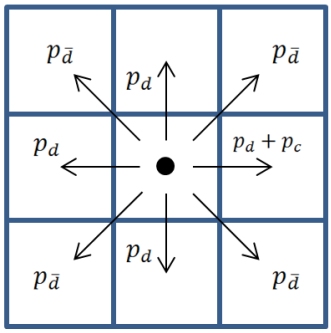

Figure 4.18: The Moore neighborhood and the transmission probabilities are shown.

Regarding the Moore neighborhood a new probability is introduced $p_{overlined}$ as shown in 4.18. It is not the same as p_d. Due to the longer way towards these cells the probability to reach this cell has to be lower. The parameter $p_{\overline{d}}$ can either be calculated using p_d or be chosen arbitrary. In the following simulation results the value was chosen dependent of p_d.

$$p_{\overline{d}} = \frac{1}{2} p_d$$

Despite the same simulation duration is used in all three graphics in figure 4.19 the results are different. In the first picture the relation $\frac{dx}{dt}$ is $\frac{1}{2}$. Therefore the concentration center is located at $x = 5$. In the second graphic the pollution distribution is greater than in the first one. The concentration center is at $t = 10$ due to the fact that the ratio changed to $\frac{dx}{dt} = 1$. In the last figure other parameter are used and the perspective changed. The new used ratio is $\frac{dx}{dt} = \frac{1}{4}$ and therefore the center is located at $x = \frac{5}{2}$. One can see that there is a linear connection between the location of the center and the relation of both step sizes.

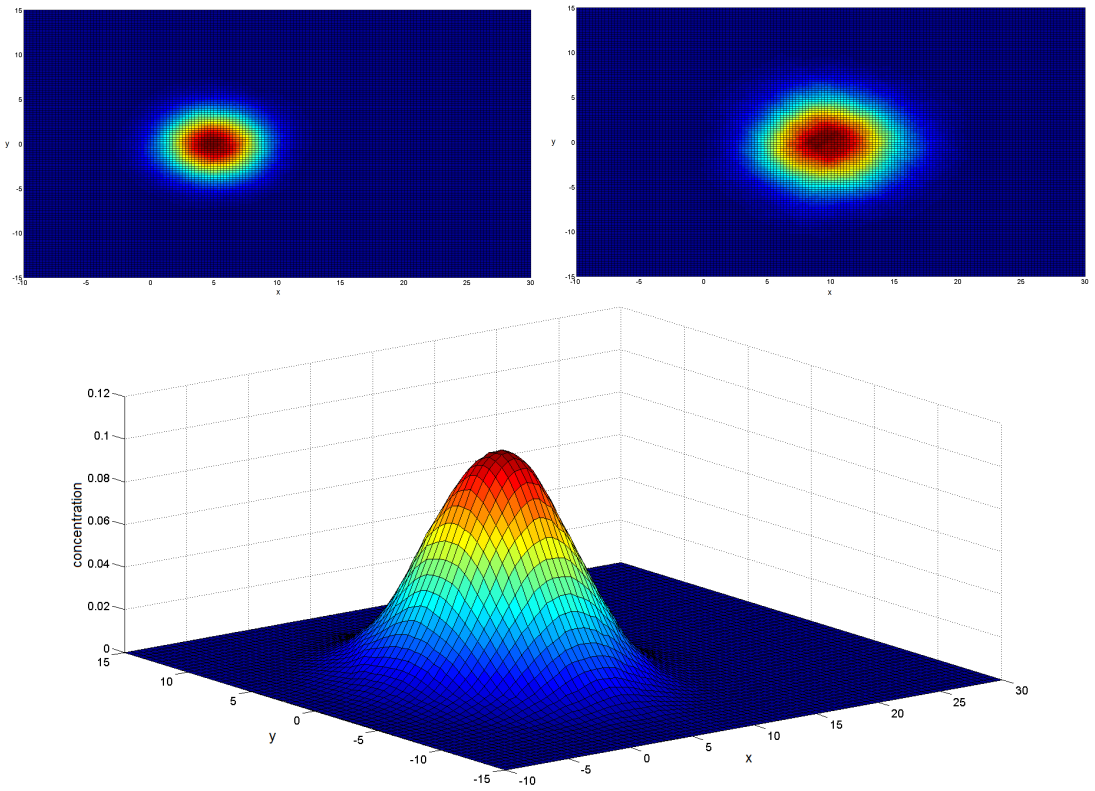

Figure 4.19: Simulating Convection diffusion using lattice random walk with Moore neighborhoods.

4.3.5 Lattice Bolzmann Method

This method was developed in the 1980s and is mainly used for the numerical simulation of fluids. Depending on the used grid and collision rules these models have special names.
In the following the regarded area is a two dimensional rectangle covered with a certain grid. The used boundary conditions differ from the analytical and numerical solutions. This time the Neumann boundary conditions explained in 1.5 are used. That means that there is no flow of pollution through any boundaries. No particles can leave the area. In case of reaching the edges the particle is reflected.
Regardless of whether a square, triangle or any other geometry is used to realize the grid the particles are always arranged in the same way. Every edge leading away form a node can be occupied by a particle. The allocated edge defines the moving direction of this particle, directed away from the node. The first used model is called HHP. The connected grid consists of small squares. There is only one collision rule defined.

Figure 4.20 a) presents the basic principle of the Lattice Bolzmann HPP models. Particles can occupy all four directions at every node. That means that there are maximal four particles

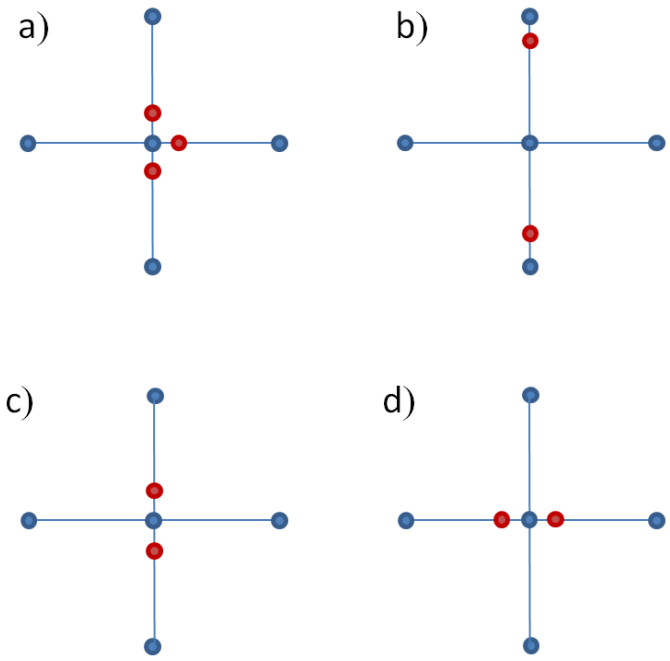

Figure 4.20: The schematic illustration of the HPP-model is shown.

per node. Picture b) shows the particle after the next time step. The furthermost right particle leaves the outlined area due to a move to the right. The other particles jump to the next node located in the opposite direction of the past node. In part c) and d) the 'head-on' collision rule is sketched. Both particles change their direction after the run-in.
Unfortunately no useful results can be produced using the HPP-model. It is not possible to simulate the convection-diffusion in an appropriate way. The initial complication of the Lattice Bolzmann method is that only a minimal number of particles can be set at one node. Therefore the realization of a point source as used in this thesis is not possible. There was a attempt to realize the source by four particles occupying all directions of node $(0, 0)$ in every time step. The particles can only move to the next node in one of the four cardinal directions until collision or reflection changes their direction. The only adjustment of direction happens when a particle reaches the edge of the domain. Then it is reflected and a collision with particles coming from the source is possible. In the simulation the particles spread in the shape of a cross and finally gather at the left and the right edge.

Another form of the Lattice Boltzmann method is the so called LHP-model. In this particular method a hexagonal grid is used.

This approach has the same disadvantages as the HPP-model. There is one difference regarding the distribution of pollution. In figure 4.21 a) the hexagonal grid with some particles is shown. Instead of spreading in cardinal directions this shape leads to an astral distribution of

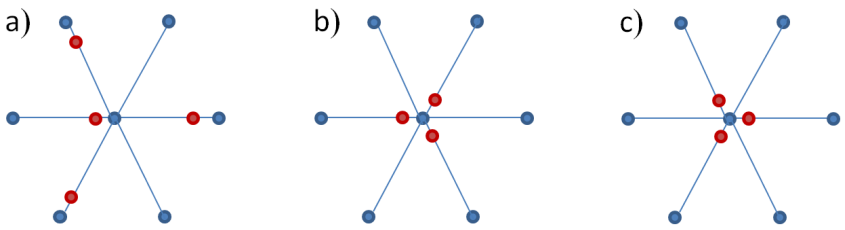

Figure 4.21: The schematic illustration of the LHP-model is shown.

particles. The collision rules are more complex. Picture b) and c) describe one of these rules. Due to the fact that the movement is again deterministic and along fixed directions towards the next node using the LHP model it is also not possible to simulate the convection-diffusion equation with a point source in an appropriate way.

Both methods are very useful to implement flux behavior in general and especially around obstacles with arbitrary geometry but not expedient for simulating any kind of diffusion problems.

CHAPTER 5

Two-dimensional Results

In this chapter the results of different convection-diffusion approaches are discussed. In chapter 4 the analytical solution is only given for an instantaneous releasing source. Therefore this solution is compared to the numerical and the random walk implementation. Due to the fact that FEM is only realized using COMSOL this approach is not compared. Regarding the random walk the stochastic and Gaussian approach, respectively is used for analysis. As shown in the one-dimensional results the diffusion coefficient has to be modified and included into the intuitive approach to gain a good approximation. This modification transfers the intuitive into the Gaussian-based approach. Hence, only the stochastic approach is used for comparison. In the end both versions of the Lattice random walk approaches are used for analysis. At first the analytical and numerical solutions are compared.

5.1 Analytical vs. Numerical

Before the analytical and numerical solutions are compared the properties of the finite difference method are analyzed.

Δt	Δx	explicit Euler	Δt	Δx	explicit Euler
1	1	0.79489	$\frac{1}{2}$	$\frac{1}{4}$	25.7700
$\frac{1}{2}$	1	1.60922	$\frac{1}{4}$	$\frac{1}{4}$	51.68385
1	$\frac{1}{2}$	3.18382	$\frac{1}{4}$	$\frac{1}{8}$	208.9761
$\frac{1}{2}$	$\frac{1}{2}$	6.41569	$\frac{1}{4}$	$\frac{1}{8}$	412.67604

Table 5.1: The calculation times for different parameters using FDM are listed.

The relation of time step size Δt and the simulation time is nearly linear. If the step size is halved the calculation time is approximately doubled. Regarding the spatial step size Δx the relation is not linear. Changing Δx has an greater impact on the simulation time than changing

Δt. Comparing the execution time in one and two dimensions regarding FDM the difference is enormous. The number of nodes on the regarded domain enlarges to the power of 2. Therefore also the duration increases quadratic.

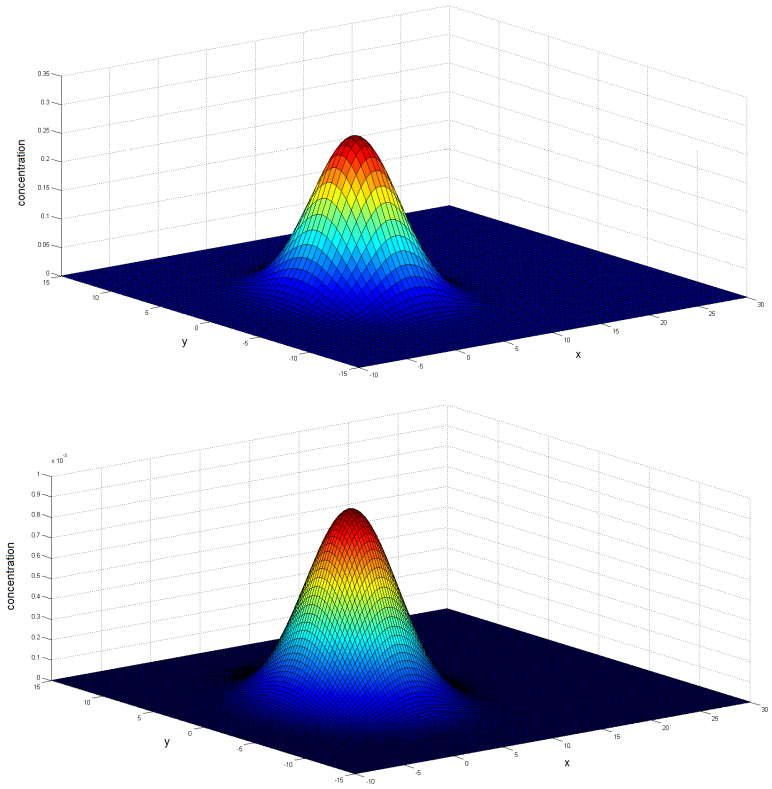

Figure 5.1: The analytical and numerical solution is shown.

The upper surface plot in figure 5.1 shows the concentration of the analytical solution dependent on the coordinates x and y. The lower graphic shows the related numerical result. The simulation time is set to $t_{end} = 250$. The other parameters are mostly similar to the figures in chapter 4. The diffusion coefficient and the velocity are both $D = v = 0.02$ and the time step is $\Delta t = 0.5$. A small difference can be found in the choice of the spatial step size Δx. This value is set to $\Delta x = \frac{1}{2}$ in the analytical and $\Delta x = \frac{1}{4}$ in the numerical solution. In the following the error values are studied in detail.

Table 5.2 shows the error values for different parameter choices. In two cases the disadvantage of the used explicit Euler algorithm is visible. For $\Delta t = 1$ and $\Delta x = \frac{1}{4}$ the proportion of these two values causes oscillations using explicit Euler. The scenario occurs also using the values $\Delta t = \frac{1}{4}$ and $\Delta x = \frac{1}{8}$. If both values are minimized simultaneously no oscillations happen. The smaller the used step sizes the smaller the error results. Except one result all the simulations uses the parameter setting $v = 0.02$, $D = 0.02$ and $t_{end} = 250$. The last results are marked with $.^*$ which means that the used simulation duration changed to $t_{end} = 500$. The approximation

		explicit Euler				explicit Euler	
Δt	Δx	$\|.\|_\infty$	$\|.\|_1$	Δt	Δx	$\|.\|_\infty$	$\|.\|_1$
1	1	0.0027	$1.5624E^{-4}$	$\frac{1}{2}$	$\frac{1}{4}$	$9.1479E^{-4}$	$1.4640E^{-5}$
1	$\frac{1}{2}$	0.0017	$3.7791E^{-5}$	$\frac{1}{4}$	$\frac{1}{8}$	$.E^{119}$	$.E^{120}$
$\frac{1}{2}$	$\frac{1}{2}$	0.0016	$3.8172E^{-4}$	$\frac{1}{8}$	$\frac{1}{8}$	$4.7570E^{-4}$	$8.5291E^{-6}$
1	$\frac{1}{4}$	$.E^{32}$	$.E^{33}$	$\frac{1}{2}$	$\frac{1}{4}$	$4.4790E^{-4}*$	$9.7584E^{-4}*$

Table 5.2: The error values for FDM using Explicit Euler are shown.

using the FDM in the two-dimensional domain is working very well.

5.2 Analytical vs. Random

5.2.1 Gaussian Approach

In order to compare the analytical solution to a random walk approach the results have to be adapted. In the random walk the output describes the smoothed amount of particles in every cell. Due to the initial Dirac-function the integral at the beginning is 1. The area of the random walk domain is discretized. Therefore the output has to by divided not only by the number of particles but also by the area of the cells used for the flattening.

Figure 5.2 shows the concentration results of the analytical solution, in the upper, and the random walk approach in the lower graphic. The difference between these two implementations can not be read out exactly. Therefore a closer look to the simulation data itself is given.

				Gaussian RW	
Δt	Δx	r	N	$\|.\|_\infty$	$\|.\|_1$
1	1	3	4000	$3.3953E^{-3}$	$6.3494E^{-4}$
1	$\frac{1}{2}$	8	4000	$5.0333E^{-3}$	$3.7366E^{-5}$
$\frac{1}{2}$	$\frac{1}{2}$	15	4000	$1.0632E^{-2}$	$1.0711E^{-3}$
$\frac{1}{2}$	$\frac{1}{4}$	15	4000	$4.5255E^{-3}$	$1.0048E^{-4}$
$\frac{1}{2}$	$\frac{1}{8}$	20	4000	$2.8011E^{-3}$	$2.2063E^{-3}$
1	$\frac{1}{4}$	20	8000	$6.7640E^{-3}$	$3.3383E^{-5}$
$\frac{1}{2}$	$\frac{1}{4}$	20	8000	$6.8246E^{-3}$	$1.8259E^{-4}$

Table 5.3: Error values for the Gaussian approach are shown.

This table 5.3 shows the approximation results. The parameter r describes the used radius for the flattening. If the spatial step size is decreasing a greater radius r can be used. If r is chosen to big compared to Δx the result loses the shape of a bell curve. Compared to the results of the numerical simulation the random walk approach leads to greater error values but it is a quite good approximation.

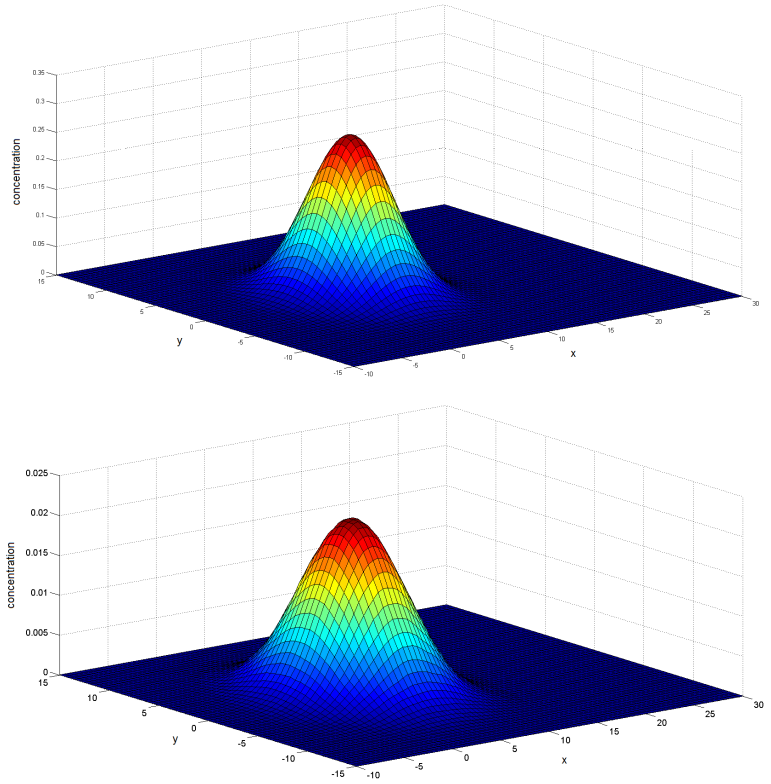

Figure 5.2: Analytical and Gaussian solution are shown.

Δt	Δx	t_{end}	N	Gaussian RW
1	$\frac{1}{2}$	250	4000	31.57182
1	$\frac{1}{4}$	250	4000	31.71316
$\frac{1}{2}$	$\frac{1}{2}$	250	4000	62.75965
$\frac{1}{2}$	$\frac{1}{4}$	250	4000	64.6670
$\frac{1}{4}$	$\frac{1}{4}$	250	4000	129.1143
1	$\frac{1}{4}$	250	8000	63.9175
$\frac{1}{2}$	$\frac{1}{4}$	250	8000	128.57107

Table 5.4: Different simulation times for the Gaussian random walk are shown.

The execution times in table 5.4 show a clear pattern. A change of the spatial step size Δx has no or minimal effects on the simulation time, whereas the modification of the time step Δt influences the needed time. If Δt is halved the simulation time doubles. The increasing number of particles also enlarges the duration. The relation is again linear.

5.2.2 Lattice Approach

In the following the two different lattice random walk approaches are used for comparison. Due to the fact that the implementation of both random walks differs only in the amount of transmission probabilities the simulation duration is nearly the same.

Δt	Δx	t_{end}	N	Neumann RW	Moore RW
1	$\frac{1}{2}$	500	4000	0.152719	0.214491
1	$\frac{1}{4}$	500	4000	0.163539	0.190734
$\frac{1}{2}$	$\frac{1}{2}$	500	4000	0.291376	0.381923
$\frac{1}{2}$	$\frac{1}{4}$	500	4000	0.280214	0.385576
$\frac{1}{4}$	$\frac{1}{4}$	500	4000	0.559355	0.725062
1	$\frac{1}{4}$	500	8000	0.290346	0.369469
$\frac{1}{2}$	$\frac{1}{4}$	500	8000	0.550393	0.741931

Table 5.5: Different simulation times for the two random walk approaches are shown.

In table 5.5 the execution times of both implementations are shown. Due to the fact that the iteration steps stay the same no matter if the spatial step size Δx is changed or not the execution time remains the same, whereas the modifications of the time step Δt influences the simulation time directly. There are more time steps for calculation. If Δt is halved the simulation time doubles. The relation of particles and duration is linear. If there are twice as many particles used for simulation the calculation time doubles. Compared to the Gaussian-based random walk the execution time is very short. Also the numerical solution needs much more time for all the calculations. This is a big advantage of the random walk implementations.

Figure 5.3 shows the concentration results of the analytical solution and both lattice random walk approaches. In the upper row the left image shows the random walk using Neumann and the right using Moore neighborhood. To validate the behavior simulations for certain parameter are compared.

				Neumann RW		Moore RW	
Δt	Δx	N	r	$\|.\|_\infty$	$\|.\|_1$	$\|.\|_\infty$	$\|.\|_1$
1	$\frac{1}{2}$	4000	5	0.0048	0.4870	0.0273	3.0004
$\frac{1}{2}$	$\frac{1}{2}$	4000	10	0.00417	0.2209	0.0115	1.8126
$\frac{1}{2}$	$\frac{1}{2}$	4000	20	0.0107	0.10438	0.0062	1.6583
$\frac{1}{2}$	$\frac{1}{4}$	4000	20	0.00481	0.10513	0.1760	9.7079
$\frac{1}{4}$	$\frac{1}{4}$	4000	40	0.01079	0.05124	0.0400	9.43712
$\frac{1}{8}$	$\frac{1}{8}$	4000	40	0.00636	0.05127	0.7281	40.775
$\frac{1}{4}$	$\frac{1}{4}$	8000	20	0.0048	0.10513	0.1287	9.7079
$\frac{1}{8}$	$\frac{1}{8}$	8000	40	0.00653	0.05127	0.7162	40.775

Table 5.6: Error values of the two random walk approaches are shown.

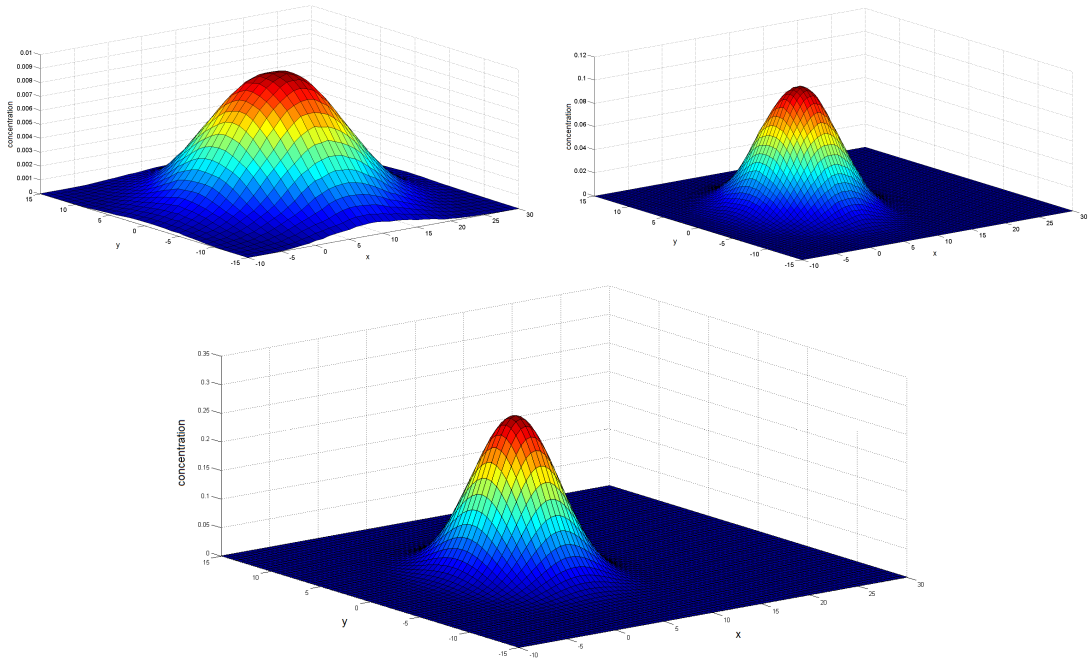

Figure 5.3: Analytical and random approach is shown.

This table 5.6 shows the error values of both random walk approaches. The Lattice random walk using the Neumann neighborhood is obviously a better approximation. The Moore neighborhood moves to fast compared to the analytical solution. One can see that the usage of different r values influences the error very much. The variable r stands for the used cells for flattening, in other words the radius. If r is chosen to big the Gaussian shape disappears in the random walk results. Therefore the error increases. As mentioned in chapter 4 the relation between Δx and Δt has to fulfill a certain condition to approximate the analytical solution. In this case it is $\frac{dx}{dt} = 1$. This condition restricts the choice of values enormous. Using the right relation regarding step sizes and radius the Neumann random walk is a good approximation of the analytical solution.

CHAPTER 6

Conclusion

Convective-diffusion is a very important topic and used in various scientific disciplines to simulate or verify many different processes in nature. In this thesis a restriction to the one- and two-dimensional problem is considered. Regarding the one-dimensional convection-diffusion equation depending on the initial and boundary conditions different analytical solutions can be given. If an analytical solution can be found of course all the approximation approaches are not necessary. In case of difficult geometries and conditions the analytical solution can be hard to find. Therefore it is important to analysis possible approximations.

In the one-dimensional convection-diffusion equation two different types of approximations are used. One the one hand the well known numerical methods, the finite difference and finite element method, are compared to the analytical solution. Additionally an analysis of the Explicit vs. Implicit Euler is made. Due to the fact that the Explicit Euler is an unstable algorithm for certain choices of Δx and Δt the comparison to the Implicit Euler is necessary. The results show that the Implicit Euler is a better approximation and not only because it is a ultra-stable algorithm. Regarding the finite element method a third algorithm, called Implicit Heun, is used. Comparing all three algorithms the Implicit Heun implementation yields the best approximation results. Of course there is a wide range of different possible algorithms which are not used in this thesis. An enlarged comparison can be worked out for future analysis.
Comparing the finite difference method and the finite element method it is also well known or expected that the finite element method approximates the analytical solution in a better way. This part of analysis can be continued regarding the usage of different base functions as well as different element shapes. This work is focusing only on linear base functions and triangular elements.

The second part of the analysis is represented by stochastic approaches connected to the Brownian motion. Different implementations of the random walk are used for comparison. The random walk approach based on the Gaussian curve approximates the analytical solution best. Due to the fact that the analytical solution is connected to the Gaussian function this result is not surpris-

ing. An advantage of the random walk approaches is the independence of the spatial step size. Comparing the error values of the finite element method and the random walk approximation the finite element approach produces better results. However, the efficiency of the random walk approaches can be increased using matrix calculations instead of loop implementations. But the accuracy won't change.

In the two-dimensional domain the same two implementation types are used. Regarding the numerical solutions only the finite difference method using Explicit Euler is compared. This approach has very bad execution times. Using complex matrix structures this disadvantage could be corrected. Also an implementation of the Implicit Euler and other algorithm would be necessary for further analysis of the numerical solutions.
Due to the instability of the Explicit Euler used for the numerical implementations the random walk approaches show their advantages. In the two-dimensional case four different random walk implementations are introduced. Two of them are extensions of the one-dimensional approaches. One of the new methods is based on the principle of Markov models and uses transmission probabilities to simulate diffusive behavior. This approach has short execution times and quite useable results. The forth implementation examines the Lattice Bolzmann method. Unfortunately this method is not useable for the regarded initial problem. Using a different problem definition this mehtod could be a useful tool. As expected the comparison of all the results lead to the same statement as in the one-dimensional case. The Gaussian based random walk is the best approximation regarding random walk approaches. In general the accuracy of the finite element method can not be reached using random walk.

List of Figures

Bibliography

[AEM98] K. J. Astrom, H. Elmqvist, and S. E. Mattsson. Evolution of continuous-time modeling and simulation. *The 12th European Simulation Multiconference, EMS*, June 1998.

[Bon97] E. Bonabeau. From classical models of morphogenesis to agent-based models of pattern formation. *Artificial Life*, Vol3:191–211, 1997.

[CJ70] Carslaw and Jaeger. *Conduction of Heat*. Springer, UK, 1970.

[Coe02] N. Coelen. Black-scjoles option pricing model. *script*, 2002.

[Cra75] J. Cran. *The Mathematics of Diffusion*. Oxford University Press, United States., 1975.

[IK03] D. M. Imboden and S. Koch. *Systemanalyse: Einführung in die methematische Modellierung natürlicher Systeme*. Springer, Germany., 2003.

[JÖ8] A. Jüngel. *Vorlesungsskript zu Partielle Differentialgleichungen*. Technische Universität Wien, Austria., 2008.

[LT05] S. Larsson and V. Thomee. *Partielle Differentialgleichungen udn numerische Methoden*. Springer, Netherlands., 2005.

[Mur89] J. D. Murray. *Mathematical biology*. Springer, New York., 1989.

[OB61] A. Ogata and R.B. Banks. A solution of the differential euqation of longitudinal dispersion in porous media. *US Geological Survey*, Professional Paper 411-A, 1961.

[PF56] B.O. Pierce and R.M. Foster. A short table of interals. *Boston, Mass., Ginn and Co.*, page p.189, February. 1956.

[Seg12] Ir. A. Segal. *Finite element methods for the incompressible Navier-Stokes equations*. Delft University of Technology, Netherlands., 2012.

[SFGGH06] P. Salamon, D. Fernandez-Garcia, and J.J. Gomez-Hernandez. A review and numerical assessment of the random walk particle tracking method. *Journal of Contaminant Hydrology*, 87:277–305, 2006.

[SK00] K. Schulten and I. Kosztin. *Lectures in Theoretical Biophysics*. University of Illinois at Urbana, USA., 2000.

[SMF10] A. H. Salas, L.J. Martinez, and O. S. Fernandez. Reaction-diffusion equations: a chemical application. *Scientia et Technica Ano XVII, Universidad Tecnoloica de Pereira*, No 46, 2010.

[Tur52] A. M. Turing. The chemical basis of morphogenesis. *Philosophical Transactions of the Roxal Society of London*, Series B, 237:37–72, 1952.

[ZK99] C. Zoppou and J.H. Knight. Analytical solution of a spatially varible coefficient advection diffusion equation in up to three dimensions. *Appliedn Mathematical Modelling*, Series B, 237:667–685, 1999.